An Improved Device to Measure Human Response to Dorsiflexion and Plantar Flexion Perturbations

by
Fourie Gildenhuys

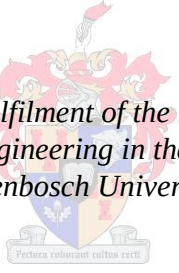

Thesis presented in partial fulfilment of the requirements for the degree of Master in Mechanical Engineering in the Faculty of Engineering at Stellenbosch University

Supervisor: Mr R.T. Dobson

December 2014

Declaration

By submitting this thesis electronically, I declare that the entirety of the work contained therein is my own, original work, that I am the sole author thereof (save to the extent explicitly otherwise stated), that reproduction and publication thereof by Stellenbosch University will not infringe any third party rights and that I have not previously in its entirety or in part submitted it for obtaining any qualification.

Signature: .....
F. Gildenhuys

Date: December 2014 .....

Abstract

An Improved Device to Measure Human Response to Dorsiflexion and Plantar Flexion Perturbations

F. Gildenhuys

Thesis: MEng (Mech)

December 2014

The Dorsiflexometer is a device designed and built for the assessment of a patient's balance capabilities. The birth of the Dorsiflexometer is due to a serious need for physiological balance assessment equipment, capable of conducting dynamic tests in the clinical setting. This is accomplished by recording and analysing the patient's response to sagittal plane perturbations. The Dorsiflexometer is operated from a computer software interface program. It uses the measurements from a single force plate to calculate four balance metrics' characterising a patient's ability to maintain balance. These balance metrics include the sway index, equilibrium score, postural stability index and radius parameter.

A single and a double inverted pendulum model of the human body is derived to calculate a patient's centre of mass movement in the sagittal plane with the measured force plate data and body parameters. Three experiments, involving 48 subjects, were conducted. The experimental tests proved the competency of the machine, the accuracy of both inverted pendulum models and the balance response of seafarers aboard an Antarctic research and supply vessel during rough sea conditions.

The tests concluded that the inverted pendulum models can be used to calculate the body centre of mass displacement. The double inverted pendulum model results are more accurate compared with the single inverted pendulum model. During rough sea conditions, the body movement and postural response of seafarers are increased in order to keep themselves upright. The body is furthermore exposed to a fluctuating ground reaction force which may lead to the progression of osteoarthritis and musculoskeletal injuries. The Dorsiflexometer proved to be capable of conducting repeatable assessments and

yielding accurate results which can be used to distinguish between balance capabilities.

Uittreksel

'n Verbeterde Apparaat om Menslike Reaksie as gevolg van Dorsifleksie en Plantarfleksie versteuringe te Meet

("An Improved Device to Measure Human Response to Dorsiflexion and Plantar Flexion Perturbations")

F. Gildenhuys

Tesis: MIng (Meg)

Desember 2014

Die Dorsiflexometer is 'n apparaat wat die balansvermoë van pasiënte analiseer. Die masjien is ontwerp en vervaardig weens die groot behoefte aan fisiologiese balans assesserings toerusting wat dinamiese toetse in die mediese sektor kan bepaal. Dit word bereik deur pasiënte se liggaamsreaksie in die sagittale vlak te meet en te assesseer.

Die Dorsiflexometer is beheerbaar vanaf 'n rekenaar sagteware koppelvlak program. Die masjien maak gebruik van 'n enkele kragplaat om pasiënte se balans statistieke te meet. Hierdie balans statistieke wat die pasiënte se balans vermoë beskryf en karakteriseer behels die sogenaamde: swaai indeks, balans telling, posturale stabiliteit indeks en die radius parameter.

'n Enkel en dubbel inverse slinger model van die liggaam is afgelei. Hierdie modelle maak gebruik van 'n pasiënt se kragplaat metings en sy liggaamlike parameters om die swaartepunt tydens beweging te bereken.

Drie eksperimente, waarin 48 persone betrokke was, is gedoen. Die eksperimente is gedoen om die apparaat se bevoegdheid te bewys, die akkuraatheid van altwee inverse slinger modelle te toets en verder die balans van seevaarders op die Antarktiese navorsings en toevoer skip tydens rowwe see toestande te analiseer. Die toetse het bewys dat die inverse modelle gebruik kan word om die liggaam se swaartepunt te bereken. Die dubbel inverse slinger model resultate is wel akkurater as die enkel slinger model. Daar is bevind dat seevaarders van meer liggaamsbeweging en posturale reaksies gebruik moet maak

om orent te bly tydens rowwe seetoestande. Verder word hul liggame blootgestel aan 'n wisselende grond reaksie krag wat kan lei tot die ontwikkeling van osteoarthritis en muskuloskeletale beserings.

Die Dorsiflexometer is bewys as 'n aparaat wat wat akurate resultate lewer vir herhaalbare assesserings. Dit kan gebruik word om te onderskei tussen verskillende balans vermoëns.

Acknowledgements

I would like to express my sincere gratitude to the following people for their valuable assistance during the course of this study:

- First and foremost I would like to thank Mr. Robert Dobson, as thesis supervisor, for his perseverance through all my arguments, inspirational life lessons, guidance and insight that has added inestimable value to this project. Without Mr. Dobson, none of this would have been possible.
- Dr. Annie Bekker and the Sound and Vibration team, for allowing me to accompany them on the 2013-2014 SANEA Antarctic expedition. It was truly a life altering experience.
- The Stellenbosch writing lab and Dr. Annie Bekker for assisting me with the write-up of this project.
- My brother, my father and my mother for the two years of moral support.
- Gideon Joubert and Guy Gafney for agreeing to let their pictures be used for demonstration purposes.

Contents

List of Figures

List of Tables

Nomenclature

Engineering Symbols

a	Length, m
COM	Centre of mass length, m
COP	Centre of pressure length, m
d	Pitch diameter, mm
ES	Equilibrium score
e	Gear ratio
F	Force, N
g	Gravitational acceleration, m/s^2
H	Total body stature, m
h	Length, m
I	Inertia, kg·m^2
k	Sub−depth teeth number
L	Length, m
l	Lever arm length, m
M	Body mass, kg
m_i	Segment mass, kg
m_{mod}	Module, mm
N	Number of teeth on gear
n	Rotational speed, rev/s
OSI	Overall stability index
PSI	Postural stability index
R	Ground reaction force, N
r	Radius, m
SD	Standard deviation
SF	Safety factor
SI	Sway index
T	Kinetic energy, J
t	Time, s

U	Potential energy, J
W	Vertical body weight, N
WF	Weight factor
x	Length, m
$\dot{x}$	Linear velocity, m/s
z	Length, m

Greek Engineering Symbols

θ	Angle, $\circ$
$\dot{\theta}$	Angular velocity, rad/s
$\ddot{\theta}$	Angular acceleration, rad/s^2
ϕ	Angle, $\circ$
$\dot{\phi}$	Angular velocity, rad/s
υ	Velocity, m/s
τ	Torque, N·m

Subscripts

$actual$	Actual
$axis$	Axis
$calc$	Calculated
COM	Centre of mass
DIP	Double inverted pendulum
$error$	Total error
F	Final gear
G	Gear
i	Measurement number
L	First gear
max	Maximum
max, ant	Maximum anterior
$max, post$	Maximum posterior
$mean$	Medianvalue
min	Minimum
mod	Module
$model$	Modelresults
n	Number of measurements
o	Rotation point
p	Pinion

r	Ground reaction
s	Friction
seg	Segment
SIP	Single inverted pendulum
T	Total
t	Time
$video$	Video measured results
x	X direction
$Xavg$	Average value in the X direction
y	Y direction
$Yavg$	Average value in the Y direction
z	Z direction

Acronyms

AMTI Advanced Mechanical Technology Incorporation

BOS Base of support

CNS Central nervous system

COG Centre of gravity

COM Centre of mass

COP Centre of pressure

DIP Double inverted pendulum

ES Equilibrium score

GUI Graphical user interface

ID Identification document

OA Osteoarthritis

OSI Overall stability index

PSI Postural stability index

RMS Root mean square

RMSE Root mean square error

SANAE South African National Antarctic Expedition

SD Standard deviation

SF Safety factor

SI Sway index

SIP Single inverted pendulum

USB Universal serial bus

WF Weight factor

Chapter 1

INTRODUCTION

In everyday life, people are unaware that their bodies are continuously adjusting the position of their body centre of mass (COM) in order to maintain balance while performing activities. Only once people fall or come close to falling do they realise how important balance is to daily functioning.

The act of achieving, maintaining or restoring a state of postural equilibrium during any activity can be defined as the ability to balance (Pollock *et al.*, 2000). Balance gives us the capability to stand upright without having to move our feet even though our bodies are inherently unstable. As we get older, get injured or suffer from balance disorders, our ability to maintain balance becomes impaired, which increases the risk of falling due to a lack of stability (Lockhart *et al.*, 2003). Undetected balance disorders are a serious health hazard which can lead to severe injuries or even death. If such individuals could have been diagnosed before a serious incident, their falls could have been prevented and most would not require a new hip or knee replacement. Some balance impairments are undetectable by physical examinations but are still severe enough to lead to falls. A device capable of detecting these slight impairments could prevent numerous accidents from occurring. Furthermore, such a device can be used to determine the response of subjects to therapy.

The Dorsiflexometer is a machine which was designed with the aim to detect even the slightest impairment in a subject's ability to maintain balance (Botha, 2005). This is accomplished by measuring the rate and the range within which a subject's centre of pressure (COP) moves during both static and dynamic support surface conditions. This idea was first proposed by an orthopaedic surgeon, Dr Driver-Jowitt (Botha, 2005). Various balance metrics, such as the sway index (SI), overall stability index (OSI), equilibrium score (ES) and postural stability index (PSI), can then be calculated using the COP trajectories (Botha, 2005; Arnold and Schmitz, 1998; Chaudhry *et al.*, 2005). These factors quantitatively captures the subject's ability to maintain balance.

The Dorsiflexmeter records a subject's ground reaction forces while standing on a platform which is perturbed in the sagittal plane. The sagittal plane is a vertical plane which passes from the anterior to posterior of the body dividing it into a left and right halve as shown in Figure 1.1. This perturbation of the platform forces the subject to react by shifting their COP to prevent themselves from falling over. The machine then uses the recorded ground reaction forces to calculate the continuous position and rate of change of the COP. The rate of change and location data are subsequently used to calculate the various balance metrics which allows for the assessment of a subject's ability to maintain balance.

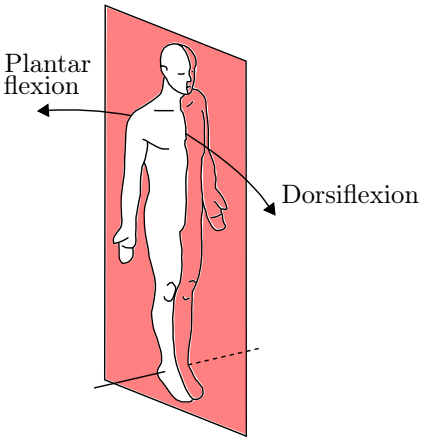

Figure 1.1 Sagittal plane of the human body.

The use of a Dorsiflexometer can contribute in the following fields: Firstly, to help diagnose patients with balance disorders, particularly the elderly. In 2001, no less than 15400 deaths occurred in the United States alone due to fall related accidents among the elderly (Bloem *et al.*, 2003). Bloem *et al.* (2003) furthermore states that medical expenses related to falls amounts to more than 20 billion dollars each year in the United States. Many of these incidents can be prevented by medically treating subjects with a high risk of falling. The effects of certain medication on the ability of the elderly to balance, can further be monitored. Secondly, the Dorsiflexometer can be used to monitor the balance improvement of sport players as a result of certain activities. The machine can aid in the rehabilitation of injured athletes. Due to the large amounts of money involved in professional sport, the performance capabilities of the athletes is of interest. The performance of athletes in many fields is directly influenced by the player's balance. The Dorsiflexometer can therefore be used to monitor the improvement in a sport player's ability to balance due to certain activities or exercises. Additionally it can be used to monitor the recovery process of injured athletes and indicate activities which can speed up the recovery process.

This thesis describes the methodology that was used to improve the old Dorsiflexometer (Botha, 2003) which was originally designed, built and patented by Botha (2005). The machine is however no longer available. The old Dorsiflexometer made use of two foot plates, with three load cells, to measure a subject's ground reaction forces. This yielded two reaction forces, one for each foot, which then had to be combined to give an overall reaction force. The aim of this project is to redesign and build a new Dorsiflexometer machine based on the old machine's principles. The new Dorsiflexometer must be operated from a laptop computer and utilise a single force plate which oscillates from the same pivot axis as the ankle joint of an average human being. Furthermore, this thesis discusses how two models of the machine were designed, built, tested and benchmarked against each other. An algorithm was coded to operate the machine from a computer based user interface. Two analytical models were derived to calculate the position of the COM of the subject in the sagittal plane. The first model simulates the human body as a single inverted pendulum (SIP). The SIP model rotates only about the ankle joint. The second model simulates the human body as a double inverted pendulum (DIP) model which can rotate about the ankle and hip joints.

An experiment involving 10 subjects was conducted to verify how closely the inverted pendulum models reflect the actual COM movement. A second experiment involving 18 subjects was conducted aboard the S.A. Agulhas II, which is a polar supply icebreaking vessel. The aim of this experiment was to measure the ground reaction forces which seafarers are exposed to during rough sea conditions. A third experiment was conducted to evaluate the final design and compare the testing accuracy of the Dorsiflexometer to a commercially available balance measuring machine. The commercial balance machine does however not have the same testing capabilities as the Dorsiflexometer. In the thesis, 'Dorsiflexometer' refers to the new Dorsiflexometer which was designed and built for this project.

Chapter 2

LITERATURE STUDY

2.1 Introduction

An analysis of balance or postural stability is essential to gain sufficient knowledge about postural control systems for the assessment and documentation of rehabilitation treatments. This can be accomplished by monitoring and analysing the stability performance of a subject during static and dynamic conditions. According to Browne and O'Hare (2001) most of the balance assessment instrumentation which is currently available is better suited for research conducted in laboratories. These machines should rather be more user friendly and easily accessible in order that they can be used routinely with ease in a clinical setting.

The purpose of this study is to develop a machine which can be easily operated by an untrained person. It is specified that this machine should yield accurate results which can be analysed by a certified medical practitioner to evaluate a subject's ability to balance. Firstly, this chapter defines balance and how it is accomplished by human beings. It continues to summarise the three different sensory systems humans use in order to balance, followed by the current physiological assessment methods used to evaluate a subject's ability to balance. Lastly the current available theoretical models which are used to simulate a static erect human body as either a single or double inverted pendulum are revised.

2.2 Human Balance

Human balance is often referred to as stability or postural control (Pollock *et al.*, 2000). In terms of mechanics, balance refers to an object in the state of equilibrium with no or zero resultant load actions acting upon it. Human balance can be viewed as a state in which the body continuously adjusts joint positions. These adjustments are made with the use of muscle activity to keep

the posture upright and the body COM above the COP in order to maintain a state of equilibrium (Galley and Forster, 1982). The COM is a point in the three dimensional global reference system which is equivalent to the total body mass. The COP is the point location of the vertical ground reaction force vector as a result of the forces exerted by the human body on the ground (Winter, 2009). The COP represents a weighted average of all the pressures over the surface of the area in contact with the ground (Winter, 1995).

The body parts in contact with the ground are known as the base of support (BOS). For example, when a person is standing erect on both feet, the surface area of the feet acts as the BOS. To statically balance, the body has to keep its centre of gravity (COG) within the BOS by adjusting its COP (Pollock *et al.*, 2000). However, when the body is erect, the COG is higher than half the body length, and has a relatively small BOS, which makes it inherently unstable and complicates the maintenance of stability. The COG is the vertical force component of the COM. Murray *et al.* (1975) reports that the COG changes according to positional changes of body segments to keep itself upright. These postural changes are carried out by an intricate process involving neurons from the sensory system. Afferent or sensory neurons convey information from certain receptors to the central nervous system (CNS). The CNS then makes a decision as what to do and conveys these commands to the intact skeletal muscle system with the use of efferent neurons (Duncan *et al.*, 1990). The human body therefore uses an intricate continuous feedback control system to keep itself upright and stable by sensing its relative position and then reacting accordingly.

2.3 Sensory Systems of Balance

Human balance entails three major sensory systems to maintain stability: vestibular, vision or visual, and somatosensory (Chaudhry *et al.*, 2011). The vestibular system is responsible for processing information about body dynamics and movements in relation to gravity. It specifically gathers information relating the acceleration, rotation and relative positions of certain body segments. The vestibular system is situated in the inner ear and consists of a semicircular canal system and the otoliths. The semicircular canal system and otoliths sense rotational movements and linear accelerations respectively (Fox, 2009).

Vision, or the visual system, provides the body with object-to-object orientation by giving it the ability to identify objects, their movement, and relative positions. Vision conveys proprioceptive information to the CNS about the body's position in the environment or the position of body segments relative to one another. The visual system consists of a combination of both pe-

ripheral and central vision. However, according to Guskiewicz *et al.* (2001), peripheral vision is more important for balance and stability than central vision. Guskiewicz *et al.* (2001) further states that the vestibular system works in conjunction with the visual system to stabilise the eyes and maintain posture, which is also known as the vestibulo-ocular reflex. The brain compares information such as segment velocities and rotation conveyed from visual and vestibular systems (Guskiewicz *et al.*, 2001).

The somatosensory system provides important feedback to the CNS regarding a multitude of sensors, involving body sway, impact and contact with external objects, body positioning in space and the velocity of segments. It consists of numerous receptors and processing centres. The main process centres used for balance is proprioception and mechanoception. These process centres sense the relative position of connected parts of the body to one another and the pressure or distortion of body parts respectively (Fox, 2009). This allows the body to make uninterrupted automatic muscle adjustments to avoid falls and to keep the body stable. Considerable research has been conducted regarding the contribution each of the three sensory systems make towards human balance.

It is remarkable how the remaining senses adjust and compensate if one of the systems fail (Winter, 1995). The body can not fully compensate for lost or injured systems and a subject's balance will be impaired to some extent as a result. Assessment methods have therefore been developed to determine which sensory system has failed or is impaired along with methods to assess the extent of sensory damage (Guskiewicz *et al.*, 2001).

2.4 Balance Assessment Methods

Balance disorders can be evaluated at both functional and physiological level (Browne and O'Hare, 2001). *Functional assessments* are subjective tests conducted by medical practitioners. These functional tests normally involve the assessment of the reach and mobility of subjects. Functional balance assessment tests are quick to perform and can be conducted without the use or need for expensive equipment. These tests are successful in identifying the presence of balance disorders or disabilities and can detect gross changes in a person's balance. However, these tests only function as a screening tool to identify subjects in need of a more thorough evaluation. Functional tests can not differentiate between levels of impairment since they are unable to detect small objective changes in a subject's balance (Browne and O'Hare, 2001).

Physiological assessments, such as those involving the use of force plates, are capable of detecting small changes in a subject's ability to maintain balance. Physiological tests are therefore suitable for thorough evaluations and monitoring of the recovery processes (Browne and O'Hare, 2001). These assessments measure the contribution of sensory, motor and effector components under both static and dynamic conditions. This is done by measuring a subject's sway which is directly calculated from the movements of their COG (Browne and O'Hare, 2001). The COG is approximated from the movement of the COP (Winter, 2009).

Assessing a subject's balance with the use of a force plate has existed for several decades and is a commonly known field of study in posturography (Kapteyn *et al.*, 1983). The initial concept involved the monitoring of the sway movements of a subject which are unobservant with the naked eye. The use of a force plate equipped with strain gauges to measure certain forces and moments made it possible to capture these minute sway movements (Diener *et al.*, 1984). Posturography rapidly advanced with the improvement of computers and their computational abilities. Faster computers and more advanced equipment enabled continuous recordings with higher data densities and aided in the analysis of the recorded results. The higher accuracy and repeatability of these experiments in turn, enabled advances in measurement techniques. These advancements lead to dynamic tests which measure the subject's sway while moving the support platform (Nashner and Peters, 1990).

Currently there are only a few physiological balance assessment test instruments commercially available (Browne and O'Hare, 2001). These instruments include: the potentometric displacement transducer, mechanical ataxia meters, sway magnetometer, static force plates and dynamic force plates.

For *potentiometric displacement transducer* recordings, a subject is required to wear an aluminium pad around the waist with a fishing line connected from the waist pad to a displacement transducer. The displacement transducer records the subject's anterior-posterior sway exclusively under static ground conditions (Fernie and Holliday, 1978). The test provides information about anterior-posterior sway. This method loads the subject with a heavy pad around the waist and is therefore not recommended for the use by frail patients (Browne and O'Hare, 2001).

Mechanical ataxia meters comprise of a perforated wheel which is attached by a taut string to a subject's waist. The subject's anterior-posterior sway is assessed by recording the number of rotations of the perforated wheel (Wright, 1971). These meters are used to evaluate and identify subjects with a history of falls. The instrumentation is limited in that it can only measure balance in the anterior-posterior direction under static conditions (Wright, 1971). Ataxia

meters are commonly used by physiotherapy departments due to simplicity of their design.

A *sway magnetometer* measures the distance a subject sways, from the middle point, in both the anterior-posterior and mediolateral directions. This information is used to evaluate the subject's balance. The magnetometer sway distances are measured with two channels each consisting of one transmitter and one receiver coil. The transmitter in the first channel transmits a magnetic field which is picked up and measured by the receiver coil in channel two and vice-versa. This enables the two channels to be correlated, and by using the strength of the measured magnetic field the distance between them can be calculated (Dean *et al.*, 1986). The magnetometer measurement method is however not reliable as Elliott and Murray (1998) found that is has a test-retest reliability of less than 14 % for daily measurements.

Static force plates make use of force transducers to measure COP displacements of standing subjects while stationary (Murray *et al.*, 1975). These platforms are commercially available and can be used to evaluate elderly people with a history of falling. Subjects with balance disorders as a result of neurological damage and balance disorders caused by the ageing process are also evaluated with these platforms (Browne and O'Hare, 2001). Static force plates are used in both audiology and physiotherapy departments and have been found to have a test-retest reliability greater than $0,6$ % (Levine *et al.*, 1996; Benvenuti *et al.*, 1999).

Dynamic force plates make use of force transducers to record displacements of a subject's COP under dynamic conditions while a moor is used to displace the support surface of the force plate. This test method assesses the contribution of the somatosensory, the visual and the vestibular system (Furman, 1994; Ishida *et al.*, 1997; Redfern *et al.*, 2001). Dynamic force plates are used in the fields of physiotherapy and audiology. They are used to evaluate elderly people with a history of falls. Any subjects suffering from balance disorders as a result of neurological damage, but still having the ability to stand, can also be assessed. These machines have been found to have a test-retest reliability greater than $0,6$ % (Clark *et al.*, 1997; Liston and Brouwer, 1996). Browne and O'Hare (2001) report that the dynamic force plate is the most favourable balance measurement instrument as it provides information about several components of the postural control system under dynamic conditions whilst also detecting small changes in a subject's ability to balance.

2.5 Balance Metrics

Balance metrics are used to quantify or quantitatively express a subject's ability to maintain balance with the use of the measured results from the various balance assessment methods discussed. These metric factors aid in the assessment and documentation of rehabilitation treatments (Önell, 2000) and quantify the postural strategies used by subjects to maintain balance (Colobert *et al.*, 2006). The measured COP is a key parameter utilize to calculate the balance metrics. Various balancing factors have been formulated. However, for the purpose of this project, only the four relevant factors will be considered: SI, ES, PSI and Radius parameter.

The *Sway index* is an objective quantification of the sway movement of a subject during a balance test. It is mathematically expressed as the average rate at which a subject changes their COP in the anterior-posterior and mediolateral position (Botha, 2005). The SI is used for both static and dynamic balance assessments. Unstable subjects tend to have a higher SI as they sway more and for longer durations before reaching equilibrium when perturbed.

The *Equilibrium score* is used to give an indication of a subject's overall stability compared to the normative total sway of the average healthy human being. ES reflects the overall coordination of the visual, the proprioceptive and the vestibular systems used to maintain a standing posture (Chaudhry *et al.*, 2004, 2005). It is computed by comparing the subject's maximum anterior and posterior sway angle in the sagittal plane with the normative total sway angle of $12,5$ degrees. The ES is scored from zero to one hundred where 100 indicates perfect balance. If a subject falls during the test, they receive a score of zero. This assessment method is however not consistent as it is only uses the maximum sway angles and not the complete set of sway angles recorded during a test. Chaudhry *et al.* (2004) proposed a new factor, known as PSI, to overcome the ambiguities and shortcomings of ES.

Postural stability index quantifies the percentage ratio of the total stabilizing and destabilizing ankle torque due to gravity during a balance assessment. This quantification is based on the sway angle throughout the entire test duration and depends strongly on the subject's ankle torque, mass and height. The PSI score is also measured on a scale which ranges from 0 to 100. A subject's instability is reflected in how much the PSI score is less than 100. Compared to ES, PSI provides more relevant information regarding the subject's balance since it directly relates to the average sway angle and body parameters of the particular individual and not the normative values or assumptions. PSI is particularly useful for assessing a subject's balance before and after interventions (Chaudhry *et al.*, 2011).

The *Radius parameter* can be quantified as the radius of the smallest circle that encloses a subjects' total COP movement where the centre of the circle is at the average COP location (Botha, 2005). The Radius parameter provides an indication of the range of the subject's movement abilities and sway limitations. The Radius parameter solely can not be used to give an accurate description or indication of a subjects ability to balance. Mostly a combination of the factors are weighed against one another to give a true estimate of a subject's overall balance. A detailed description of how these parameters are calculated using force plate measured results are discussed in Chapter 4.

2.6 Balance of Seafarers

Ships operating at sea are manned by seafarers holding a variety of professions and ranks on board. These seafarers often spend months at sea exposed to extreme weather conditions and large swells. They are therefore constantly exposed to pitching and rolling motions in the environment in which they work and rest. In a recent discussion with captains from the South African Navy, many complained of knee and hip pain (Stokes T, 2012). They believe this is as a result of spending a life time (20 to 30 years) on-board ships. During heavy swells, the ship pitches and rolls, causing the body to experience gravitational forces in various directions. The body's centre of weight vector, therefore varies, causing the vertical ground reaction vector on the feet to fluctuate as well. This causes the loads on all the joints, and in particular the loads on the knee and hip joints that are used to maintain balance, to fluctuate between tension to compression forces depending on the frequency and size of the swell.

In 1999, research was done on the rough condition exposure of Olympic Yacht racing sailors. Mackie *et al.* (1999) attempted to quantify the physical demands on the sailors' knees and hips. The method was however only accurate if the sailor kept his feet equidistant on the hiking strap. Hiking straps are made from rope or webbing and is used to hold the sailors feet down when leaning upwind to decrease the extent of the boat's lean away from the wind. Aagaard *et al.* (1997) conducted a similar study to investigate the peak moments about the knee by measuring knee extension and flexion movement during sailing. Both studies found that the physical demand on the knees is particularly substantial and that the applied forces are marginally close to a sailor's predicted maximal voluntary contractions.

A scientific hypothesis posed by Fischer and Dickerson (2012), used psychophysical load estimation as a method to establish capacity threshold guidelines for physical task demands and their acceptable physical forces. Excessive or abnormal loading across the lower extremity joints has been linked to the progression of osteoarthritis (OA) and musculoskeletal injuries (Haight, 2012).

Research done by Ratzlaff *et al.* (2012) suggests that certain levels of lifelong knee and hip joint forces can aggregate or increase the risk factor for developing OA. OA causes stiffness and chronic pain due to changes in the bone underneath the cartilage (Felson, 2004). It is a degenerative joint disease and can be characterized by chronic degradation of hyaline articular cartilage (Haight, 2012). The application and release of the high levels of compression forces on the cartilage may require a prolonged duration for proteoglycan synthesis rates to return, which can alternatively lead to cartilage cell death (Guilak and Hung, 2005). Cartilage is a living tissue, and therefore the threshold at which it fails, either from fatigue or excessive stress levels, is dependent on the prevalent stress arising in a joint (Seedhom, 2006).

Although navigation on large vessels does not demand the same physical activities as sailing a yacht, the seafarers are still exposed to rough sea conditions, often for much longer durations. To the knowledge of the author, no research has been conducted aboard large vessels to measure the ground reaction forces which a seafarer's body experiences while at sea. These measurements can indicate how a person's ability to balance is affected during rough seas and further show what these forces potentially contribute to knee and hip injuries.

2.7 Human Single and Double Inverted Pendulum Models

Model trajectory estimation of body links and COM movement is a practical means of gaining quantitative information on basic parameters of postural sway (Winter, 2009). The COM can either be directly measured or calculated. Numerous methods such as: videographic imagery, optoelectronic sensors, electromyography and skin mounted markers are used to directly measure kinematic movements of the body. However, Colobert *et al.* (2006) state that these direct kinematic measurement methods are time consuming and require expensive equipment which are not suited for routine clinical use. An alternative method is to calculate the position of the COM based on human body simulations. The body can either be simulated as a single or double inverted pendulum model. Force plate readings, human anthropometric data and these simulated models can then be used to calculate the trajectory of body links.

The trajectory of the simulated body links are used to estimate the COM location of the body. These simulations further offer insight into the functional behaviour and motor feedback units needed in the stabilization of the body. Studies conducted by Colobert *et al.* (2006) and Browne and O'Hare (2001) showed that force plate measurements is the most favourable method used to

determine COM since these machines consume less set-up space. Force plate tests are conducted much quicker since they do not require any additional attachments to the body such as skin mounts. Compared to various kinematic measurement equipment, force plates are cheaper and more user friendly.

Force plates record forces and moments in the X, Y and Z axes as it is discussed in Chapter 3. The measured forces and moments can be used to calculate the COP location. A few methods and hypotheses exist to determine the COM location using the calculated COP. A force plate can however not directly measure the COM movement of the body. Karlsson and Lanshammar (1997) developed a SIP model to predict the position of the COM by using force plate data. Their model did not incorporate shear components of the ground reaction force and are only suited for static balance assessments. Ji *et al.* (2004), Botha (2005) and Levin and Mizrahi (1996) improved Karlsson and Lanshammar (1997) model by including the shear component of the ground reaction force mathematical model used to calculate the position of the COM. Neither of these papers, Ji *et al.* (2004), Botha (2005) and Levin and Mizrahi (1996), states how accurately these improved models predict the COM to the true body COM.

Winter (2009) formulated an equation which predicts the COM from the COP in the sagittal plane. His method assumes the body sways about the ankles and requires both the height and body weight to compute the moment of inertia of the body about the ankles. The SIP model developed by Winter (2009) is comprised of relatively simple and robust equations. The SIP model formulas are however only applicable if a subject behaves with similar characteristics as a SIP thereby only makes use of ankle strategy to balance. Colobert *et al.* (2006) and Gatev *et al.* (1999) states that standing subjects typically make use of both ankle and hip joint motions to control their balance. Therefore, a two link model incorporating ankle and hip strategies is a more appropriate model to simulate body link movements.

Colobert *et al.* (2006) developed a two dimensional DIP model which uses force plate data as well as anthropometric data, such as the subject's height and weight to calculate the body link locations and COM. Colobert *et al.* (2006) claim that their computational algorithm can be used as a routine clinical protocol to evaluate the postural strategy which a subject uses to maintain balance. In Colobert *et al.* (2006), the body movements and angles computed with the DIP model computational algorithm is compared to videographic results. The maximum root mean square (RMS) error between the DIP model and videographic results differed by 7,9 %. This is reasonably accurate considering the simplicity of the method used. The application methods can easily be used in real-time evaluations of a patient's state. Colobert *et al.* (2006) only tested and compared the results of four subjects. This is a concern which

brings the viability of the computational algorithm into question. A thorough comparative evaluation is recommended involving more subjects to prove the validity of the method.

2.8 Conclusions

The evaluation of human balance is important in diagnosing and treating balance disorders and monitoring rehabilitation recovery (Botha, 2005). Balance disorders can occur from a wide variety of factors. These disorders can lead to the tendency to fall, resulting in serious injuries, suppression of activities, a loss of independence and even death (Schaafsma *et al.*, 2003). It is therefore critical to identify subjects with balance disorders in order to prevent balance-related accidents from occurring.

Two distinct methods exist to identify balance disorders: functional and physiological assessments. Functional assessments are subjective, can be inaccurate as a result of human error and are unable to detect slight impairments in a subject's balance capabilities. The use of physiological assessments, which is less prone to human error is therefore a necessity. Various physiological assessment methods have been developed. These assessment methods however require tedious time to set up, are problematic to operate and are not suited for routine clinical use. This research aims to develop a machine, based on Botha's (2005) thesis, capable of conducting a physiological balance assessment which requires no set up time, is easily operated and still produce accurate results.

Chapter 3

DORSIFLEXOMETER STRUCTURE DESIGN

The function of the machine is to measure and assess a subjects' ability to maintain balance during both static and dynamic conditions using a force platform. Since there are very few machines with similar capabilities commercially available, the specific engineering requirements were difficult to define due to the lack of procedural information. This chapter discusses the user requirements, followed by the engineering specification of the machine. A short description is provided of the structure of the machine and the measurement equipment that is used to determine the ground reaction forces of a subject. Further, the two methods of rotating the platform, which the subject stands on, are discussed. The rationale behind the selection of a platform rotation method is discussed. The chapter concludes with a short description of the structure of the machine and its operating procedure.

3.1 User Specifications and Requirements

The research and machine design is a continuation of Botha's (2005) work on the development of the Dorsiflexometer. Botha designed, built and patented the first Dorsiflexometer in 2005 as part of his thesis project. However, this machine was not ready to be mass produced or commercially sold, since it was still in its early engineering development and testing phase. After Botha completed his thesis the Dorsiflexometer research came to an end. The Mechanical and Mechatronic Engineering Department disposed of the Dorsiflexometer machine since the equipment and software became outdated and were no longer in use. In 2011, Edmayr (2011) reopened the Dorsiflexometer research for his final year project. Edmayr attempted to redesign the Dorsiflexometer. A single force plate replaced the two load-cells which was originally used in Botha's design. When the author started with the project, only the Dorsiflexometer which was built by Edmayr along with Edmayr's final report and Botha's

thesis were available. The Dorsiflexometer which was built by Edmayr was however, not in a working condition due to the following problems: the platform was positioned above the point of its rotation causing it to be unstable, the platform could further not rotate due to a misalignment of the gears and no working software was available to operate the machine.

This thesis aims to redesign and improve the Dorsiflexometer machine using the existing theories and primary measurement techniques as developed by Botha and Edmayr. The requirements were mainly adapted from recommendations proposed by Botha (2005). The main requirements include:

- The machine structure must be stable, rigid and have a hand railing for support as it will be used by patients with balance disorders who are unstable on their feet.
- The machine must assess static as well as dynamic balance as a result of dorsiflexion and plantar flexion in the sagittal plane.
- A single platform must be used to measure the resultant reaction forces of the subjects.
- The platform must hang such that it rotates about the ankle of an average human being.
- The machine must be operated from a laptop computer interface and the output of results is required to be in digital format.
- The machine must be capable of conducting a balance assessment test in less than 90 seconds.
- Testing should be conducted allowing for easy repeatability.
- The design of the machine must be based on the original design by Botha (2005).

3.2 Engineering Specifications

The user requirements and current balance assessment methods were used to compile the engineering specifications. The specifications for the improved Dorsiflexometer is summarised in the following section.

The improved machine must be capable of performing a single assessment test on a subject weighing up to 120 kg in less than 90 seconds. Furthermore, the machine should have a support railing which subjects can grab hold of in case they lose balance while undergoing a balance assessment on the machine. The platform must be capable of being rotated 15 degrees to either side from

its static position in the sagittal plane. This enforces both dorsiflexion and plantar flexion of the ankle as shown in Figure 3.1. For safety reasons, the platform's rotational speed may not exceed $0,008$ rad/s and must have an emergency stop button to instantly freeze the platform. The platform must rotate about an axis corresponding to the average person's ankles. The average person is $1,7$ meters tall (Zinke-Allmang, 2008) and has an ankle to ground length of $0,039$ times the total body height as indicated by the anthropometry body model in Section 5.2. The platform radius of rotation should therefore be $0,066$ meters.

Figure 3.1 Dorsiflexion and plantar flexion of the ankle in the sagittal plane.

3.3 Mechanics of the Improved Dorsiflexometer

The structure of the Dorsiflexometer was redesigned and built according to the engineering specifications discussed. This section describes the hardware of the Dorsiflexometer and the design of the machine's structure. Two new structural designs to oscillate the platform were built and tested. The first design makes use of spur gears to oscillate the platform. The second design incorporates a linear actuator and actuator arm to oscillate the platform which the subject stands on. The section concludes with a discussion as to why the second design was selected.

3.3.1 Force plate measurement system

The Dorsiflexometer makes use of a force plate to measure the ground reaction forces of a subject. These forces are used to quantify a subject's ability to balance. This section describes the force plate measurement system which consists of a force platform, an amplifier and a laptop computer as shown in the system layout diagram in Figure 3.2.

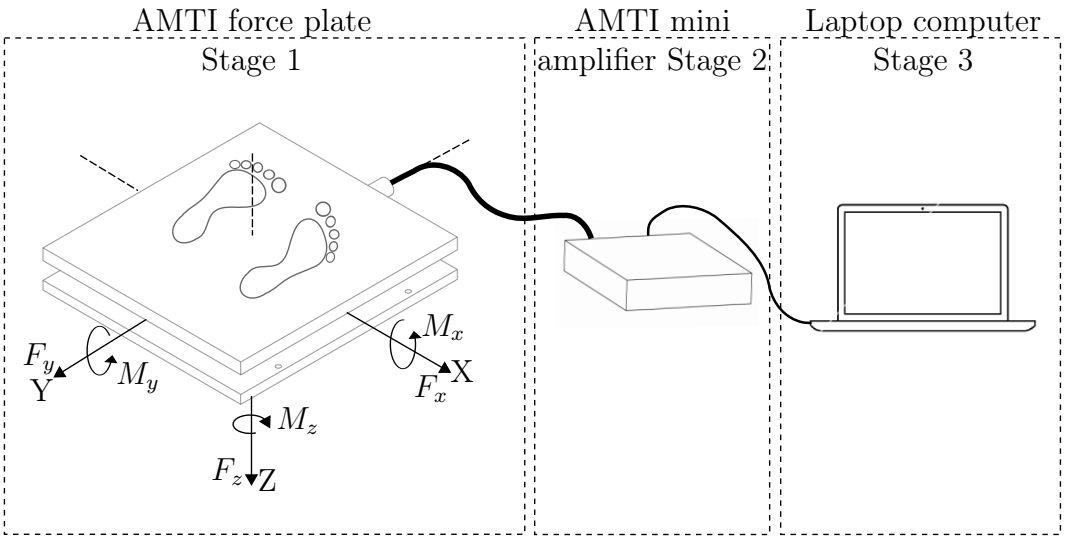

Figure 3.2 Force plate measurement system consisting of a AMTI force plate, AMTI mini amplifier and a laptop computer.

Stage 1, which consists of the force plate, measures any forces and moments within a measurable range applied to its surface area. The Advanced Mechanical Technology Incorporation's (AMTI's) force platform (OR6-7-1000 (Incorporation, 2010)) measures three forces and three moments along the X, Y and Z axes as presented in Figure 3.2. These forces and moments are measured using four strain gages which are attached to proprietary load cells near the four corners of the platform. Furthermore, six Wheatstone bridges with four active arms, are formed with the gauges. Each bridge consists of eight or more gauges. This ensures that any forces and moments that are applied to the force plate are measured within a fraction of a millimetre, typically less than $0,2$ mm (Incorporation, 2010).

In stage 2, the signals measured by the force plate are sent as analogue voltages to the amplifier. The amplifier is a AMTI MSA-6 MiniAmp Strain Gage Amplifier (Incorporation, 2010) which amplifies the signal from the force plate and converts it from analogue to digital format. For more information regarding the AMTI force plate and amplifier refer to Appendix A.

In the third stage, this digital signal is transmitted to the computer where it is interpreted as binary data. This binary data is corrected and calibrated by the computer software. The signal is corrected and multiplied by a calibration value in order to directly relate the actual physical force plate measured quantities to the interpreted results. The signal correction and calibration is discussed in Chapter 6.

The results are displayed on the computer in such a way that it can be interpreted by a medical practitioner. Any information on the subject is stored to the computer and can be accessed at any time. The results can also be printed out.

3.3.2 Structure of the Dorsiflexometer

Since there were no specifications provided about the machine weight or material to be used, it was decided to manufacture the machine using steel plates and pipes. Steel is conveniently available, inexpensive, strong, easily bent and welded into the desired shape. Furthermore, it has enough structural strength to support the weight of a patient and still maintain its rigidity. In this section the structural design of the Dorsiflexometer is described.

The structure of the Dorsiflexometer refers to the load-bearing frame of the machine, which comprises of five parts: a base plate, supporting struts, an oscillating platform, bearings and a support railing. The structure is shown in Figure 3.3. The manufacturing and assembly drawings are presented in Appendix B.

The base plate was laser cut from 5 mm thick steel plate. It acts as the foundation of the structure which mostly everything is mounted onto. The four supporting struts were laser cut from 10 mm thick steel plate and bent to the desired shape. The struts raises the platform for two reasons: The platform was firstly raised such that it hangs and rotates around an axis which is at the same level as the ankle joint of a standing subject. Secondly, the platform was raised to ensure that there was adequate space for the platform rotation mechanism and sufficient storage space for the force plate measurement equipment. The struts further ensure platform stability and ample strength to support the weight of test subjects.

The oscillating platform consists of two side brackets and a plate. The platform oscillates back and forth to force plantar and dorsiflexion movement of the subject's ankle. The mechanisms that are used to oscillate the platform are secured to the bottom of the platform. The force plate is bolted to the top of the platform. Two bearings are used to hang the platform from the supporting struts. These bearings were used to ensure smooth oscillation of the platform and to support the weight of the force plate and subjects.

A support railing, made from stainless steel pipe, encloses the sides of the machine. The railing acts as a support system for the subject to grab hold of in the case of a loss of balance or to be used as support when climbing onto the raised force plate. The stainless steel railings are strong enough to support the weight of a subject and furthermore create an appealing aesthetic.

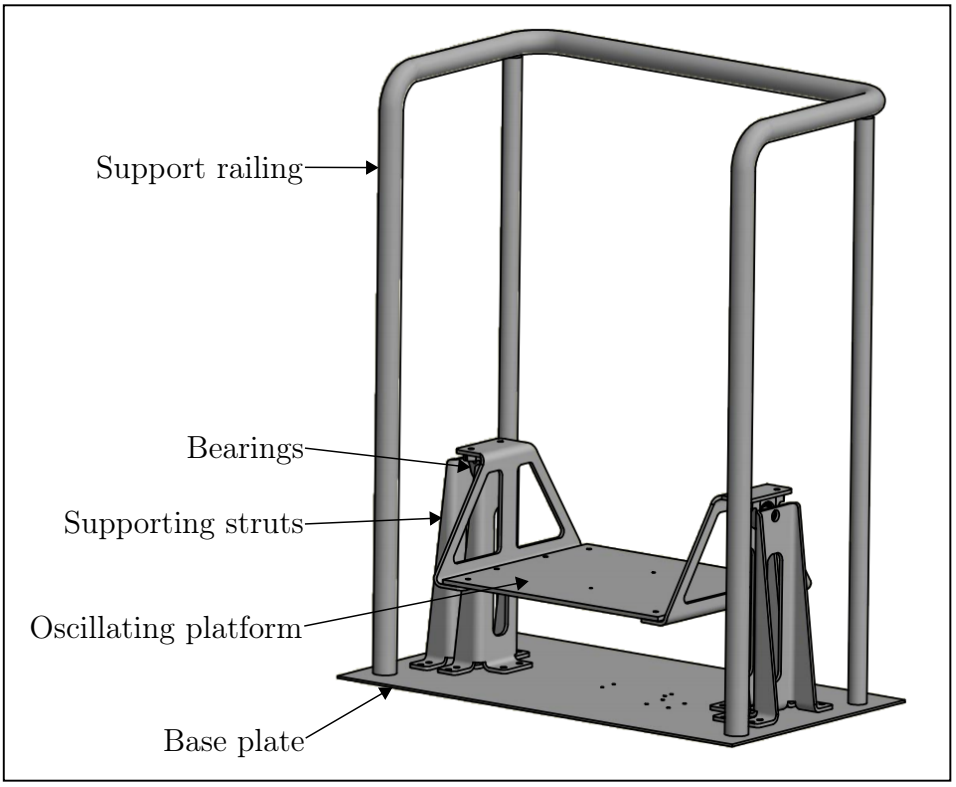

Figure 3.3 Skeleton structure of the Dorsiflexometer.

3.3.3 Design phase 1: platform oscillation using gears

This section describes the selection process and calculations that was used to specify the appropriate spur gear sets and motor to oscillate the platform. Figure 3.4 shows the iterative loop of actions that were followed to select the gear sets and motor.

The first step was to determine the forces which the gears and motor must be capable of withstanding. As an engineering specification, the machine must be able to assess subjects weighing up to 120 kg. The maximum torque (τ_0) exerted on the gears will occur as a subject steps onto the tip of the platform as shown in Figure 3.5. Equation 3.3.1 shows that a subject weighing 120 kg will therefore exert a maximum torque of 442 N·m about point O, the rotation point of the platform.

$$\tau_0 = m_1 g L_1 SF \tag{3.3.1}$$

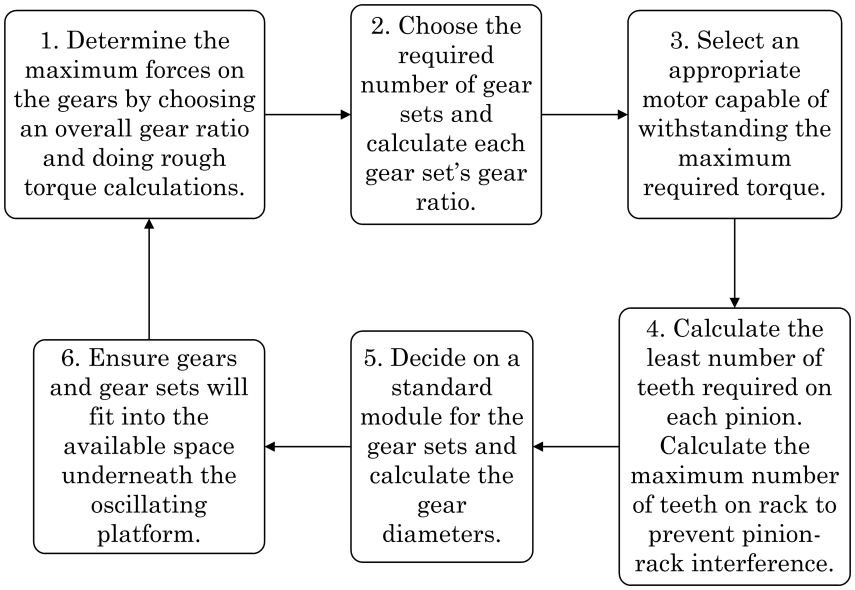

Figure 3.4 Design steps for the gear selection procedure.

The mass of the subject is represented by m_1, the gravitational acceleration by g and the length parallel with the applied force, which is equal to $0,25$ m, by L_1. A safety factor (SF) of $1,5$ was included in the calculation. It was assumed, as a rough estimate, that the torque reduction is calculated in the same way and therefore equal to the overall gear ratio (e) as shown in Equation 3.3.2. The rotational speed of the first and final gears are indicated as n_F and n_L respectively. The torque on the final gear is represented by τ_F.

$$e = \frac{n_L}{n_F} \approx \frac{\tau_0}{\tau_F} \tag{3.3.2}$$

Since the tests must be conducted in a slow, accurate and repeatable manner, a stepper motor was used instead of a direct current motor. The stepper motor used, is a Nema 34 which has a holding torque of $7,7$ N·m. This stepper motor was one of three options: the Nema 23, Nema 34 or Nema 42. The holding torque of the Nema 23 is too little and the shear size of the Nema 42 is too great to fit into the available space underneath the platform and therefore these motors were not used. The Nema 34 fits into the available space and has adequate torque to oscillate the platform with a subject on it. Refer to Appendix A for more information regarding the stepper motor specifications. Using Equation 3.3.2, a gear ratio of 45:1 is required. A guideline by Budynas (2008) recommends the use of a two stage compound gear for this particular gearbox as the overall gear ratio is greater than 10:1 but less than 100:1.

A two stage compound gear consisting of two gear sets comprised of two gears each was used. The four gears and their positions are indicated in Figure 3.5. Gear 1 must rotate about point O, and therefore, as shown in Figure 3.5

The maximum number of teeth (N_G) on the largest gear which would operate interference-free with the smallest pinion can be calculated with the use of Equation 3.3.5 (Budynas, 2008).

$$N_G = \frac{N_p^2 \sin^2(\phi_p) - 4k^2}{4k - 2N_p \sin^2(\phi_p)} \tag{3.3.5}$$

Each gear sets' module (m_{mod}) was calculated using Equation 3.3.6. The minimum teeth of the smallest gear and gear pitch diameters (d in mm) which would fit into the available space, as shown in Figure 3.5, were used to calculate the modules.

$$m_{mod} = \frac{d}{N} \tag{3.3.6}$$

A desirable module of 4 mm for gear set one and $1,25$ mm for gear set two was selected. With these standard modules, the diameter of each gear was calculated. The final values of each gear is shown in Table 3.1. Gear set one has a gear ratio of 10:1 and gear set two a gear ratio of 4,5:1. The gears were manufactured by CVC Gear Corporation in Paarl.

Table 3.1 Gear and gear set specifications.

	Gear 1	Gear 2	Gear 3	Gear 4
Number of teeth on gear	170	17	72	16
Facewidth (mm)	15	15	15	15
Module (mm)	4	4	1,5	1,5
Pressure angle (deg)	20	20	20	20
Helix angle (deg)	0	0	0	0
Gear set centre distance (mm)		374		55

3.3.4 Design phase 2: platform oscillation using linear actuator

The second design option was to oscillate the platform using a linear actuator. This section describes the design phase of a custom linear actuator, which is used to oscillate the platform of the Dorsiflexometer. The design process for the linear actuator involves an iterative loop of calculations, that can be summed up in 6 steps. Figure 3.6 shows the 6 steps that were used to design the actuator.

The linear actuator is mounted to the base plate. The platform can be oscillated using a lever arm connected from the linear actuator to the platform as shown in Figure 3.7. Prefabricated linear actuators are expensive

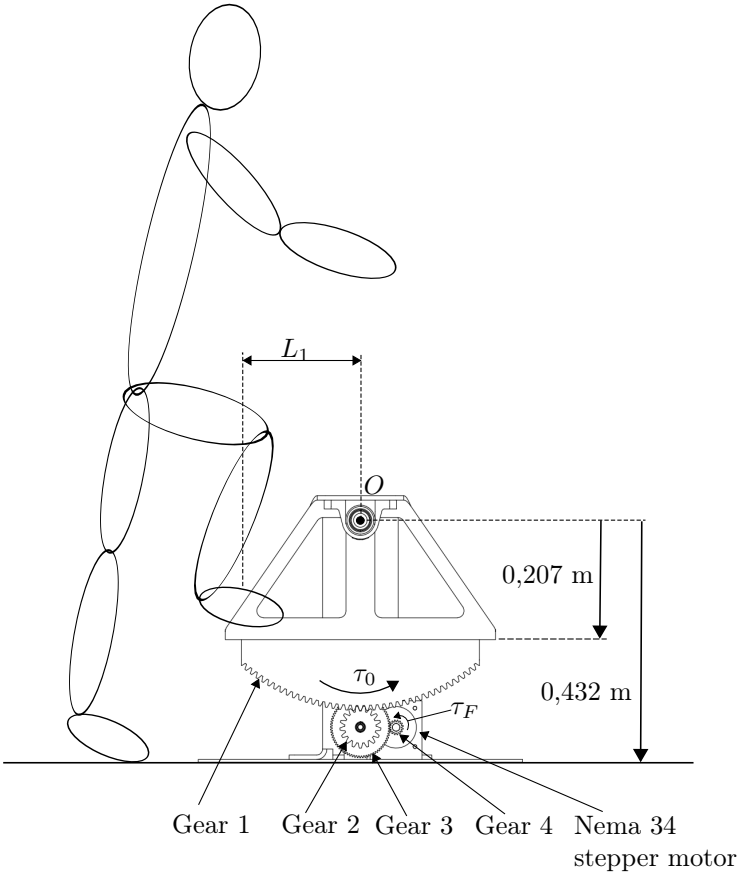

Figure 3.5 Subject stepping onto platform which is rotated using two gear sets.

its diameter must be greater than $0,414$ m but less than $0,864$ m to fit in the available space. It was beneficial to make the gear ratio of gear set one as large as possible since gear 1 had to be more then four times the diameter of the rest of the gears. A gear ratio of 10:1 was chosen for the first gear set consisting of gears 1 and 2. Using Equation 3.3.3, gear set two would require a gear ratio greater then 4,5:1 for the overall gear ratio to be 45:1. The gear ratios of gear sets one and two are indicated as e_1 and e_2 respectively (Budynas, 2008). The number of teeth on each gear is represented by N.

$$e = \frac{N_1}{N_2}\frac{N_3}{N_4} = e_1 e_2 \tag{3.3.3}$$

To eliminate gear interference from occurring, the least number of teeth for each gear set's pinion was calculated using Equation 3.3.4 (Budynas, 2008). The smallest number of stub-depth teeth ($k = 0.8$) on the pinion is represented by N_p, where ϕ_p is the pressure angle which is cut at a standard of 20 degrees.

$$N_p = \frac{2k}{(1+2e)\sin^2(\phi_p)}(e + \sqrt{e^2 + (1+2e)\sin^2(\phi_p)}) \tag{3.3.4}$$

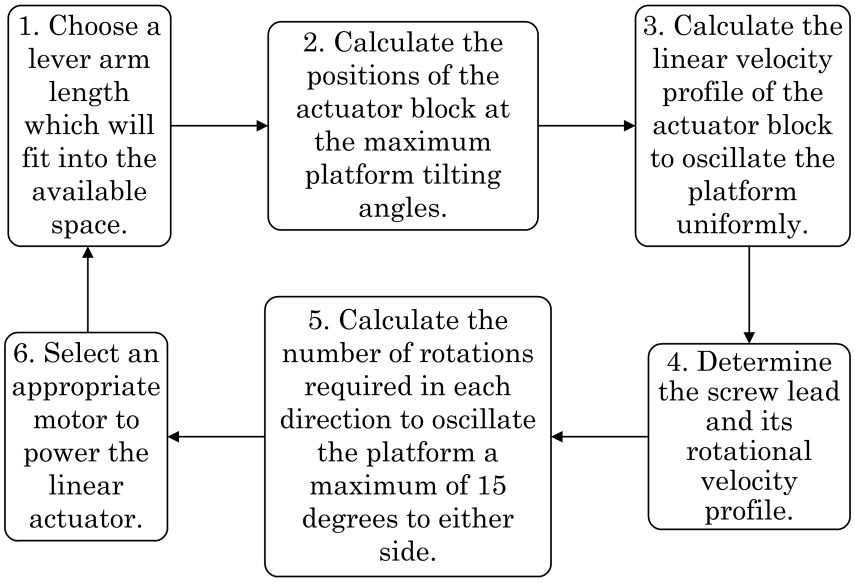

Figure 3.6 Linear actuator design procedure.

($\pm$ R18 000), therefore due to budget limitations, it was decided to design and have a custom linear actuator manufactured by the mechanical workshop at the Department of Mechanical and Mechatronic Engineering of Stellenbosch University. Firstly, the length of the lever arm (l) was chosen. The lever arm link BC with a design length of $0,195$ m connects the linear actuator with the existing platform. The lever arm is used to oscillate the platform around point O by pushing or pulling the platform back and forth as the linear actuator block (part C) slides from side to side.

With the help of the geometry sketch of the machine structure as shown in Figure 3.7, Equations 3.3.7 and 3.3.8 were set up, which relate the position of the actuator block to the tilt angle (ϕ) of the platform. The actuator block displacement along the global X axis is represented by x, θ is the angle of the lever arm and ϕ the angle of the platform from the horizontal X axis. The vertical distance from the point of rotation to the actuator block is equal to $0,4$ m and represented by z. The radius around which the platform is being oscillated is equal to $0,303$ m and represented by r. When the platform is exactly level with the ground, $\phi = 61,4°$ and $\theta = 43°$.

$$z = r\sin\phi + l\sin\theta \tag{3.3.7}$$

$$x = r\cos\phi - l\cos\theta \tag{3.3.8}$$

These two equations can be solved simultaneously to give the actuator block position at any given platform angle. Equation 3.3.9 shows the two equations solved simultaneously and expressed in terms of ϕ. This equation was used to

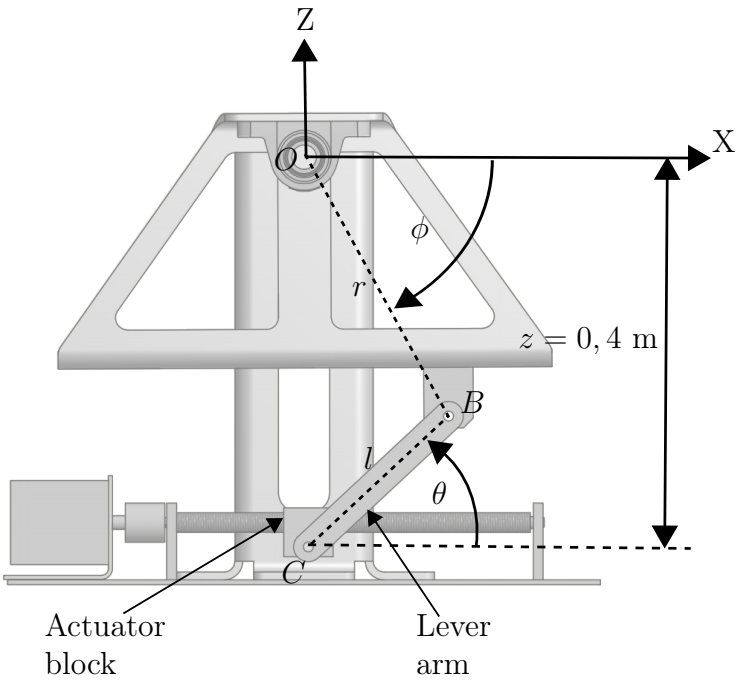

Figure 3.7 The geometry of the platform which is oscillated with the use of a linear actuator.

determine the outermost positions of the actuator block when the platform is tilted to a maximum of 15 degrees to either side from its starting position, as shown in Figure 3.8. The actuator block positions at the start and at both outermost points (A and B) were calculated to ensure that the selected lever arm would fit into the available space underneath the platform. Additionally this analysis provide the required length and reach of the linear actuator.

$$x = r\cos\phi - l\cos\left(\arcsin\left(\frac{z - r\sin\phi}{l}\right)\right) \tag{3.3.9}$$

Figure 3.8 shows the outline of the platform tilted to either side, x_{min} and x_{max} were calculated to be $-0,093$ m and $0,133$ m respectively. The linear velocity equation of the actuator block is formulated by differentiating Equation 3.3.9 with respect to time.

$$\dot{x} = -r\dot{\phi}\sin\phi - \frac{\dot{\phi}r\cos\phi(z - r\sin\phi)}{l\sqrt{1 - \dfrac{(z - r\sin\phi)^2}{l^2}}} \tag{3.3.10}$$

Equation 3.3.10 shows the linear velocity of the actuator block. The linear velocity of the actuator block has to be adjusted according to its relative position since the platform has to oscillate at a constant angular velocity ($\dot{\theta}$) of $0,008$ rad/s.

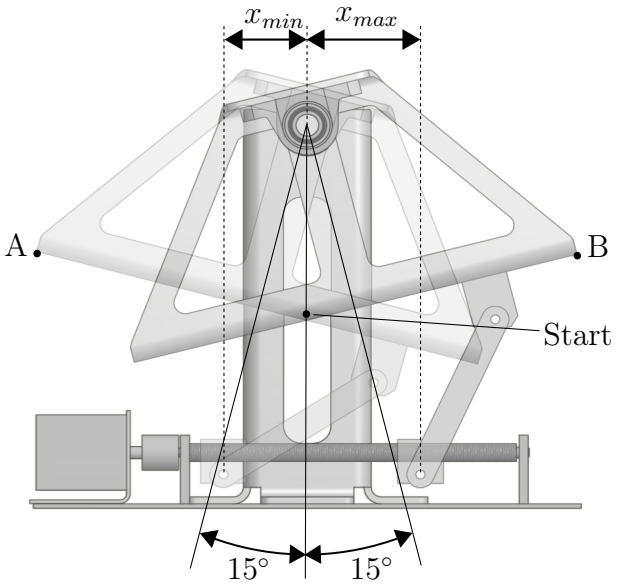

Figure 3.8 Linear actuator tilting to the extremity points on either side.

Using the newly acquired linear velocity equation of the actuator block, a maximum linear velocity of $0,006$ m/s is required to rotate the platform at $0,008$ rad/s. This velocity is used to calculate the required pitch and rotation speed for the linear actuator screw. For a single lead screw, one revolution causes a linear displacement equal to one pitch length. Furthermore, one revolution per second will result in a linear velocity of one pitch length per second as shown in Equation 3.3.11.

$$1\ revolution/second = 1\ pitch\ length/second \tag{3.3.11}$$

A M20 single lead screw with a pitch length of $2,5$ mm was selected. A Nema 34 stepper motor is used to drive the linear actuator, which in turn oscillates the platform. A general purpose coupling was used to connect the stepper motor to the linear actuator. The linear actuator screw acts as a self braking mechanism. The stepper motor was programmed to rotate according to the velocity profile as shown in Figure 3.9. For each test, the platform first rotates forward from 0 degrees (start) to 15 degrees (point A), then backwards to a position of -15 degrees (point B), and then forwards with 15 degrees to end up at the starting position of 0 degrees. Therefore, the motor rotates 54 revolutions clockwise, pauses for a second, rotates $90,4$ revolutions anticlockwise, pauses for another second, and then rotates $36,4$ revolutions clockwise to its starting position. Refer to Appendix C for the torque calculations of the linear actuator.

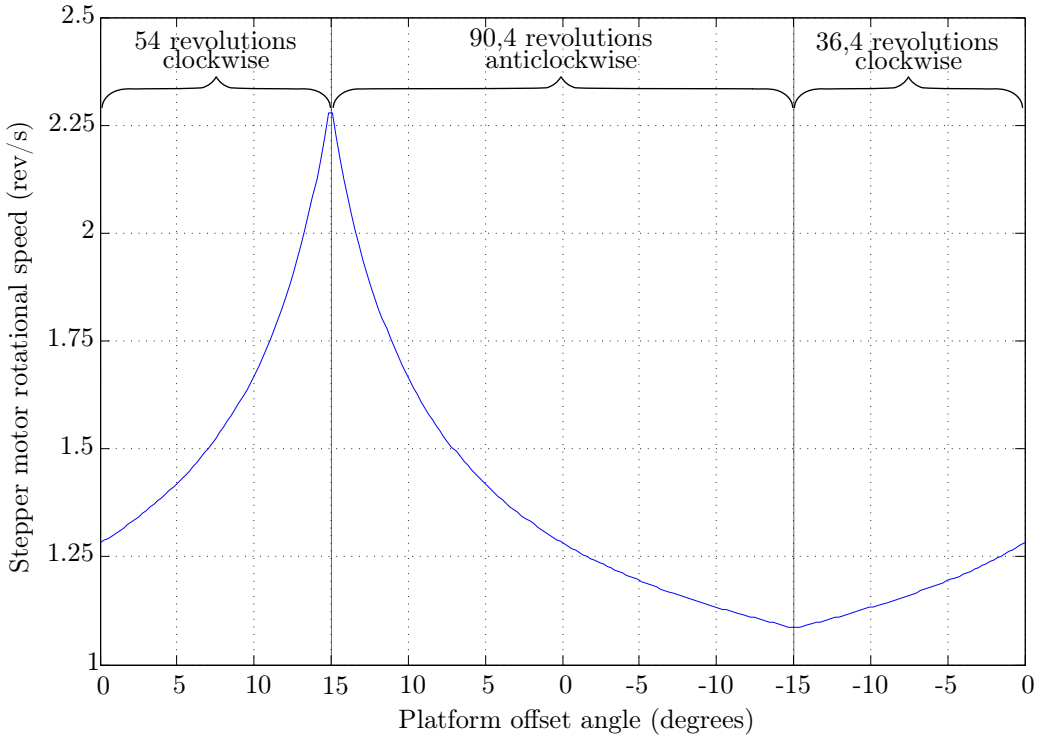

Figure 3.9 Stepper motor rotational speed relative to the platform offset angle.

3.3.5 Design selection

In order for the machine to conduct a dynamic balance assessment test, the platform that the subject stands on has to be oscillated back and forth. Two methods to oscillate the platform using a Nema 34 stepper motor was conceptualised, built and tested. This section describes why design phase 2 is used in the Dorsiflexometer instead of design phase 1.

The first design method uses two gear sets, each consisting of two spur gears to rotate the platform. After the machine and gear sets were assembled, it was found that the gear sets had an unusual amount of play or backlash between meshing gears. Upon further investigation, it was found that the gears were poorly manufactured. It was visible that not all the teeth on certain gears had the same working depth. The largest gear, gear 1, was straight cut and did not have a curved face or flank on the gear teeth profile. This caused the gears to have interference and backlash, which resulted in a non-smooth platform oscillation with extensive frequency vibration and noise.

The second design method uses a custom linear actuator driven by the stepper motor to oscillate the platform. There is much less noise and vibration compared to the oscillating gear design. The small amount of vibration caused by the stepper motor is not detectable by the feet and does not influence the readings of the force plate as it oscillates. Rotation of the platform with the use

of the linear actuator runs noticeably smoother than the first design method. The second design method was therefore selected as the desired method to oscillate the platform. Figure 3.10 presents the final design assembly of the complete Dorsiflexometer.

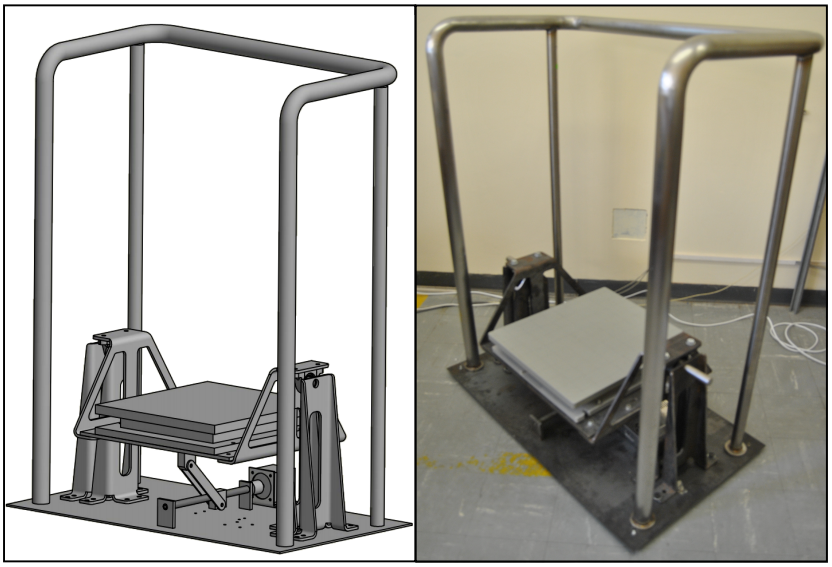

Figure 3.10 Final structure of the Dorsiflexometer.

3.4 Conclusion

The Dorsiflexometer structure is constructed from stainless steel pipe and steel plate to ensure its rigidity and stability. It features a linear actuator driven by a Nema 34 stepper motor which is used to oscillate the platform back and forth. An AMTI force plate and MiniAmp amplifier is used to measure the ground reaction forces of the subjects, which are converted to a digital signal and calibrated by a laptop computer. The machine is further able to assess the balance performance of subjects weighing up to 120 kg and can complete an assessment in less than one and a half minutes.

Chapter 4

USER-INTERFACE

A computer software interface was developed to enable the operation of the machine from a computer. By computerising the machine operation the opportunity for human error and subjectivity is minimised. It further assures that all tests are conducted in a repeatable manner. This chapter discusses the development of the user interface and provides guidance on how the program should be used by the operator. In the text, the person being tested is referred to as the subject or the patient, and the person operating the machine is referred to as the operator. The operator controls the test from the computer and inputs the commands while the subject is required to follow the operator's commands.

4.1 Program User Interface and Instructions

The software program acts as an interface through which the operator can control the machine. The intent of the software design was to be as user friendly as possible. The program simplifies the measurement procedure such that the machine can be operated by medical personnel with minimum training required. However, the interpretation of the measured results would require the skill of a qualified medical practitioner. The program consists of numerous graphical user interfaces (GUI's) and sub-functions. The GUI's appear as menues with click-buttons and commands and requires inputs from the operator. The sub-functions are algorithms which are not visible to the operator. These functions execute the operator's commands in the background.

The diagram in Figure 4.1 explains the interaction of the GUI's during the test process. It also shows what sub-functions are executed in the background of the GUI's. The remainder of this chapter discusses the logic of the test algorithm. The importance and sequence of the GUI's is discussed followed by an in-depth description of each sub-function's purpose and how these are executed from commands from the GUI's.

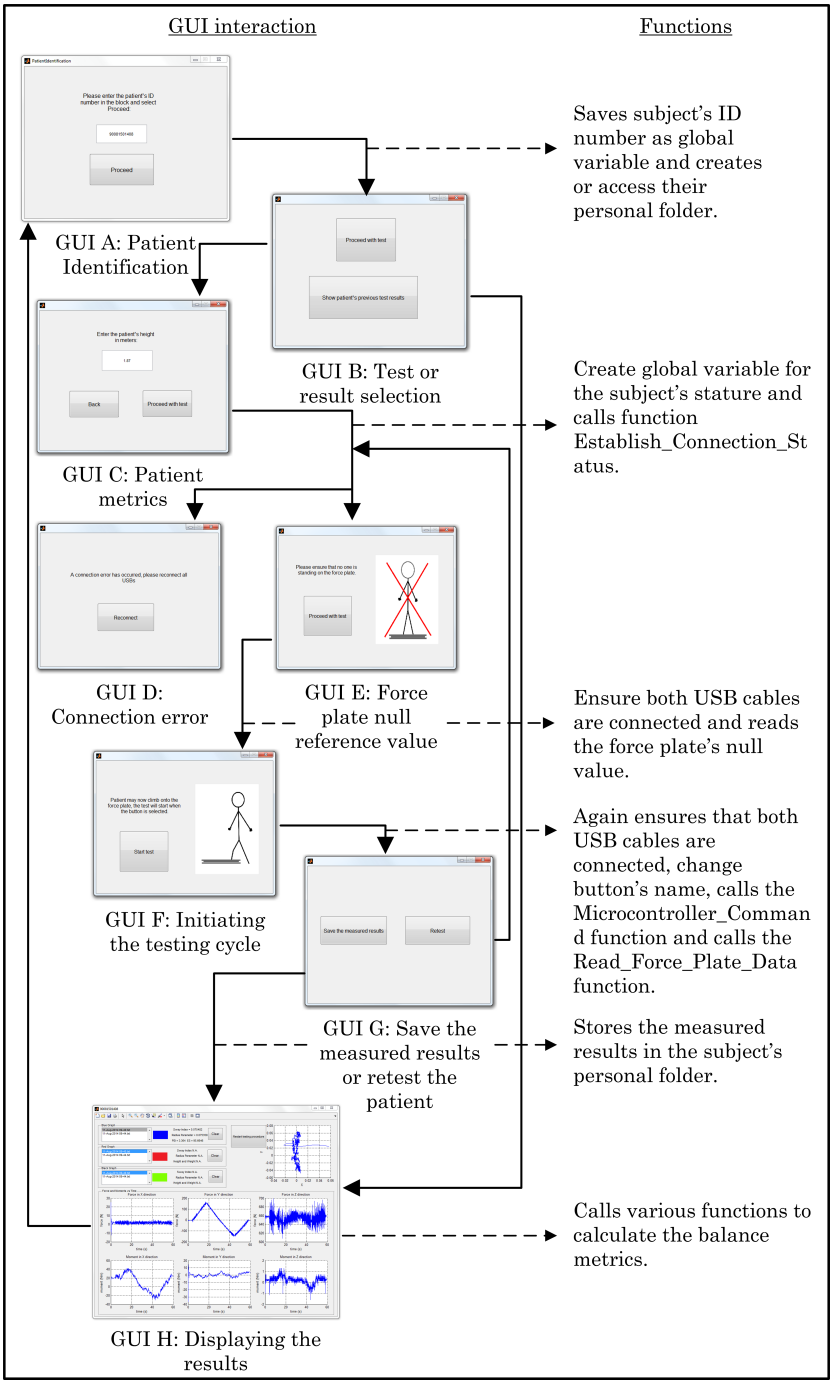

Figure 4.1 GUI interaction diagram.

The software program was written in an educational version of MATLAB. The program makes use of GUI's to gather relevant information about the subject, to retrieve the operator's commands and to display the measured results in a manner interpretable by a doctor. GUI's ensure that the operator does not have to create a script or type a command in the command line to

accomplish tasks. To conduct a balance assessment test the operator simply has to follow the step-by-step instructions provided by the GUI's and select the 'proceed' and 'test' buttons. Before the program is opened, the operator must first ensure that both universal serial bus (USB) cables are connected to the computer.

GUI A: Patient Identification opens at the start of the program, as shown in Figure 4.2. GUI A consists of a button, a text box and some static text. The static text and the text on the button prompts the operator what inputs are required. For this particular GUI, the static text prompts the operator to enter the subject's Identification (ID) number in the text box. The text box is used to retrieve and store the subject's ID number. It was decided to enter an ID number as this allows easy and unique identification of subjects. Each subject has their own ID number which makes it easy to keep a record of the test results. The button, 'Proceed', can be selected after the operator has entered the subject's ID number. Upon selecting the proceed button, GUI A will close and GUI B will open. The subject's ID number is stored as a global variable which is eventually used to create a single folder containing all the test information of the subject.

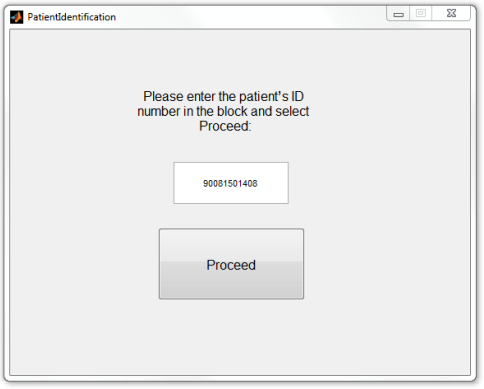

Figure 4.2 GUI A: Patient identification.

GUI B: Test or result selection, shown in Figure 4.3, provides the operator with two options: the operator can either proceed to view previously tested results by selecting the 'Show patient's previous test results' button or proceed with the current test by selecting the 'Proceed with test' button. If the operator selects the 'Show patient's previous test results' option, GUI B will close and GUI G displaying the subject's previous test results will open. Note that no results will be displayed if the subject has not been tested on the system before. However, if the operator decides to continue with the testing procedure by selecting the 'Proceed with test' button, GUI B, will close and GUI C will open.

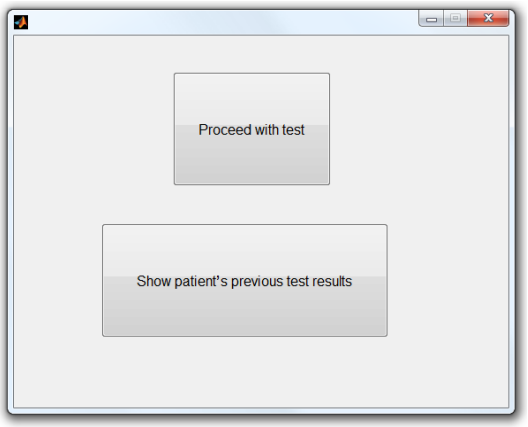

Figure 4.3 GUI B: Test or result selection.

GUI C: Patient metrics window is shown in Figure 4.4. It requires the subject's current stature. This information is used to calculate several balance metrics which gives an indication of the subject's ability to balance as discussed in Section 4.2. The height is required in meters. After the the subjects height has been entered, the operator can proceed by selecting the 'Proceed with test' button. This button closes GUI C and opens either GUI D or GUI E depending on the connection status of both USB cables. The USB cables connect the measurement equipment, as discussed in Section 4.2, with the computer. If there is a USB cable connection error, GUI D will open.

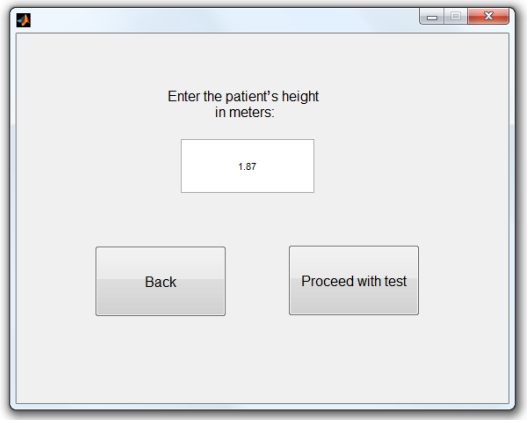

Figure 4.4 GUI C: Patient metrics window.

GUI D: Connection error, informs the user that one or both USB cables are not connected to the computer. To proceed with the test, the operator has to connect the missing USB cables and proceed by selecting the 'Re-connect' button, as shown in Figure 4.5. GUI E will open if both USB cables are connected and operational.

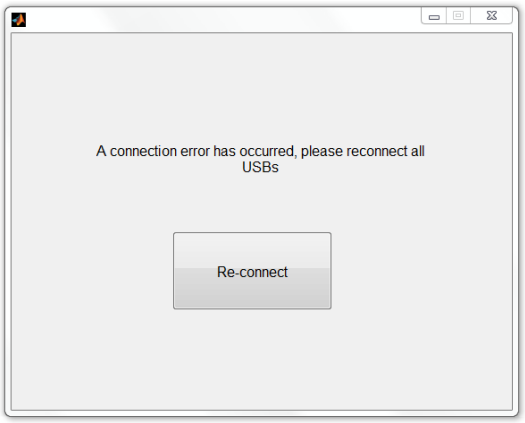

Figure 4.5 GUI D: Connection error.

GUI E: Force plate null reference value, informs the user that both USB cables are connected. The operator is informed that the patient must stand clear of the machine upon selecting the 'Proceed with test' button. This operation resets the Mini Amplifier such that it has a null reference value. Thereafter, GUI E is closed and GUI F is opened. If any connection problems occurred from GUI E onwards, GUI D will re-open and the test procedure will be restarted from GUI E. GUI E is presented in Figure 4.6.

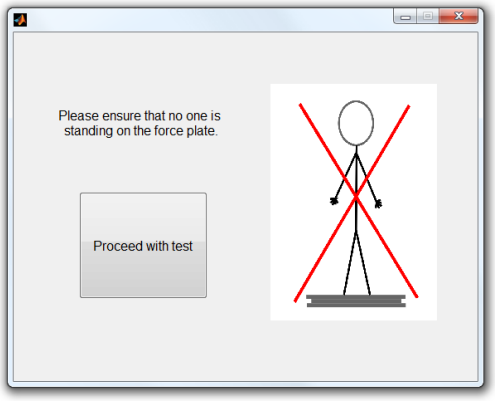

Figure 4.6 GUI E: Force plate null reference value.

GUI F: Initiating the testing cycle, opens to instruct the subject to step onto the force plate in order for testing to begin. The subject should position their feet such that their ankles are in line with the rotation axis of the machine which is also indicated by the grid on the force plate. Furthermore the subject should stand at ease with their feet positioned as they would normally stand. As soon as the subject is ready, the 'Start test' button can be selected as shown in Figure 4.7 (a). When the button is selected, the it's name changes to 'Testing under way' to inform the operator that actual testing has commended, as presented in Figure 4.7 (b). The machine will be operated by a sub-function

to perform the balance test cycle. After the test has been completed, GUI F will close and GUI G will open.

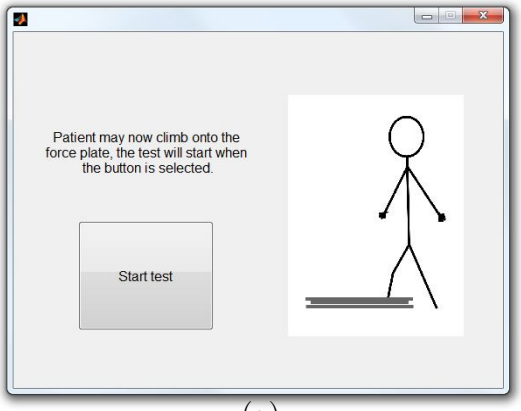

(a)

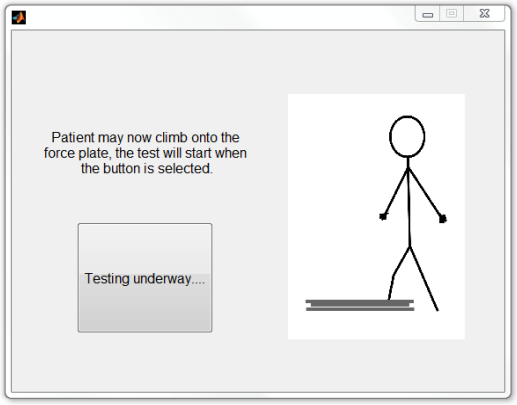

(b)

Figure 4.7 GUI F: Initiating the testing cycle: (a) before actual testing has started; (b) after the testing button has been selected.

GUI G: Save the measured results or retest the patient, is shown in Figure 4.8. It provides the user with two options: either to re-test the patient or to save the measured results. In the case of re-testing, the results of the proceeding test will be deleted, GUI G will be closed and GUI F will re-open. This particular option will be chosen if an error occurred during the first test. If the test went according to plan, the 'Saved the measured results' button should be selected. The measured results and subject information will be saved to a folder with the subject's ID. When the saving process is completed, GUI G closes and GUI H opens.

GUI H: Displaying the results, as shown in Figure 4.9, is the final GUI and displays the test results of the subject. There are three listboxes in the top right hand corner. The listboxes list the test history of the subject. When a test history is selected from the listbox, that test's results are plotted in the

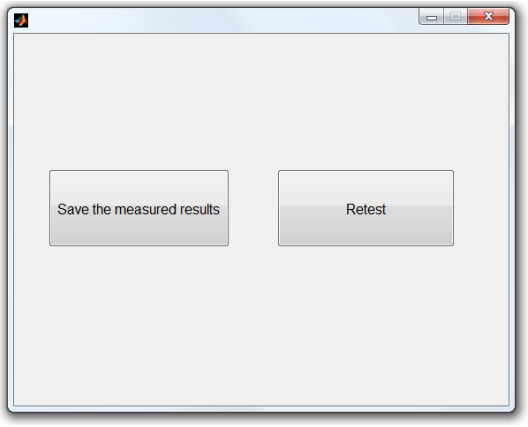

Figure 4.8 GUI G: Save the measured results or retest the patient.

seven graphs and the various balance metrics are displayed next to the listbox. There are three different list boxes available, each with a different colour and a reset button next to it. This enables the operator to compare up to three different test results at the same time. If the operator wishes to remove certain results from the graphs the reset button next to the listbox can be selected. The graph in the top right hand corner displays the COP movement of the subject throughout the test. The six remaining graphs display the forces and moments in the X, Y and Z directions through the duration of the test. The calculation of the various balance metrics, forces and moments are discussed in Section 4.2. Once the medical practitioner has analysed the test results the 'Restart testing procedure' button can be selected. This will close GUI H and return to the start of the test procedure. The system is now ready for another test to be conducted on either the same or a different subject.

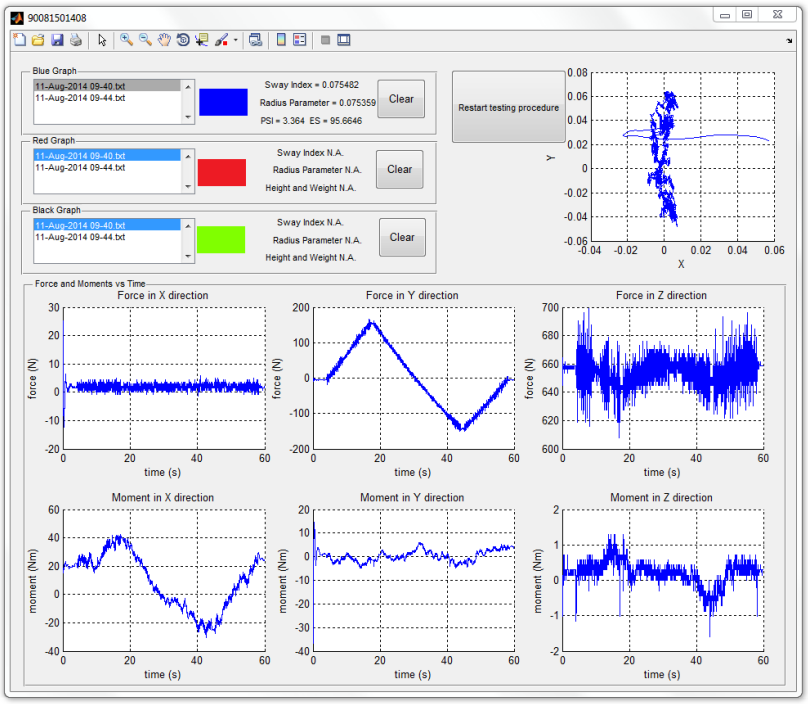

Figure 4.9 GUI H: Patient results.

4.2 Program Callback Functions

The callback functions execute the operator's commands. These are the functions running in the background and remain unknown to the operator. The callback functions are called by the GUI's as a consequence of a command provided by the operator, for example by selecting a button. The benefit of these functions are that the operator doesn't need to understand the details of how the commands are performed or that the functions exists, as long as the commands are executed. The functions enable the execution of advanced operations.

As shown in Figure 4.2, the program starts with GUI A. Once the only button on GUI A is selected, the subject's ID number is stored as a global variable. A global variable is a variable accessible by other functions besides only the function in which it is initially defined in. This global variable known as 'ID_number' is used to search through the program database to find a folder with the same name. If such a folder exists, it means that this is not the first time this subject is being evaluated. However, if no such folder is found, a folder is created with the subject's ID number as the folder name. This also indicates that the subject is a first time user. A balance performance database is therefore built up with a separate folder for each subject.

GUI B does not require the execution of any functions, it simply directs the operator to GUI C or GUI H. The 'Back' button in GUI C re-directs the operator back to GUI B. If the 'Proceed with test' button is selected in GUI C, the stature of the subject is stored as global variable , 'Subject_height'. The subject's height are stored as a global variable such that it can be accessed by another function at a later stage. The command also calls a function named the 'Establish_Connection_Status'. This function ensures that both the micro-controller and the force plate's USB cables are connected to the computer. Refer to Appendix A for the micro-controller specifications. The function tries to open and close the serial connection to each USB port. If one of the ports can not open, GUI D is opened indicating that there is a cable connection problem. The 'Re-connect' button in GUI D also calls the 'Establish_Connection_Status' function. GUI E is opened if no connection errors occurred.

The 'Proceed with test' button in GUI E first re-establishes if both USB cables are still connected thereafter opening the serial port to the force plate. After opening the serial port, 'S' in binary code is sent to the force plate and the serial port is closed again. Binary 'S' is an instruction command for the force plate hardware to zero. After the force plate has been zeroed, GUI F opens. The procedure is initiated by selecting the 'Start test' button in GUI F. The test procedure starts by again ensuring that both USB cables are connected, thereafter calling the 'Microcontroller_Command' function. The Microcontroller_command function opens the serial port to the micro-controller, sends the command '1' to it and closes the serial connection. The micro-controller has its own code stored on it. When '1' is sent to it, it activates the code stored on the micro-controller to rotate the stepper motor a number of steps in either direction. After the 'Microcontroller_Command' function is executed, the button's name in GUI E is changed from 'Start test' to 'Testing under way' to indicate that the testing procedure is under way. The 'Read_Force plate_Data' function is called up next.

The 'Read_Force plate_Data' function opens the force plate serial port and sends a binary 'Q' followed by a binary 'R' to it. The binary 'Q' sets the force plate sampling frequency to 200 Hz. The binary 'R' initiates the recording of the force plate. The force plate measures six readings at 200 Hz. These readings are the forces in the X, Y and Z axis directions and the moments about the X, Y and Z axes respectively. One measurement containing the six readings is recorded as a 12 bit binary array. For a recording of 60 seconds at 200 Hz, the serial port buffer size is set to 144 000 bytes as shown in Equation 4.2.1.

$$Buffer\ Size = 12 \times 200 \times 60 \tag{4.2.1}$$

As the buffer fills up to the pre-set number of bytes the binary data is converted to decimal numbers and stored as a global matrix named 'Forces_and_Moments'. This matrix is multiplied by a calibration and transformation factor to convert the values to SI units of Newton and Newton meter for the forces and moments respectively. GUI G is opened after the 'Read_Force plate_Data' function has been executed.

GUI G has two buttons. The 'Retest' button calls the 'Establish _Connection_Status' function which restarts the procedure. The 'Save the measured results' button creates a text file containing the test's data. This text file is saved in the subject's folder as the current time and date as shown in Figure 4.10. The text file contains the data as a $n \times 7$ matrix, where n is equal to the product of the test duration and sample frequency of the recordings. The first six columns of the matrix contains the measured forces and moments. Row 1 and row 2 in the last column contains the height and weight, which was entered in GUI C and calculated with the measured force plate data respectively. In Figure 4.10, an example of a subject's folder containing the test results are shown. The subject's ID number is 90 081 501 408. The test was conducted on 13 June 2014 at 08:15. The subject was 2 meters tall and weighed 100 kilograms when the test was conducted.

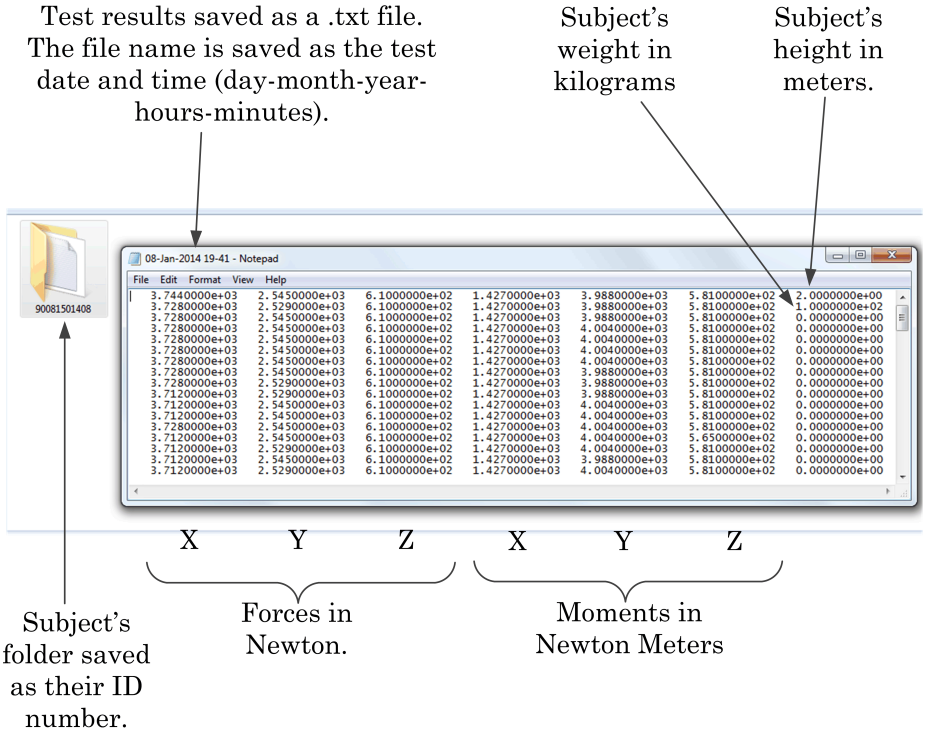

Figure 4.10 Subject's folder and text file which is created after a test.

After the results have been saved, GUI H, which displays the results, opens. GUI H makes use of a callback function which calculates the necessary balance factors from the raw results in the text file. The callback function firstly calculates the COP location in the X and Y direction of the i^{th} measurement using Equation 4.2.2 and 4.2.3. $M_{x,i}$ and $M_{y,i}$ represents the measured X and Y moments and $F_{z,i}$ the measured Z force of the i^{th} sample measurement respectively. The calculated COP is displayed on the graph in the top left hand corner of GUI H as discussed in Section 4.1 (Winter, 2009).

$$COP_{x,i} = \frac{-M_{y,i}}{F_{z,i}} \tag{4.2.2}$$

$$COP_{y,i} = \frac{M_{x,i}}{F_{z,i}} \tag{4.2.3}$$

The calculated COP is further used to calculate the SI of the subject as shown in Equation 4.2.4. The SI expresses a subject's ability to balance according to the average rate at which they shift their COP location (Botha *et al.*, 2007). It is an indication of the response time of a subject when a change in balance occurs or is required. The change in time between every sample measurement is represented by Δt. Measurements are sampled at 200 Hz and therefore Δt is $0,005$ seconds.

$$SI = \frac{\sum_{i=1}^{n-1} \frac{\sqrt{(COP_{x,i+1}-COP_{x,i})^2+(COP_{y,i+1}-COP_{y,i})^2}}{\Delta t}}{(n-1)} \tag{4.2.4}$$

In order to calculate both the ES and PSI, the subject's body balance behaviour is simulated as a single inverted pendulum as discussed in Chapter 5.3.1. A single mass is used to represent the total body mass which rotates about the ankle joint as shown in Figure 4.11. Equation 4.2.5 shows how the body sway angle is calculated using the measured force plate data (Ji *et al.*, 2004).

$$\theta_i = \frac{Mh[F_{r,i}COP_{y,i} + F_{y,i}L_0 - mga] + IF_{y,i}}{M^2gh^2 - I[(M+m)g - (\frac{F_{r,i}}{k+1})]} \tag{4.2.5}$$

The total mass of the body segments above the ankles is represented by M and the remaining mass of the feet and the force plate is expressed as m. The body sway angle relative to the line perpendicular to the force plate is represented by θ and the inclination of the force plate is ϕ. The resultant ground reaction force (F_r) perpendicular to the force plate acts at a norm distance of COP_y from the ankle joint. F_y is the horizontal force directly measured by the force plate in the Y direction. The norm distance between the ankle joint O and the surface of the force plate is represented by L_0 and the gravitational acceleration force by g. The body inertia, the height from the

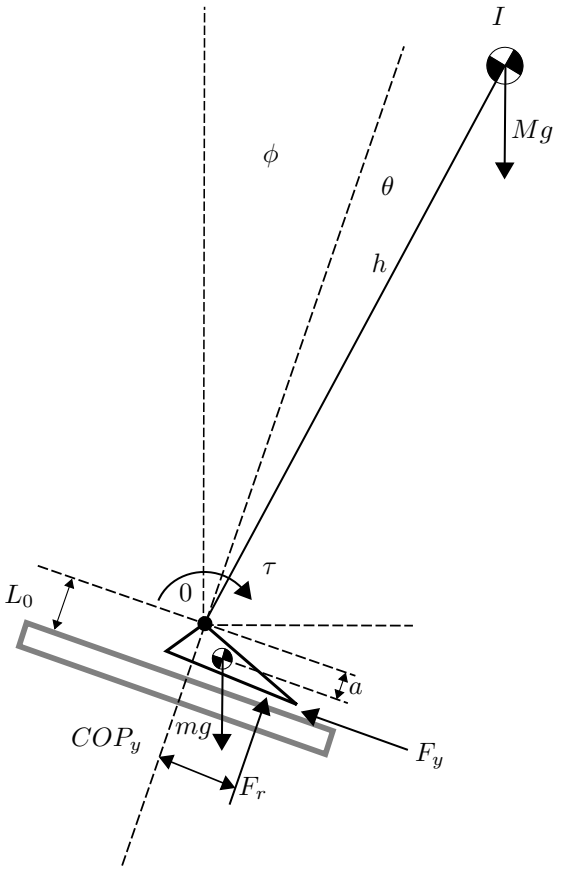

Figure 4.11 Free body diagram of the human body modelled as an inverted pendulum.

ankle joint to the COM and the perpendicular distance from the ankle to the foot COM is represented by I, h and a respectively, and is calculated using the anthropometric body data as discussed in Chapter 5.2. The gain k is the ratio of the rotation angle of the base to the body sway angle of the previous measurement (θ_{i-1}). For the calculation of the first angle, k is equal to 1. This single inverted pendulum model is used to calculate the body tilt angle as the balance performance test progresses.

The subject's ES is calculated as shown in Equation 4.2.6 using the calculated data from the inverted pendulum model. The subject's maximum anterior and maximum posterior sway angles (degrees) recorded during the test is represented by $\theta_{max,ant}$ and $\theta_{max,post}$ respectively. The limited tilting angle of the average human is $12,5$ degrees. No movement of the subject results in a perfect score of 100 and a subject who falls during the test receives a score of 0. The ES gives an indication of the subject's balance compared to that of the average human being (Chaudhry *et al.*, 2011).

$$ES = 100 \times \frac{12,5 - (\theta_{max,ant} - \theta_{max,post})}{12,5} \tag{4.2.6}$$

The model is then further used to define the torque (Equation 4.2.7) of the body which is used to calculate the subject's PSI score.

$$\tau_i = (F_{r,i})COP_{y,i} + F_{y,i}L_0 - mga(\cos(\frac{k\theta_i}{k+1})) \tag{4.2.7}$$

The PSI incorporates a broader range of biomechanical aspects of the upright stance. PSI is defined as the percentage ratio of the total stabilizing and destabilizing ankle torque (τ_i) due to gravitational forces. Equation 4.2.8 shows the mathematical expression of the PSI factor, where m_T is the total mass of the subject, g the gravitational acceleration, h is $0,55$ the total height of the subject, τ_i the stabilizing torque, and θ_i (Equation 4.2.5) the sway angle of the i^{th} measurement in radians (Chaudhry *et al.*, 2005).

$$PSI = \frac{\sum_{i=1}^{n} |m_T g h \theta_i|}{\sum_{i=1}^{n} |\tau_i|} \tag{4.2.8}$$

To calculate the Radius parameter, the average COP position is first calculated using Equation 4.2.9 and 4.2.10. The maximum radius enclosing all the COP positions is then calculated as the maximum R value of Equation 4.2.11.

$$COP_{Xavg} = \frac{\sum_{i=1}^{n} COP_{x,i}}{n} \tag{4.2.9}$$

$$COP_{Yavg} = \frac{\sum_{i=1}^{n} COP_{y,i}}{n} \tag{4.2.10}$$

$$R_i = \sqrt{(COP_{x,i} - COP_{Xavg})^2 + (COP_{y,i} - COP_{Yavg})^2} \tag{4.2.11}$$

These calculated values along with the measured forces and moments are displayed on GUI H for the doctor to observe and analyse.

4.3 Conclusion

In this chapter an overview about the computer program, which is used to operate the Dorsiflexometer, was given. The program has a graphical user interface which interacts with the operator by specifying the steps and required subject information to complete the testing procedure. Numerous functions executes the commands of the operator which controls the force plate and the oscillating mechanism of the machine. The computer program was created with the intent of making the testing procedure as easy and understandable as possible for the medical personnel operating the computer.

Chapter 5

INVERTED PENDULUM MODELS OF THE HUMAN BODY

During a force plate balance assessment test, a subject is asked to stand at ease on a platform while the platform records the subject's reaction forces for a certain time. The force plate measures the X, Y and Z reaction forces and the X, Y and Z moments as described in Section 3.3.1. Typically, these forces are then used to calculate balance parameters, such as SI an PSI, which gives an estimation of the subject's ability to balance. However, these balancing factors only indicate how the COP changes and does not consider the body COM movements. Tracing the movement of the COM aid in the study of the stiffness of the muscles around the moving joints and their correlation to destabilise the force of gravity on the body (Ji *et al.*, 2004). Therefore, in this chapter, two models are developed to calculate a subject's COM movement from the subject's initial body conditions and force plate recordings. The first model simulates the body as a SIP by assuming the subject only makes use of ankle flexion to maintain balance. The second model simulates the body as a DIP, thereby assuming the subject uses a combination of ankle and hip flexion.

5.1 Human Balance Strategy

The ability to balance is of fundamental importance to human beings to function normally and perform everyday tasks. While a subject is standing stationary and erect, the body sways back and forth subconsciously to maintain balance. The COP of the subject perpetually shifts around to keep the COM within the range of the foot surface area, which is in contact with the ground. As soon as the COM extends beyond the foot contact area, the subject is forced to take a step in the direction in which their COM is moving to prevent

themselves from falling over. This section describes the balance strategy used by a stationary subject to keep their COG within range of their foot surface area.

The human body is inherently unstable. Therefore, the COM of a subject standing erect is continuously moving around and constantly in a falling state. The COP dictates the movement of the COM which results in a continues movement of the COP in order to keep the COM in the most upright position possible. This can be explained by comparing a subject to an inverted pendulum and further assuming that the subject only rotates its body about their ankle joints in the sagittal plane. The inverted pendulum consists of a massless rod with all the weight placed at the top. Figure 5.1 shows a subject in the sagittal plane rotating about its ankle. The figure further shows how the subject can be described as a pendulum model. Since the model is only described in the sagittal plane, the location of the COM is referred to as the COM_x. The COM_x is the normal length from the vertical projection of the COM to the point of rotation which is the ankle joint. COM_x can either be in the positive or negative X direction. W represents the vertical body weight vector of the COM. As a result of the body weight, a vertical ground reaction vector R is formed. COP_x represents the normal length from R to the ankle joint. It is assumed that W is equal to R and that both are constant while a subject sways. Therefore only the COM_x and COP_x changes during static standing.

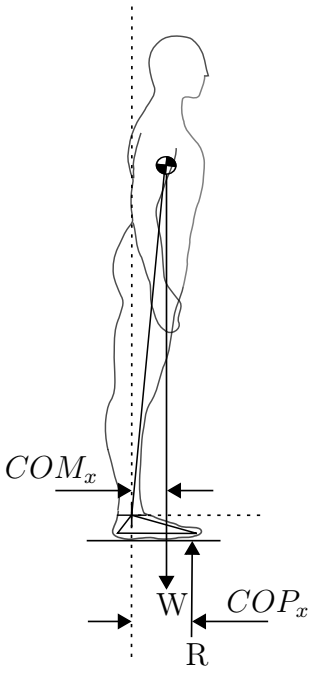

Figure 5.1 Subject rotating about their ankle in the sagittal plane.

Figure 5.2 (a) shows a body at an instant in time with zero angular acceleration ($\ddot{\theta}$), a clockwise angular velocity ($\dot{\theta}$) and a COP_x greater than its COM_x. The vertical projection force W of the COM is ahead of the ankle pivot point and will thus cause the body to fall forward. To prevent this from happening, the COP_x will be increased, thus increasing the angular acceleration in the anticlockwise direction as shown in Figure 5.2 (b). As the angular acceleration becomes greater in the anticlockwise direction, the angular velocity decreases to such a point that it becomes zero as shown in Figure 5.2 (c). While the COP_x is still grater than the COM_x and the angular acceleration is positive in the anticlockwise direction, the angular velocity will increase in the anticlockwise direction as presented in Figure 5.2 (d).

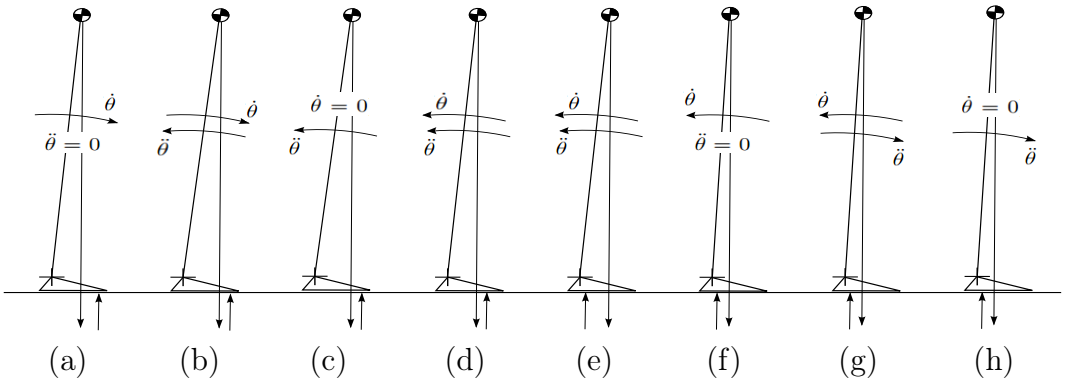

Figure 5.2 Human balance strategy free body diagrams with: (a) clockwise angular velocity and zero angular acceleration; (b) clockwise angular velocity and anticlockwise angular acceleration; (c) zero angular velocity and anticlockwise angular acceleration; (d) anticlockwise angular velocity and anticlockwise angular acceleration; (e) COP less than COM; (f) anticlockwise angular velocity and zero angular acceleration; (g) anticlockwise angular velocity and clockwise angular acceleration; (h) zero angular velocity and clockwise angular acceleration.

At a certain point the subject will subconsciously realise that the COP_x will have to decrease to prevent themselves from falling over backwards. The subject therefore shifts their COP_x such that it becomes less than their COM_x, as shown in Figure 5.2 (e). The angular acceleration of the subject decreases such that it becomes zero as the COP_x becomes less than the COM_x. This is shown in Figure 5.2 (f). Thereafter, the angular acceleration starts to increase in the clockwise direction as a result of the location of the COP_x, shown in Figure 5.2 (g).

The angular velocity will decrease until it becomes zero as a result of the angular acceleration being in the opposite direction to the angular velocity.

This is shown in Figure 5.2 (h). The angular velocity will then increase in the clockwise direction, due to the angular acceleration, and the subject will have to increase their COP_x to prevent themselves from falling over forwards. As the COP_x becomes greater than the COM_x, the angular acceleration in the clockwise direction will decrease until it becomes zero. This brings the subject back to the position as shown in Figure 5.2 (a).

This cycle of maintaining the body upright continues indefinitely. It is interesting to note that when the angular velocity is in the clockwise direction, the COP_x should be greater than the COM_x and when the angular velocity is in the anticlockwise direction, the COP_x should be less than the COM_x. The rate and the range in which the subject shifts their COP around characterises the subject's ability to maintain balance. If the COP rate is too slow, the subject will have to step in the direction in which the COM is moving to prevent itself from falling. If the COP rate is too fast, the subject overcompensates by shifting their COM too much. These subjects tend to have a high risk of falling when perturbed since they overcompensate and go beyond their COP range.

5.2 Human Anthropometry

The analytical models simulating the COM movement of a subject, either as a single or double inverted pendulum, make use of the body inertia to calculate the overall COM location of the body. This section describes the anthropometric models that were used to calculate the location of the COM of the body and its inertial moment about the points of rotation. Human anthropometry refers to the physical dimensions and proportions of the body segments (Ben-Abdelkader and Yacoob, 2008).

Figure 5.3 (a), constructed by Drillis *et al.* (1964), shows the location of the COM of the body parts. The COM location of each part is expressed as an average of it's total length from the proximal joint centres. Figure 5.3 (b) shows the basic body segment lengths between joints and expresses each segment's length as a percentage of the total body height H. This model was summarised by Dempster (1955). The black dots and black and white circles in Figure 5.3 indicate the pivot points and COM locations of the body segments respectively.

Table 5.1 contains the mass of each body segment as a percentage of the total body mass (m_T). The values in this table was obtained from Winter (2009). Using the segment masses in the table, the segment lengths and their COM locations, along with Equation 5.2.1, the COM location for a number of combined body parts were calculated as a function of the total body height. The overall COM radius from a global axis system is referred to as r_{COM}. The

mass of each segment is represented by m and the radius of the segment's COM from the global axis system as r_{axis}.

$$r_{COM} = \frac{\sum m_{seg} \cdot r_{axis}}{\sum m_{seg}} \tag{5.2.1}$$

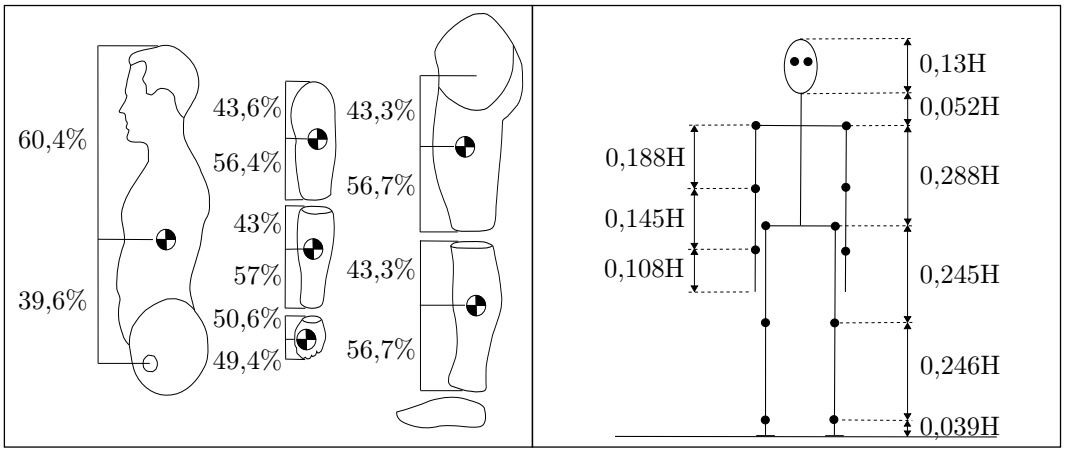

(a) (b)

Figure 5.3 COM locations of body segments (a) and human anthropometric data (b).

Table 5.1 Body segment masses as a percentage of the total body mass.

Body segment	Segment weight (m_{seg})
Trunk head neck	0.578 m_T
Upper arm × 2	0,056 m_T
Forearm × 2	0,032 m_T
Hand × 2	0,012 m_T
Thigh × 2	0,2 m_T
Leg × 2	0,093 m_T
Foot × 2	0,029 m_T

The body segments were combined to form two main body parts: the upper body and the legs. The upper body segment consists of the head, trunk and arms. The lower body segment consists of the thigh and the lower leg. The body parts were combined to form two main segments since the DIP model simulates the body as two pendulums pivoted at the ankle and hip joints. Note that the foot does not form part of the leg since the models rotate about the ankle joint. These two segments were then further combined using Equation 5.2.1 to form one single segment. This was done since the SIP model simulates the whole body as a single pendulum which only rotates about the ankle joint.

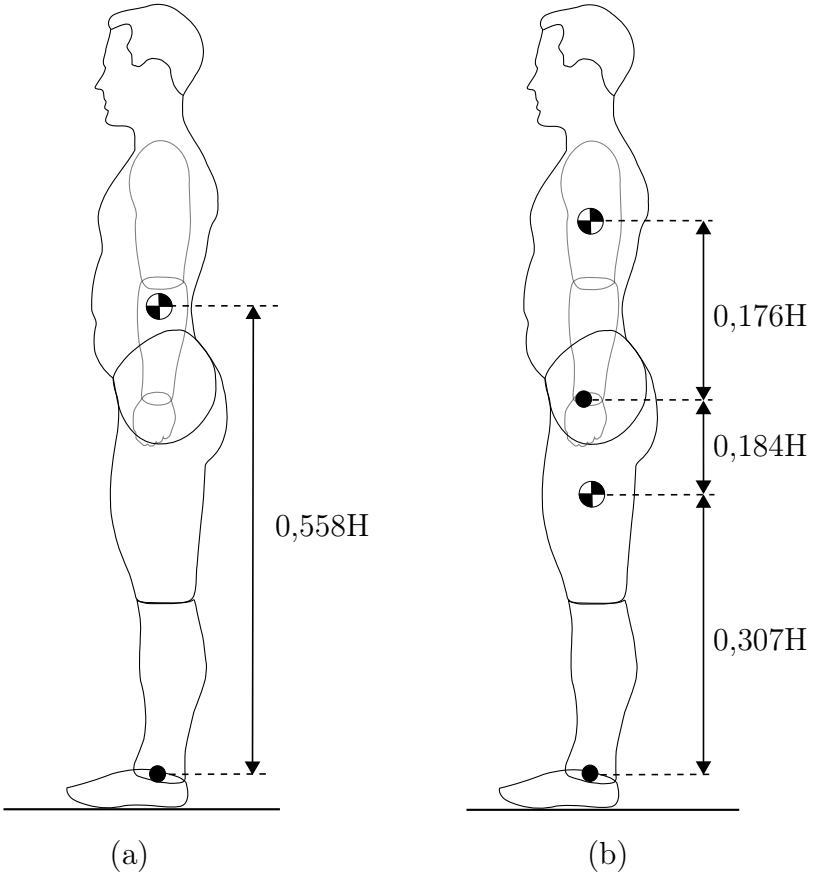

Figure 5.4 COM location for a single (a) and double (b) inverted pendulum models of the human body.

The moment of inertia (I_{axis}) for the segments were calculated using Equation 5.2.2.

$$I_{axis} = \sum m_{seg} \cdot r_{COM} \tag{5.2.2}$$

The SIP and DIP models only consider anterior-posterior oscillations in the sagittal plane and therefore the COM locations were only calculated for the sagittal plane. Figure 5.4 (a) and (b) show the locations of the COMs' and the relative distance these are from the ankle pivot point for both the single and double segmented bodies. It should be noted that these lengths my vary with body build, racial origin and sex, and are not specific to the subjects that were tested in Chapter 6.3.

5.3 Single Inverted Pendulum Model

A subject's ability to balance can quantitatively be defined by monitoring how much and at what rate the subject shift their total body mass around. Total body mass monitoring equipment is very expensive, take a lot of time to set up and needs a trained professional operator. Inverted pendulum models are therefore used to simulate how a subject's COM shifts. The pendulum models use force plate measured data, which is much easier and quicker to obtain, to calculate the location of the COM. This section starts by formulating the equations of motion for a SIP. It further explains how a subject's COM movement can mathematically be modelled using dynamic and explicit time step equations.

5.3.1 Dynamic equations of a single inverted pendulum

The human body can be compared to a SIP by only considering ankle postural control to keep the body upright. This section describes the dynamic equations that were formulated to predict the movement of the SIP model's COM in the sagittal plane. The equations formulated in this section were used for the experiments as described in Section 6.3.

It is important to monitor the COM movement of a body as it enables the study of the control strategies used by subjects to maintain their balance. Current equipment available to measure the movement of a subject's COM is however, very expensive and difficult to operate. A SIP model was therefore formulated to relate the force plate measured COP to the body COM movement. To model a subject as a SIP, it was assumed that the entire body rotates only about the ankle joints and therefore only makes use of ankle postural control to stay upright. Figure 5.5 (a) shows the subject modelled as an inverted pendulum in the sagittal plane. The model only rotates about the ankle joint O and is placed on a tilted force plate. The model is then broken up into two free body diagrams: the entire body above the ankle (b) and the feet (c).

Figure 5.5 (b) shows the body above the ankle. This model consists of the entire body excluding the feet and will from now on be referred to as the entire upper body. The entire upper body mass (m_1) is a distance L_1 from the ankle joint O. θ_1 represents the sway angle of the pendulum with respect to the fixed global Y axis. The location of m_1 is the COM of the entire upper body. I_1 represents the COM's inertia, υ_1 its velocity, and g the gravitational acceleration constantly acting upon it. F_x and F_y are the horizontal and vertical forces acting at the ankle joint respectively. Torque (τ_1) is the resultant moment acting at the ankle joint keeping the inverted pendulum upright.

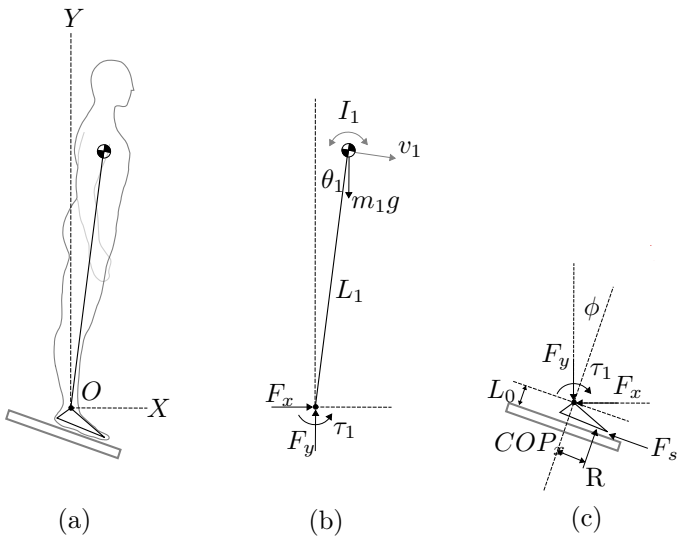

Figure 5.5 Human body simulated as a SIP with a free body diagram of the: (a) entire body; (b) body above the ankles; (c) feet.

Figure 5.5 (c) shows the lower segment consisting of the feet and the force plate. The mass of the feet and the force plate is ignored since it rotates at a negligible small velocity about the hinge point O. This is coincidently the same reasoning Colobert *et al.* (2006) followed in their model. The platform is rotated by an electrical motor about point O as described in Section 3.3. The frictional force preventing the feet from slipping when the force platform is at an inclined angle ϕ is represented by F_s. The frictional force is measured by the force plate as the force vector in the force plate's Y direction and not the global X direction as shown in Figure 5.5. L_0 is the distance between the ankle joint O and the surface of the force plate. R is the resultant ground reaction force measured by the force plate. The resultant ground reaction force is equal to force Z measured by the force plate. COP_x is the normal distance between the ankle joint O and the resultant ground reaction force.

The dynamic equations describing the sway of the model can be formulated using Lagrangian formulation. Lagrangian formulation describes the dynamic behaviour of a system in terms of work and energy stored in it (Greenwood, 2003). The Lagrangian (L) is defined by Equation 5.3.1 in terms of the generalised coordinates (q_i) and their time derivatives ($\dot{q}_i$).

$$L(q_i, \dot{q}_i) = T(q_i, \dot{q}_i) - U(q_i) \tag{5.3.1}$$

The total kinetic and potential energy stored in the dynamic system is represented by T and U respectively. The equation of motion for a dynamic system is defined by Equation 5.3.2. The generalised forces is represented by Q.

$$\frac{d}{dt}\frac{\partial L}{\partial \dot{q}_i} - \frac{\partial L}{\partial q_i} = Q_i \tag{5.3.2}$$

Since this model is only two-dimensional, it is more convenient to make use of a polar coordinate system where the radius can be expressed as L_1 and the angle as θ_1. The upper body velocity (υ_1) in the Cartesian coordinate system can be converted in terms of θ_1 in the polar coordinate system using Equation 5.3.3.

$$\upsilon_1 = L_1\dot{\theta}_1 \tag{5.3.3}$$

The total kinetic energy of the system can then be expressed as shown in Equation 5.3.4. The total potential energy of the system is expressed in Equation 5.3.5.

$$T = \frac{1}{2}m_1(L_1\dot{\theta}_1)^2 + \frac{1}{2}I_1\dot{\theta}_1^2 \tag{5.3.4}$$

$$U = m_1 g L_1 cos(\theta_1) \tag{5.3.5}$$

Substituting both the kinetic and potential energy equations into Equation 5.3.1, gives the Lagrangian of the system as shown in Equation 5.3.6.

$$L = \frac{1}{2}m_1(L_1\dot{\theta}_1)^2 + \frac{1}{2}I_1\dot{\theta}_1^2 - m_1 g L_1 cos(\theta_1) \tag{5.3.6}$$

Taking the partial derivative of the derived Lagrangian with respect to time and substituting this into Equation 5.3.2, gives the equation of motion. Equation 5.3.7 expresses the dynamic system in terms of the angular acceleration and the angle of the inverted pendulum.

$$m_1 L_1^2\ddot{\theta}_1 + I_1\ddot{\theta}_1 + m_1 g L_1 sin(\theta_1) = \tau_1 \tag{5.3.7}$$

The torque acting at the ankle, as shown in Figure 5.5 (c), is formulated from summing all the moments about point O and setting them equal to zero. The sum of all the moments are equal to zero since the mass of the foot is ignored and therefore it has zero moment of inertia. Equation 5.3.8 gives the torque about point O.

$$\tau_1 = COP_x R - F_s L_0 \tag{5.3.8}$$

Equation 5.3.7 and 5.3.8 can then be combined to form Equation 5.3.9. This is the full equation which is used for the experiments in Section 6.3. The equation is use to calculate the COM movement of a subject using their COP measured results.

$$m_1 L_1^2\ddot{\theta}_1 + I_1\ddot{\theta}_1 + m_1 g L_1 sin(\theta_1) = COP_x R - F_s L_0 \tag{5.3.9}$$

5.3.2 Single inverted pendulum modelling

This section describes the methodology used to model a subject's body behaviour as a SIP model during a balance assessment test. The model uses force plate recordings to simulate the body's movement during the test. It is assumed that the subject balances in the same manner as a SIP by only making use of ankle flexion to stay upright.

The human body can be modelled as a SIP by viewing the entire body above the ankle as a single rigid segment. A force plate is used to measure the ground reaction forces of the subject undergoing a balance assessment test. The force plate measures the X, Y and Z forces and the X, Y and Z moments at 200 Hz. Thus for every $0,005$ seconds there is a recording containing three forces and three moments. These recordings are used to calculate the subject's COP movement. The subject's COM location at each time step can then be calculated using the equations of motion for a SIP, the body's initial conditions, and the continuous COP results.

It is assumed at time zero, just before the force plate measurement started, everything is known about the subject: the subject's height, mass, the initial body angles and initial body velocity. The measured force plate data is then used to calculate the torque of the current time step as shown in Equation 5.3.10.

$$\tau_{1(t)} = COP_{x(t)} R_{(t)} - F_{s(t)} L_0 \tag{5.3.10}$$

Using the current torque and body angle the next time step's $(t+\Delta t)$ body acceleration can be calculated by rearranging Equation 5.3.7.

$$\ddot{\theta}_{1(t+\Delta t)} = \frac{\tau_{1(t)} - m_1 g L_1 \sin(\theta_{1(t)})}{m_1 L_1^2 + I_1} \tag{5.3.11}$$

In this equation, Δt is the time step size. The magnitude of each time step is equal to the difference between t_{i+1} and t_i. An explicit method of small time steps is further used to calculate the body angular velocity for the next time step as shown in Equation 5.3.12.

$$\dot{\theta}_{1(t+\Delta t)} = \ddot{\theta}_{1(t+\Delta t)} \Delta t + \dot{\theta}_{1(t)} \tag{5.3.12}$$

Using the explicit time step method, the next time step's body angle can be calculated as shown in Equation 5.3.13.

$$\theta_{1(t+\Delta t)} = \dot{\theta}_{1(t+\Delta t)} \Delta t + \theta_{1(t)} \tag{5.3.13}$$

The procedure can then be repeated for the number of time steps measured starting with Equation 5.3.10 again to calculate the new torque. The angles obtained from Equation 5.3.13 and the body anthropometry measurements as

described in Section 5.2 are then used to calculate the location of the COM of the body.

5.4 Double Inverted Pendulum Model

The exclusive use of ankle flexion is not always enough to maintain balance, therefore subjects are often forced to use a combination of ankle and hip strategies to stay upright. This section describes how the human body is modelled as a DIP by splitting the body at the hip joint. The dynamic equations of motion for this DIP is formulated in this section.

5.4.1 Dynamic equations of the double inverted pendulum

The DIP model is more complex than the SIP model, but can be derived using the same Lagrangian dynamic formulation principals. Figure 5.6 (a) shows a human model in the sagittal plane standing on a force plate as a double inverted pendulum. In this case, both ankle and hip strategies are used to keep the model upright. The model can rotate about its hip and ankle joints, point O_1 and O_2 respectively. The model is broken up into an upper body and a lower body, each having their own COM. The lower body rotates about the ankle joint O_1 and has a length of L_1. L_1 is from point O_1 to point O_2. The upper body rotates about the hinge point O_2 which is situated at the hip joint. The upper body's COM is located a radius of L_{COM2} from its point of rotation O_2.

Figure 5.6 (b) shows the separated upper and lower body parts. The upper and lower bodies are referred to as the upper and lower pendulums respectively. The lower pendulum has a torque τ_1 acting upon it which comes from the foot. The lower pendulum's COM is located at a radius of L_{COM1} from O_1. Note that the COM of the lower pendulum is not situated at the top of the pendulum. It has a mass of m_1, a linear velocity of v_1 and a moment of inertia of I_1. θ_1 represents the sway angle of the lower pendulum with respect to the fixed global Y axis. The upper pendulum is at an angle θ_2 from the lower pendulum and has a mass of m_2, a moment of inertia of I_2 and a linear velocity of v_2. The upper pendulum exerts a torque of τ_2 upon the lower pendulum.

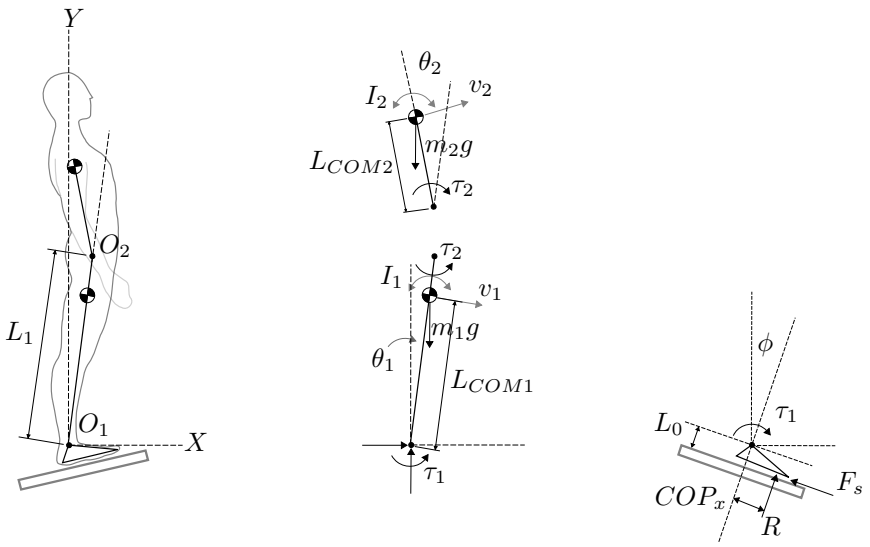

(a) (b) (c)

Figure 5.6 Human body simulated as DIP free body diagrams with: (a) the entire body; (b) the upper and lower body halves; (c) the feet.

The foot and the force plate shown in Figure 5.6 (c), rotates about point O_1. The rate at which the foot and the force plate rotates is small compared with that of the two links and therefore it is ignored. It is further assumed that the foot is massless since it is so small compared to the rest of the body. The foot has a torque of τ_1 acting upon it as a result of the entire body's mass and momentum. Due to the mass and torque of the body, the foot has a reaction force R and shear force F_s which is measured by the force plate. Force R is perpendicular to the force plate and at a normal distance of COP_x from the point of rotation, O_1. The shear force F_s is a normal distance L_0 from the point of rotation and is parallel with the force platform. The force platform is tilted at an angle of ϕ from the fixed global axis.

Lagrangian formulation is used to obtain the equation of motion for the DIP model. A polar coordinate system in the sagittal plane is used. Equation 5.4.1 and 5.4.2 show the linear velocities of both pendulums written in terms of their angles and angular velocities.

$$v_1 = \begin{pmatrix} -L_{COM1}\dot{\theta}_1 \sin(\theta_1) \\ L_{COM1}\dot{\theta}_1 \cos(\theta_1) \end{pmatrix} \tag{5.4.1}$$

$$v_2 = \begin{pmatrix} -\dot{\theta}_1\{L_1 \sin(\theta_1) + L_{COM2} \sin(\theta_1 + \theta_2)\} - \dot{\theta}_2 L_{COM2} \sin(\theta_1 + \theta_2) \\ \dot{\theta}_1\{L_1 \cos(\theta_1) + L_{COM2} \cos(\theta_1 + \theta_2)\} - \dot{\theta}_2 L_{COM2} \cos(\theta_1 + \theta_2) \end{pmatrix} \tag{5.4.2}$$

The total kinetic energy in the two links combined is expressed in Equation 5.4.3.

$$T = \frac{1}{2}\begin{bmatrix}\dot{\theta}_1 \\ \dot{\theta}_2\end{bmatrix}\begin{bmatrix}A_{11} & A_{12} \\ A_{21} & A_{22}\end{bmatrix}\begin{bmatrix}\dot{\theta}_1 \\ \dot{\theta}_2\end{bmatrix} \tag{5.4.3}$$

The coefficients in the kinetic energy matrix is given in Equation 5.4.4. The potential energy stored in the two links are given in Equation 5.4.5.

$$\begin{bmatrix}A_{11} \\ A_{12} \\ A_{21} \\ A_{22}\end{bmatrix} = \begin{bmatrix}I_1 + I_2 + m_1 L_{COM1}^2 + m_2(L_1^2 + L_{COM2}^2 + 2L_1 L_{COM2}\cos(\theta_2)) \\ I_2 + m_2 L_{COM2}^2 \\ I_2 + m_2(L_{COM2}^2 + L_1 L_{COM2}\cos(\theta_2)) \\ I_1 + I_2 + m_1 L_{COM1}^2 + m_2(L_1^2 + L_{COM2}^2 + 2L_1 L_{COM2}\cos(\theta_2))\end{bmatrix} \tag{5.4.4}$$

$$U = m_1 g L_{COM1}\sin(\theta_1) + m_2 g\{L_1\sin(\theta_1) + L_{COM2}\sin(\theta_1 + \theta_2)\} \tag{5.4.5}$$

Equation 5.4.3 and 5.4.5 is substituted into the Lagrangian. The partial derivative with respect to time is taken of the Lagrangian and gives the torques as shown in Equation 5.4.6 and 5.4.7. G_1, G_2 and G_3 in Equations 5.4.6 and 5.4.7 can be expressed as shown in Equation 5.4.8.

$$\tau_1 = A_{11}\ddot{\theta}_1 + A_{12}\ddot{\theta}_2 - G_1\dot{\theta}_2^2 - 2G_1\dot{\theta}_1\dot{\theta}_2 + G_2 \tag{5.4.6}$$

$$\tau_2 = A_{22}\ddot{\theta}_2 + A_{12}\ddot{\theta}_1 + G_1\dot{\theta}_1^2 + G_3 \tag{5.4.7}$$

$$\begin{bmatrix}G_1 \\ G_2 \\ G_3\end{bmatrix} = \begin{bmatrix}m_2 L_1 L_{COM2}\sin(\theta_2) \\ m_1 L_{COM1} g\cos(\theta_1) + m_2 g\{L_{COM2}\cos(\theta_1 + \theta_2) + L_1\cos(\theta_1)\} \\ m_2 g L_{COM2}\cos(\theta_1 + \theta_2)\end{bmatrix} \tag{5.4.8}$$

The above equations were derived using the Lagrangian principles as discussed in Craig (2005). These equations are used to calculate a subject's COM location when the subject uses a similar balance strategy as a DIP model.

5.4.2 Double inverted pendulum modelling

To maintain balance during certain situations, the body is forces to make use of both ankle and hip flexion to keep itself stable. In these instances, the balance behaviour of the body in the sagittal plane behaves as a DIP model. This section describes the methodology used to simulate a subject's body as a DIP using the recorded data from a balance assessment test. The DIP model simulation can then further be used to calculate and track the movement of the body's COM as described in Section 5.2 and applied in Chapter 6.3.

The recorded data from a balance assessment test along with the derived dynamic equations of the DIP is used to model a subject's DIP model balance behaviour. The assumption is made that at time zero, before the test started, everything is known about the subject: height, mass, initial body angles and each segment's velocity. These assumptions and recorded test data is used to calculate the variables describing the body's movement for every time step. Firstly, the torque at the ankle ($\tau_{1(t)}$) is calculated with the measured data as shown in Equation 5.3.10. The torque at the hip joint can be formulated as shown in Equation 5.4.9 by taking the sum of the upper body's moments about the hip joint.

$$\tau_{2(t)} = L_{COM2} m_2 g \sin(\theta_{2(t)}) + I_{2(t)} \ddot{\theta}_{2(t+\Delta t)} \tag{5.4.9}$$

The angular acceleration of each segment is expressed in Equations 5.4.10 and 5.4.11 respectively. These equations were formulated by solving Equations 5.4.6 and 5.4.7 simultaneously. Equations 5.4.9, 5.4.10 and 5.4.11 are solved simultaneously to obtain the angular acceleration for the upper body ($\ddot{\theta}_{2(t+\Delta t)}$), the lower body ($\ddot{\theta}_{1(t+\Delta t)}$) and the torque ($\tau_{2(t)}$).

$$\ddot{\theta}_{2(t+\Delta t)} = K_1(K_2 - G_{1(t)}\dot{\theta}^2_{2(t)} - 2G_{1(t)}\dot{\theta}_{1(t)}\dot{\theta}_{2(t)} + G_{2(t)} - \tau_{1(t+\Delta t)}) \tag{5.4.10}$$

$$\ddot{\theta}_{1(t+\Delta t)} = \frac{1}{A_{12(t)}}(\tau_{2(t)} - A_{22(t)}\ddot{\theta}_{2(t+\Delta t)} - G_{1(t)}\dot{\theta}^2_{1(t)} + G_{3(t)}) \tag{5.4.11}$$

Coefficients K_1 and K_2 is shown in Equations 5.4.12 and 5.4.13 respectively.

$$K_1 = \frac{A_{12(t)}}{A_{11(t)}A_{22(t)} - A^2_{12(t)}} \tag{5.4.12}$$

$$K_2 = \frac{A_{11(t)}}{A_{12(t)}}(\tau_{2(t+\Delta t)} - G_{1(t)}\dot{\theta}^2_{1(t)} + G_{3(t)}) \tag{5.4.13}$$

The calculated accelerations and an explicit method of small time steps are then used to calculate the angular velocities of the two segments as shown in Equations 5.4.14 and 5.4.15.

$$\dot{\theta}_{1(t+\Delta t)} = \ddot{\theta}_{1(t+\Delta t)}\Delta t + \dot{\theta}_{1(t)} \tag{5.4.14}$$

$$\dot{\theta}_{2(t+\Delta t)} = \ddot{\theta}_{2(t+\Delta t)}\Delta t + \dot{\theta}_{2(t)} \tag{5.4.15}$$

The same methodology is used to obtain each segment's new angle for the next time step, as shown in Equation 5.4.16 and 5.4.17.

$$\theta_{1(t+\Delta t)} = \dot{\theta}_{1(t+\Delta t)}\Delta t + \theta_{1(t)} \tag{5.4.16}$$

$$\theta_{1(t+\Delta t)} = \dot{\theta}_{1(t+\Delta t)}\Delta t + \theta_{1(t)} \tag{5.4.17}$$

These steps can be repeated for the total number of time steps available in the recorded data to calculate the movement of the body segments. The ratio of the upper body angle from the vertical compared to the lower body angle indicates how actively the subject uses their upper and lower body segments in conjunction to maintain balance and damp perturbations. Healthy subjects tend to use less ankle flexion and more hip flexion to maintain balance. The human anthropometry model, Section 5.2, is further used to calculate the movement of the COM of the DIP model.

5.5 Conclusion

In this chapter, the balance strategy used by human beings is explained by analysing the body as a single inverted pendulum. Human anthropometric dimensions are used to compose the segments of the body into two individual parts, known as the upper and lower body halves. These parts are used for the simulation and calculation of the human body dynamics as a single and double inverted pendulum model. The pendulum models are used to simulate the movement of a subject's COM. In Chapter 6 the accuracy of these simulated models are tested by comparing their calculated results to videographic calculated results.

Chapter 6

EXPERIMENTAL WORK

For this study, a machine known as the Dorsiflexometer was redesigned and built. The function of the machine is to measure a subject's ability to maintain balance when exposed to a perturbation. The measured results are used to calculate various balance metrics which describes the subject's balance behaviour. This chapter elaborates on the experiments which were conducted to test the competency and accuracy of the machine.

6.1 Force Plate Calibration

The force plate was calibrated before all the experiments were conducted. The calibration ensured that all the measured results were accurate. This section describes how the force plate manufacturer's calibration matrix was used to correct and scale the measured data. A test was also conducted to ensure that the calibration was done correctly.

For the calibration of the force platform, the sensitivity of each channel to all applied load components were determined by the manufacturers. This was accomplished by bolting the platform to a precision calibration stand with loads applied at various points while recording the outputs. From this recorded data a calibration report containing a unique 6×6 calibration matrix was generated. This 6×6 calibration matrix is shown in Equation 6.1.1. The matrix contains the channel sensitivities where the output for each channel is represented by the left column and the input load by the top row. The diagonal terms represents the sensitivities and actual calibration coefficients while the off-diagonal terms are the cross-talk values. The off-diagonal terms will be zero in an ideal situation in which there is no cross-talk among the channels. The calibration matrix elements are given in micro-volts per volts-of-excitation and are sent as an output analogue signal to the amplifier.

The amplifier amplifies the output analogue signal with a gain G of 1000 and an excitation voltage E of 10 V. Both the gain and the excitation voltage can be changed manually inside the amplifier to comply or fit in with the force plate measurement range. Furthermore, the amplifier also converts the output analogue signal to a digital signal which changes the units from Volts to Analogue-to-Digital converted units. This digital signal is sent to the computer as digitalized voltage levels of the channels. The computer reads 12 bit digitalized voltage levels and converts it to numbers in a vector. This vector is then calibrated with the use of Equation 6.1.1.

$$\begin{pmatrix} F_x \\ F_y \\ F_z \\ M_x \\ M_y \\ M_z \end{pmatrix} = \frac{10^6 R}{2^L GE} \begin{pmatrix} 3,01 & 0 & 0 & 0 & 0 & 0 \\ 0 & 2,99 & 0 & 0 & 0 & 0 \\ 0 & -0,01 & 0,76 & 0 & 0 & 0 \\ 0 & 0 & 0,01 & 0,19 & 0 & 0 \\ 0 & 0 & 0 & 0 & 0,19 & 0 \\ 0 & 0 & 0 & 0 & 0 & 0,38 \end{pmatrix} \begin{pmatrix} F'_x \\ F'_y \\ F'_z \\ M'_x \\ M'_y \\ M'_z \end{pmatrix} \tag{6.1.1}$$

The true calculated ground reaction forces and moments are $[F_x, F_y, F_z]$ in Newton and $[M_x, M_y, M_z]$ in Newton meter respectively. R is the voltage range which is 20 V and L the number of bits. The recorded signal for the forces and moments are $[F'_x, F'_y, F'_z, M'_x, M'_y, M'_z]$. The recorded signal is multiplied by 10^6 to scale the units.

All of the balance metrics factors are calculated with a combination of either F_x, M_x or M_y. Therefore, two tests were conducted to ensure that the calibration matrix worked correctly. To test the force in the Z direction, weights of four different masses, of which the weights are known, were compared. The masses are cylindrical with diameters less then $0,03$ m, and were used as point masses. The four masses were weighed on the Department of Mechanical and Mechatronic Engineering's scale and then compared to the force plate measured Z force. To test if the measured X and Y moments were accurate, 17 positions were marked out on the force plate as shown in Figure 6.1. The positions were marked out $0,05$ m apart on the X and Y axis of the force plate. The four masses, of which the weights are known, were then placed at all 17 positions individually. Using Equations 4.2.2 and 4.2.3, the COP_x and COP_y locations were calculated respectively. The calculated locations were then compared to the point mass positions.

The difference between the calculated values and the actual values of the two tests were compared using the Root Mean Square Error (RMSE) analysis. The RMSE is calculated as shown in Equation 6.1.2 where the actual COP_{actual} is subtracted from the calculated COP_{calc}. The number of measurements is represented by n.

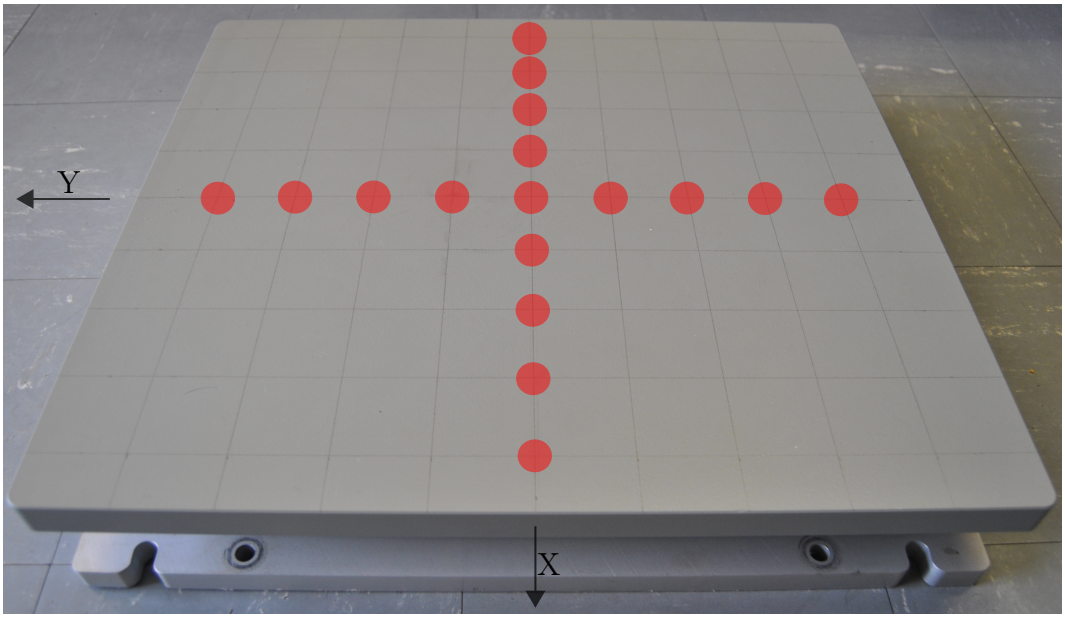

Figure 6.1 The location of the 17 marked out positions on the force plate.

$$RMSE = \sqrt{\frac{\sum_{i=1}^{n}(COP_{calc,i} - COP_{actual,i})^2}{n}} \tag{6.1.2}$$

The RMSE value comparing the known weights of the masses to the measured weights is equal to $0,23$. The RMSE value comparing the calculated locations of the weights to the actual locations is equal to $0,18$. This indicates that the force plate calibration matrix is correct and that measured results are highly accurate.

6.2 Machine Comparison Test

An experiment was conducted to compare the measured results obtained from the Dorsiflexometer to a commercially available balance assessment machine. A total of 20 subjects were tested on both machines. This section describes the experimental procedure and the compared results for the comparison test.

The Dorsiflexometer is the first balance assessment machine which can test a subject's balance capabilities for both static and perturbed, dynamic conditions. Other machines conducting dynamic balance assessments does not force the platform to rotate. Only the static assessment method was therefore compared to that of another machine. The machine to which it was compared to is called the Biodex^{TM} machine. Refer to Biodex (2014) for a full description of this machine. The subjects were first tested on the Biodex machine and thereafter retested on the Dorsiflexometer. The results

were compared to indicate how accurate the Dorsiflexometer results are and whether it follows the correct calculation procedure.

6.2.1 Methodology

A total of 20 subjects consisting of 16 males and 4 females all ranging within the age of 21 to 30 were tested. The subjects were randomly selected, none had a history with balance related issues. The only criteria for the subjects to participate was that they had to be able to stand up straight without moving their feet for at least more than 60 seconds. If a subject moved their feet during a test, the test was redone and the failed test results excluded. All the subjects agreed to partake in the tests. The tests were conducted under the supervision of Grant van Velden, manager of the Sport Technology Unit (Centre for Human Performance Sciences) at the University of Stellenbosch.

The Biodex machine and the Dorsiflexometer which was being compared were placed in the same room. Tests were conducted one subject at a time. Subjects were allowed to keep their shoes on during the tests. Each subject was first instructed to stand at ease on the Biodex machine while a fall risk test was being conducted. Figure 6.2 shows a subject standing on the Biodex machine while a test is under way.

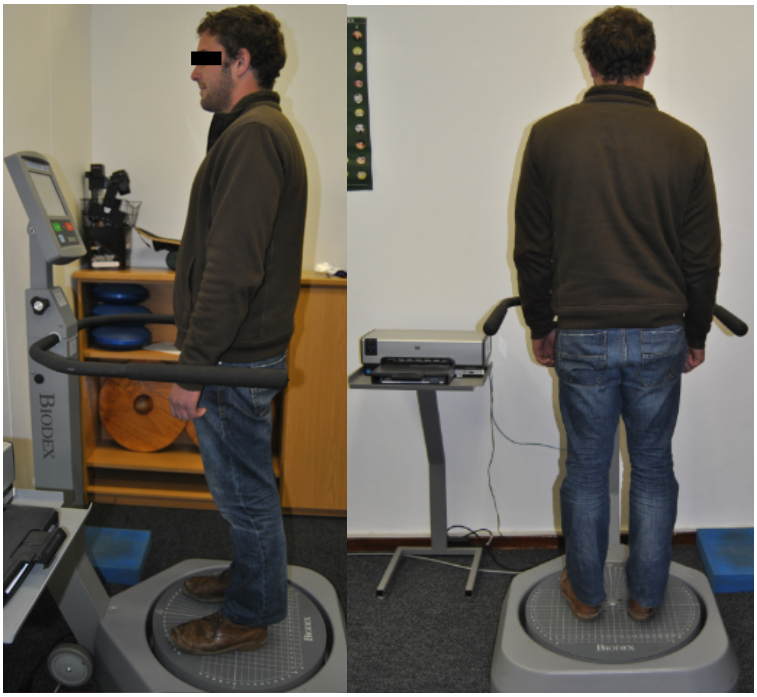

Figure 6.2 Subject standing on Biodex balance measuring machine.

The fall risk test measures the subject's Overall Stability Index (OSI) and Standard Deviation (SD) score on a static platform for a duration of 60 seconds. After the Biodex fall risk test was completed, the subject was instructed to stand at ease on the Dorsiflexometer platform. A 60 second static test was then performed with the Dorsiflexometer platform. The subject's forces in the X, Y and Z and their moments in the X, Y and Z direction were recorded at 200 Hz for the Dorsiflexometer platform test. Each subject's results were saved as a 12 000 $\times$ 6 matrix in a '.txt' file. This procedure was repeated for all 20 subjects.

The Dorsiflexometer results were used to calculate each subject's COP displacement in the X and Y direction as expressed in Equation 4.2.2 and 4.2.3 respectively. The OSI is used to express the average offset of the body COM to the median body COM position as expressed in Equation 6.2.1. The OSI is an age-related metrics which compares a subject's ability to maintain balance to their peer group's normative range. This is done by assessing the subject's COP displacement in the sagittal and frontal plane (Arnold and Schmitz, 1998). The median COP position in the X and Y direction is expressed as $COP_{x,mean}$ and $COP_{y,mean}$ respectively. The measurement count is expressed as i and the total number of measurements as n.

$$OSI = \sqrt{\frac{\sqrt{\sum_{i=1}^{n}(COP_{x,mean} - COP_{x,i})^2 + \sum_{i=1}^{n}(COP_{y,mean} - COP_{y,i})^2}}{n}} \tag{6.2.1}$$

The COP displacement was further used to calculate each subject's SD as shown in Equation 6.2.2. The SD is a static measure of the amount of variability between data points. It quantifies a subject's average COP movement per time step. For a healthy human being between the ages of 17 to 35 years, the SD score should be relatively low, less then $0,6$.

$$SD = \frac{\sum_{i=1}^{n}\sqrt{(COP_i - COP_{mean})^2}}{n} \tag{6.2.2}$$

6.2.2 Results

This experiment was conducted to compare the OSI and SD factors of the Biodex machine to that of the Dorsiflexometer. Figure 6.3 shows the plotted OSI and SD values of the 20 subjects. The plot shows how similar the two balance metrics results for both machines are for each of the 20 subjects. Each subject's Dorsiflexometer result is compared to their own Biodex machine result for both metrics. To compare the results of the two machines, the RMSE for both the OSI and SD was calculated. The RMSE indicates how close the results relate to one another. Comparing the OSI of both machines, the RMSE

is 0, 036. The RMSE of the SD is 0, 0247. These RMSE values indicate that there is an eminent correlation between the results measured by the machines. This suggests that the results obtained by the Dorsiflexometer are accurate.

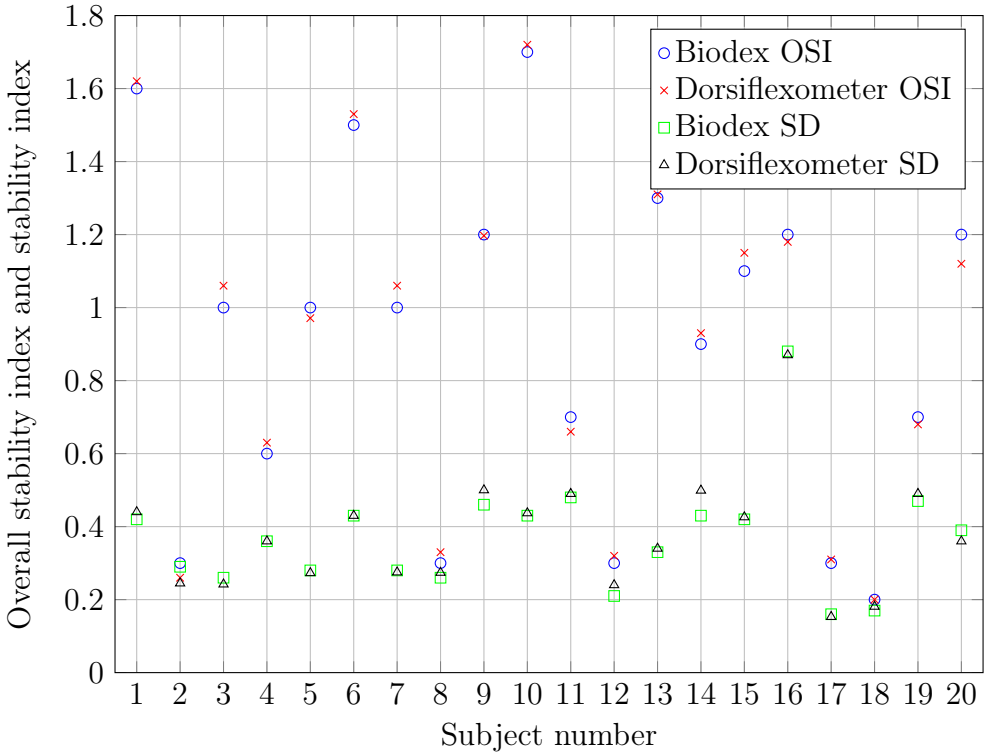

Figure 6.3 Comparison of the OSI and SD values of 20 subjects measured on the Dorsiflexometer and Biodex balance machines.

6.2.3 Conclusions

The experiment compares the balance assessment results of the Dorsiflexometer to the Biodex machine. This experiment was conducted to compare the accuracy and viability of the Dorsiflexometer results to a commercially available balance assessment machine. The OSI and SD factors of 20 subjects are compared. The Dorsiflexometer test procedure and methodology to calculate the results is accurate and deviates with a maximum RMSE of 0, 036. When comparing the operational interface of the two machines, the Dorsiflexometer was found to be easier, faster and more user friendly to operate. The Biodex machine is operated from a touch screen device situated chest height in front of the standing subject. For each subject, the operator first has to create a profile or access it (if it already exists) followed by entering the position of the patient on the platform before testing can begin. It was found that due to the location of the screen and its lack in size that it took twice as long to

enter the required information as with the computer interface software of the Dorsiflexometer.

6.3 Inverted Pendulum Model Verification and Balance Comparison

The overall function of the Dorsiflexometer is to measure a subject's ability to balance. To test weather or not the measured results of the machine can be used to detect a difference in a subject's ability to balance, an experiment was conducted to compare the balance of single-legged stance to double-legged stance. The hypothesis is that a subject's ability to balance is better when standing on both feet to maintain balance than on one. Therefore, 10 subjects ranging between the age of 22 to 24 years each underwent two dynamic balance assessment tests on the Dorsiflexometer. Firstly, subjects performed a test while balancing on both legs. For the second test, subjects were asked to balance on one leg. Each double-legged test was video recorded. These recordings were used to measure the movement of each subject's COM. Furthermore, the force plate recorded data was used to estimate each subject's model trajectory as discussed in Chapter 5. The COM movement of the model trajectory was then compared to the calculated COM movement of the video recorded data.

Anthropometric data and force plate measured results can be used to predict the movement of a subject's COM without the use of expensive video measurement equipment. The aim of this experiment was to show that the machine is capable of distinguishing between balance capabilities, and secondly to determine how closely the SIP and DIP models, which are derived in Chapter 5, predict or correlate the COM movement of a subject.

6.3.1 Methodology

A total of 10 subjects underwent two dynamic balance assessment tests on the Dorsiflexometer while being recorded with a video camera. All the subjects freely agreed to partake in the tests. The tests were conducted according to the procedure as described in Chapter 4. Markers were placed on the subjects' left hips and shoulders as presented in Figure 6.4. For the first test, subjects were instructed to stand normally on both feet. For the second test, subjects were instructed to stand on one foot while undergoing the balance test. Each test continued for a duration of 60 seconds.

The Dorsiflexometer recorded the subjects' forces and moment in the X, Y and Z directions at 200 Hz. Each subject's ES, SI, PSI and Radius parameter was computed using the recorded data from the Dorsiflexometer. The tests

were video recorded from the side to capture each subject's movement in the sagittal plane. Saggital plane movement was recorded at 25 frames per second using a Sony HDR-CX290E video camera. The markers on the hip and shoulder were used as tracking points for the video analysis software to track the movement of the body.

Figure 6.4 Subject undertaking a Dorsiflexometer balance assessment.

An open source software program, 'Tracker', was used to analyse the video footage of each subject's double-legged test. Tracker was used to track the movement of the hip and shoulder in the sagittal plane. The movement data was then used along with the dynamics of the body (as discussed in Section 5.2) to locate the position of its COM for each frame.

The Dorsiflexometer results were used to calculate the COM location using the methodology as described in Chapter 5. Both the SIP and DIP model analogy was used to calculate the COM position for the double-legged stance. The COM positions of the SIP, the DIP model and the video analysis were compared. The comparison shows how closely the models' predicted COM movement relates to the videographic analysed movement of the COM. Furthermore, the absolute error between the video analysis results and both models were calculated using Equation 6.3.1 and 6.3.2. Each subject's error was calculated for every time step and the maximum error and median was determined. The error is calculated for the COM movement along the X axis in the sagittal plane.

$$COM_{SIP\ error} = |COM_{video}(t) - COM_{SIP\ model}(t)| \tag{6.3.1}$$

$$COM_{DIP\ error} = |COM_{video}(t) - COM_{DIP\ model}(t)| \tag{6.3.2}$$

6.3.2 Results and discussions

Each subject's balance metrics were compared to themselves for the single and double-legged stance to show that the Dorsiflexometer is capable of distinguishing between balance capabilities. The metrics should indicate that each subject's balance is better when performing a two legged stance compared with single legged stance. Figure 6.5 and 6.6 compares the SI and Radius parameter values of each subject respectively. Furthermore, each subject's PSI and ES value is compared in Figure 6.7 and 6.8 respectively.

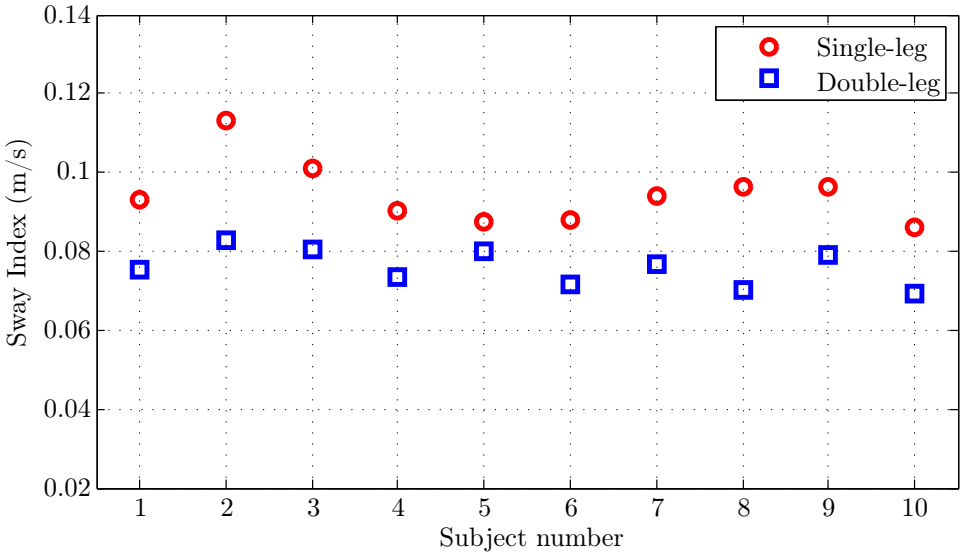

Figure 6.5 Comparison of each subject's sway index for the case of single and double-legged stance.

The SI factor reflects the average speed at which a subject's COP is shifted at the BOS. Figure 6.5 compares each subject's SI results to themselves for the single and double-legged stance cases. From the results, it is seen that each subject's SI is greater for single-legged stance compared to double-legged stance. Furthermore, the average and maximum SI for double-legged stance is less than the average and minimum SI value for single legged stance. These SI values reflect that for single-legged stance, subjects were forced to react faster and move their COP more regularly in a more jittery and twitchy manner to prevent themselves from falling over. The BOS for single legged stance is less than half the area of double-legged stance making the body even more unstable.

The radius parameter is equal to the smallest circle enclosing the area of a subject's COP movement. The measured results, as presented in Figure 6.6, show that all the subjects had a greater Radius parameter for double legged stance. The figure compares each subject's single-legged Radius parameter to their own double-legged radius parameter. Subjects with a small radius parameter are more prone to falling as a result of external perturbations since they have a smaller surface area span in which they are able to move their COP to counter the body's instability. Subjects with greater radius parameters are suited to resist falling from perturbations.

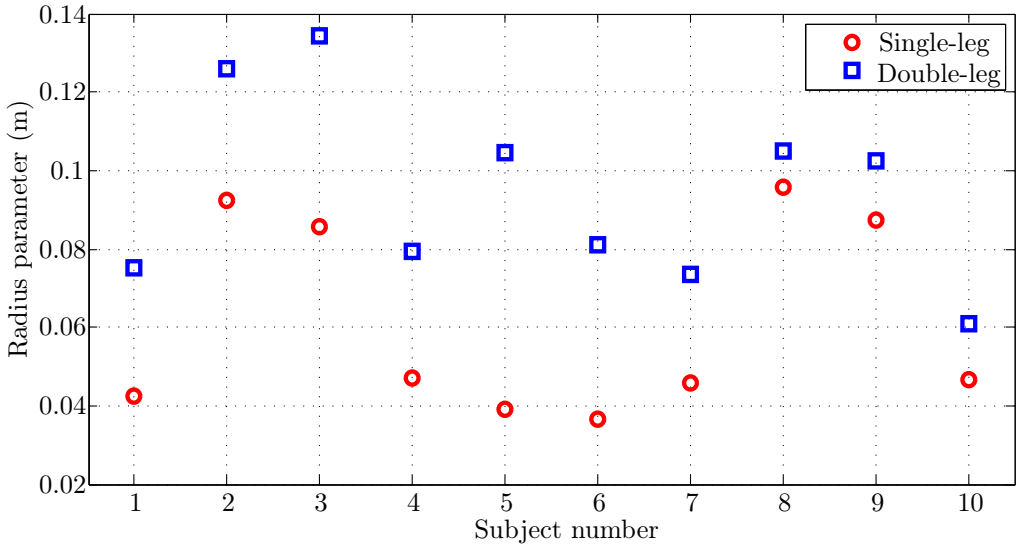

Figure 6.6 Radius parameters measured during the experiments.

The total stabilizing and destabilising ankle torque needed to keep the body upright can be characterised with the PSI. A larger PSI value signifies that greater ankle torque was used to keep the body upright. Figure 6.7 compares each subject's PSI for single and double-legged stance to themselves. The measured results presented in Figure 6.7 suggest that the PSI is greater for single legged stance. This relates strongly with the measured SI values which

indicated that subjects changed their COP at greater average speeds as large torques would be required to overcome the inertia of a fast moving body. The PSI factor is very subjective and should not be compared to a normative value, but rather to the PSI history of the individual. Only one subject had a PSI value slightly less for single leg than double-legged stance.

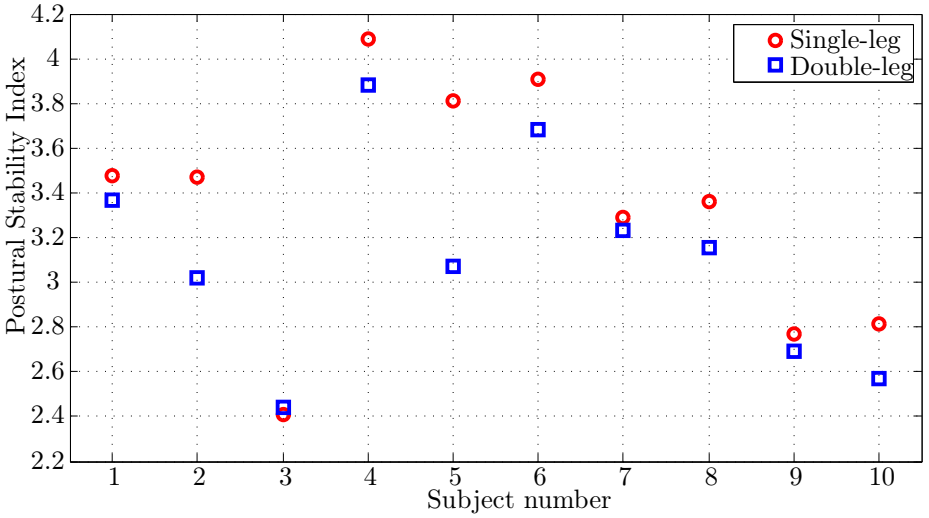

Figure 6.7 Comparison of each subject's calculated PSI.

Figure 6.8 compares each subject's single-legged stance ES value to their own double-legged stance ES value. For 70 % of the subjects the double legged stance yielded an ES value greater than single legged stance. The ES value compares a subject's maximum anterior and posterior sway angles to a normative overall sway angle. The subjects that were tested have an above normative ability to balance. The ES does however not distinguish the balance ability of subjects as directly as the SI, PSI and radius parameter.

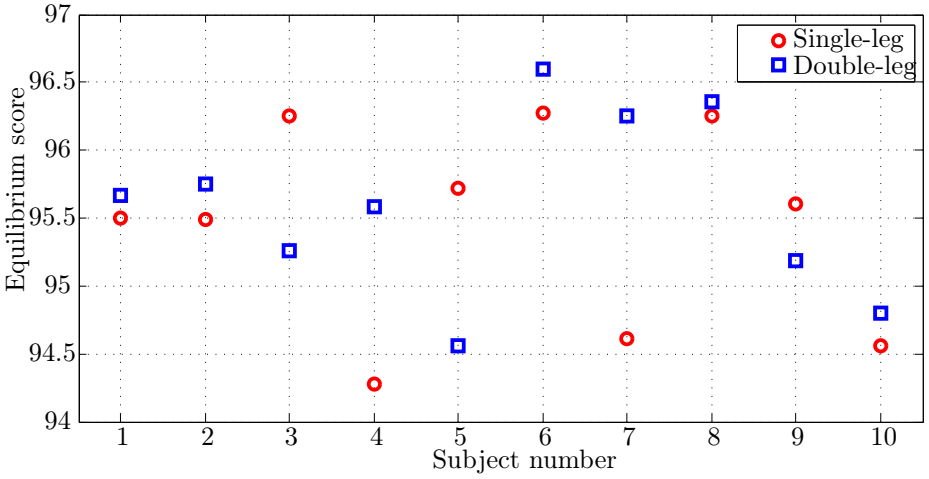

Figure 6.8 ES of single and double-legged stance.

Each subject's COM movement was calculated and modelled using the single and double inverted pendulum models and video analysis. Figure 6.9 shows an example of a randomly chosen subject's COM movement. In the figure, the COM movement of the videographic results are compared with the inverted pendulum model results. The DIP model predicted the COM movement of the subject with a higher accuracy than the SIP model. The DIP model is also very responsive and does not fall behind when the COM is displaced at greater velocities. When the subjects moved forward (positive X direction) at greater velocities the SIP model progressed very slowly resulting in inaccurate model predictions. These slower reactions of the SIP model is a result of inadequate ankle torque provided to the model. During tests, the subjects subconsciously used any means possible to maintain their balance on the perturbed platform, such as using ankle, knee, hip and torso flexion to balance their COM over their BOS. Subjects using a combination of joint flexions will have less ankle torque than a subject only making use of ankle flexion. Since the subjects did not solely make use of ankle flextion, their measured ankle torques were less, and therefore the SIP model did not follow the videographic results as accurately.

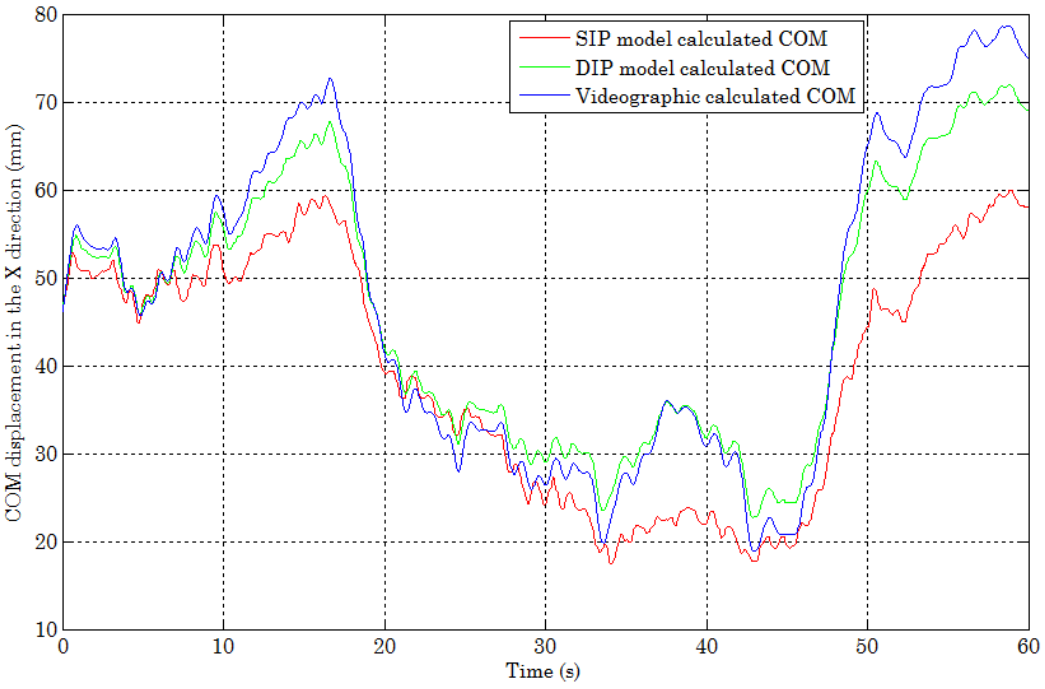

Figure 6.9 Comparison of videographic calculated and model predicted COM's.

Even though all of the subjects had different COM displacements, the model prediction trend stayed the same. The error of the inverted models compared to the video analysis results of the 10 subjects are presented in Ta-

ble 6.1. The maximum error between the video analysis and the SIP model for a subject is 36, 7 mm. The maximum error between the video analysis and the DIP model for a subject is 15, 9 mm. Furthermore, the maximum mean SIP model error is 22, 5 mm whereas the maximum mean DIP model error is less than half at 10, 1 mm. These results indicate that the DIP model simulate the body movement with less error than the SIP model. The DIP model is more accurate than the SIP model and a better means of modelling COM movement with the use of force plate data.

Table 6.1 Subject information and model accuracy.

Subject number	Subject height (m)	Maximum COM error of SIP model (mm)	Maximum COM error of DIP model (mm)	Mean SIP model error (mm)	Mean DIP model error (mm)
1	1,93	22,4	8,3	6,4	3,1
2	1,84	30,3	11,3	12,4	5,5
3	1,86	8,7	4,8	3,1	2,3
4	1,73	36,7	9,2	22,5	6,7
5	1,90	23,4	9,6	11,6	4,1
6	1,88	14,6	7,3	5,1	2,3
7	1,67	13,9	4,1	7,2	1,8
8	1,71	16,5	10,2	8,3	6,9
9	1,7	24,6	15,9	20,3	10,1
10	1,84	22,5	13,7	16,8	9,1

6.3.3 Conclusions

The aim of the experiment was to show that the Dorsiflexometer machine can be used to distinguish between levels of balance and to compare the derived inverted pendulum models to videographic analyses. A total of 10 subjects were tested. The results indicated that the calculated balance metrics can be used to categorise a subject's balance. The balance metrics indicated that when subjects balance on both legs their balance capabilities are greater compared to single leg balancing. Furthermore, both the SIP and DIP models simulate the COM movement of a subject fairly accurate. The SIP and DIP models have a maximum COM error of 36, 7 mm and 15, 9 mm respectively. The DIP model simulates the COM movement with a greater accuracy compared with the SIP model.

6.4 Balance Response of Seafarers During Still and Rough Sea Conditions

Seafarers are constantly exposed to varying ground reaction forces due to extreme weather conditions. These forces may lead to the progression of osteoarthritis and musculoskeletal injuries which strongly affect a person's ability to balance. The force plate of the Dorsiflexometer machine was therefore used to measure the ground reaction forces which seafarers are exposed to on shipping vessels during still and rough sea conditions. The ground reaction forces were used to calculate each subject's SI and weight factor (WF). Each subject's SI and WF is compared for the different test conditions.

6.4.1 Experimental procedure

The reaction forces and moments in the X, Y and Z direction of 18 subjects were measured using the AMTI force plate designed for static and gait studies. Each subject was tested on four occasions. Informed consent was obtained from each subject before any tests were conducted. The AMTI MiniAmp signal conditioner and amplification was used to digitize the readings from analogue to a 12 bit digital format. A laptop computer was used to calibrate and process the recorded data.

The AMTI MiniAmp has a standard anti-aliasing low pass filter, 1000 Hz cut-off, for each channel. All test readings were sampled at 50 Hz for a duration of 60 seconds, resulting in 3000 force and moment measurements in each direction. The force plate was calibrated before the tests were conducted. The measurements were performed on-board the S.A. Agulhas II Polar Supply and Research vessel. The vessel was built by STX Finland at the Rauma Shipyard and entered service in April 2012. The purpose of the ship is to support the South African National Antarctic Expedition (SANAE IV) base on the Antarctic continent (Soal and Bekker, 2013). The vessel is equipped with laboratories which are used for conducting scientific research in the Southern Ocean. Furthermore, the vessel is utilized to carry cargo, bunker oil, helicopter fuel and passengers. Table 6.2 contains the main dimensions of the S.A. Agulhas II and the service speed.

Table 6.2 Main dimensions of the S.A. Agulhas II

Dimension	Quantity
Beam	$\leq 21,7$ m
Draught, design	$\leq 7,65$ m
Length, bpp	$\leq 121,8$ m
Average service speed	≤ 14 knots

A total of 18 healthy subjects (range: 21 to 45 years), 8 males and 10 females, were tested on-board the S.A. Agulhas II on the 2013-2014 Antarctic voyage. Each subject was tested twice during still conditions and twice during rough conditions. Still conditions refer to conditions on-board the ship when it was stationary against an ice wall with no swell present. Rough conditions refer to when the vessel was in open seas with swells greater than 6 meters. All measurements were conducted in the starboard operations laboratory on deck 3, as indicated by 'O' in Figure 6.10.

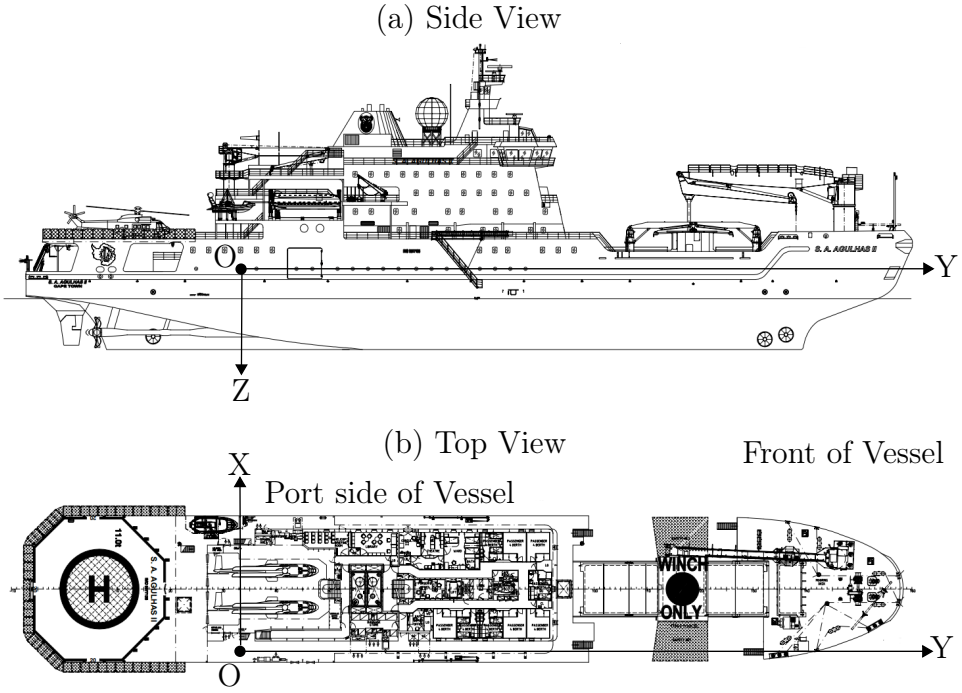

Figure 6.10 Drawing of scaled vessel and test location of data recordings.

Tests were conducted one subject at a time. Each subject was instructed to stand normally on the force plate, facing the front of the vessel. A 60 second measurement was performed without the subject leaving the force plate. The subject was then instructed to reposition themselves on the force plate to face the port side of the vessel. A second measurement was then repeated, again without the subject leaving the force plate. The same test procedure was followed during rough conditions, first facing the front and thereafter the port side of the vessel. Tests were repeated in cases where the subjects lost their balance and inadvertently stepped off the force plate.

The recorded data was used to calculate the ground reaction forces, the SI and WF of the subjects. The ground reaction force is known as the force which acts on the foot to keep a subject pastorally upright and stable during unsupported standing (Winter, 2009). This three-dimensional force vector

consists of two shear components (F_x and F_y) acting along the support surface and a vertical component (F_z) acting perpendicular to the support surface. The resultant ground reaction force R, is calculated using Equation 6.4.1.

$$R_i = \sqrt{F_{x,i}^2 + F_{y,i}^2 + F_{z,i}^2} \tag{6.4.1}$$

In the equation, $F_{x,i}$, $F_{y,i}$ and $F_{z,i}$ represents the measured forces in the X, Y and Z direction respectively of the i^{th} sample measurement in time. The resultant ground reaction forces measured during rough conditions are compared to the resultant ground reaction forces measured during still conditions as shown in Equation 6.4.2.

$$WF_i = \frac{R_{i,rough}}{R_{i,still}} \tag{6.4.2}$$

The weight factor is represented by WF. The weight factor signifies the comparison of the resultant ground reaction force measured during still and rough conditions. It gives an indication as to how a subject's weight is varied and how much extra force is applied to the joints during rough conditions as opposed to still conditions.

Human balance is the ability to maintain the body upright in an equilibrium position by moving the COG over the base of support (Browne and O'Hare, 2001). Balance can either refer to postural steadiness, i.e. static, or postural stability, i.e. dynamic. Postural steadiness captures the characteristics of postural sway during quiet standing. Postural stability characterizes the postural response of the body as a result of an external perturbation (Chaudhry *et al.*, 2011). The ability to maintain balance during still conditions around the vessel is characterized as postural steadiness and the ability to maintain balance during rough conditions is characterized as postural stability.

SI quantifies a subject's ability to balance and gives the average sway movement of the body during a test (Botha, 2005). Thus, it calculates the average speed at which the resultant ground reaction force of a subject changes its location. The SI for a 60 second test of 3000 samples is calculated using Equation 4.2.4. COP_x and COP_y is calculated as shown in Equation 4.2.2 and 4.2.3 respectively. A sample measurement was taken every 20 milliseconds.

6.4.2 Results

The results of the measured ground reaction forces, which seafarers working on vessels during rough sea conditions are exposed to, are presented below. Investigations into how the seafarers' ability to balance is affected are also presented. A total of 72 successful tests were performed.

Figure 6.11 shows how the WF, of a random chosen subject, fluctuates over a period of 60 seconds. This indicates that the ground reaction force, and therefore the forces in the knee and hip joints, varied between $1,23$ and $0,86$ times the normal force between calm and rough conditions. The WF has a varying sinusoidal waveform as a result of steady rolling and pitching of the boat with no harsh judders or slams present. The maximum and minimum WF's measured were $1,46$ and $0,66$ respectively. Thus, the ground reaction forces acting on the body through the feet can increase up to $1,46$ times the weight of the body, resulting in extra strain on the joints. The cyclic nature of the applied force may lead to possible fatigue in the cartilage as discussed in Section 2.6.

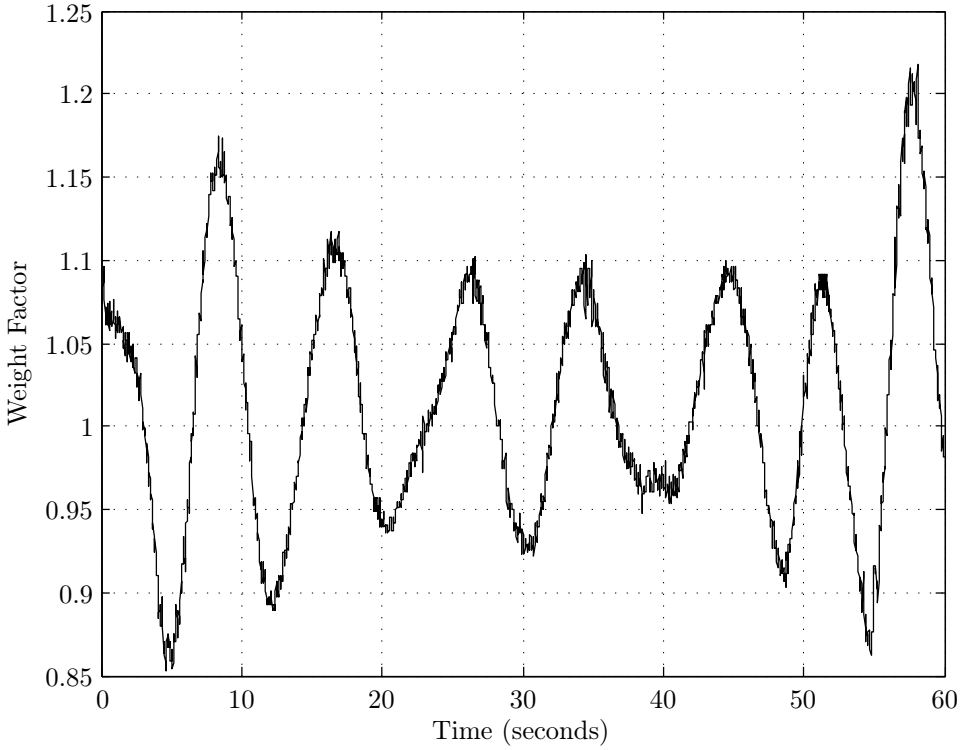

Figure 6.11 Weight factor variation during rough sea conditions.

To keep the body upright, the COP changes constantly. Figure 6.12 compares a randomly chosen subject's COP displacement during still conditions, opposed to that of rough conditions, while facing the front of the vessel. The COP is shifted around more frequently at faster speeds and is distributed on a greater surface area during rough conditions. It shows that the body sways to an extreme extent to keep itself in an upright position during rough conditions.

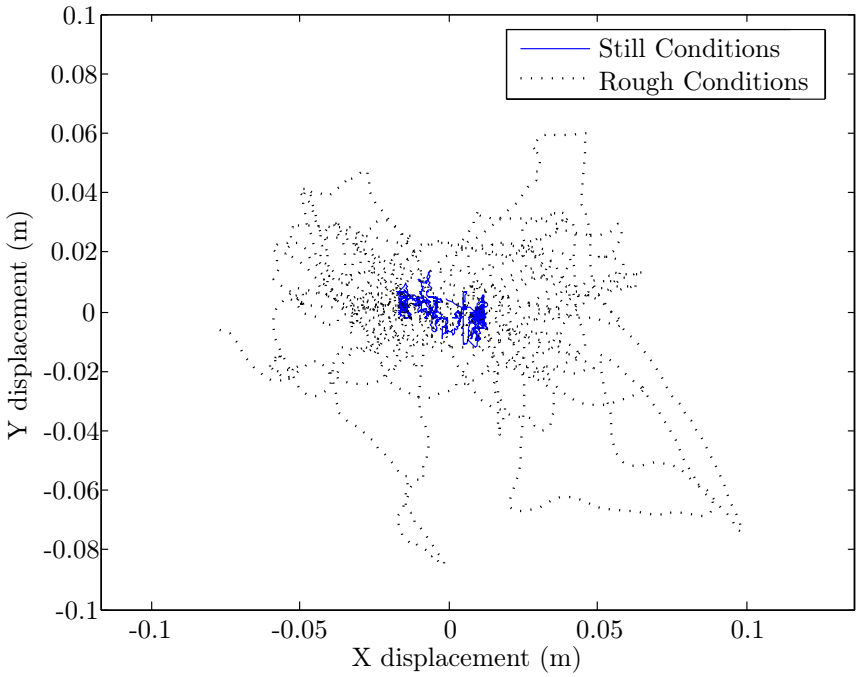

Figure 6.12 Comparison of COP during still and rough sea conditions.

Each subject's SI for all four test conditions were calculated using Equation 4.2.4 and is displayed in Figure 6.13. The results show that each subject's SI for the tests done during still conditions are mostly similar. For the majority of the subjects, the SI tested during rough conditions is also in close proximity. However, there is a noticeable difference when comparing each subject's SI tested during still and rough conditions facing the front and the port side of the ship. The SI of all the subjects tested during rough conditions is more than double that of still conditions. On closer observation, it was noted that more than 70 % of the subjects' SI is greater when facing the port side of the ship, both during still and rough conditions.

The box plot in Figure 6.14 compares the SI of the four different test conditions. During still conditions the SI results are very similar; however, the mean and maximum SI is greater when facing the port side of the vessel. During rough conditions, the mean and maximum SI is also greater when facing the port side of the vessel. This can be explained by the fact that the ship's length is much longer than the wavelength of the periodically oncoming waves, and therefore has smaller pitching moments. The breadth however, is usually similar or smaller than the wavelength of the oncoming waves, thus causing the ship to have larger rolling moments in the troughs of the waves.

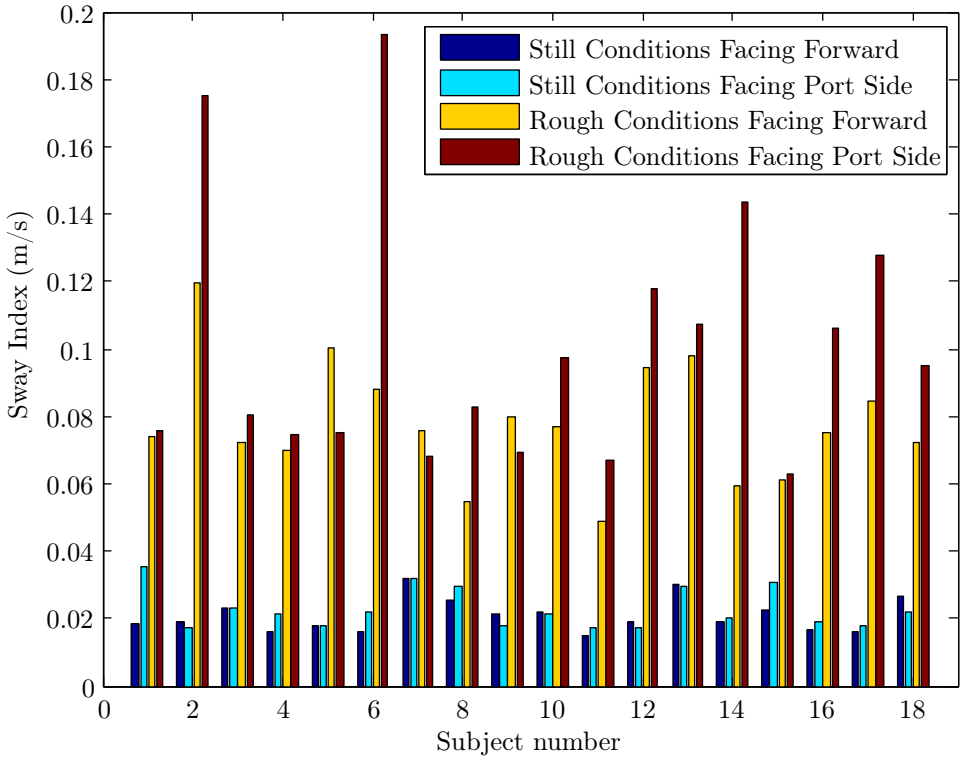

Figure 6.13 Comparison of the SI during four different testing conditions.

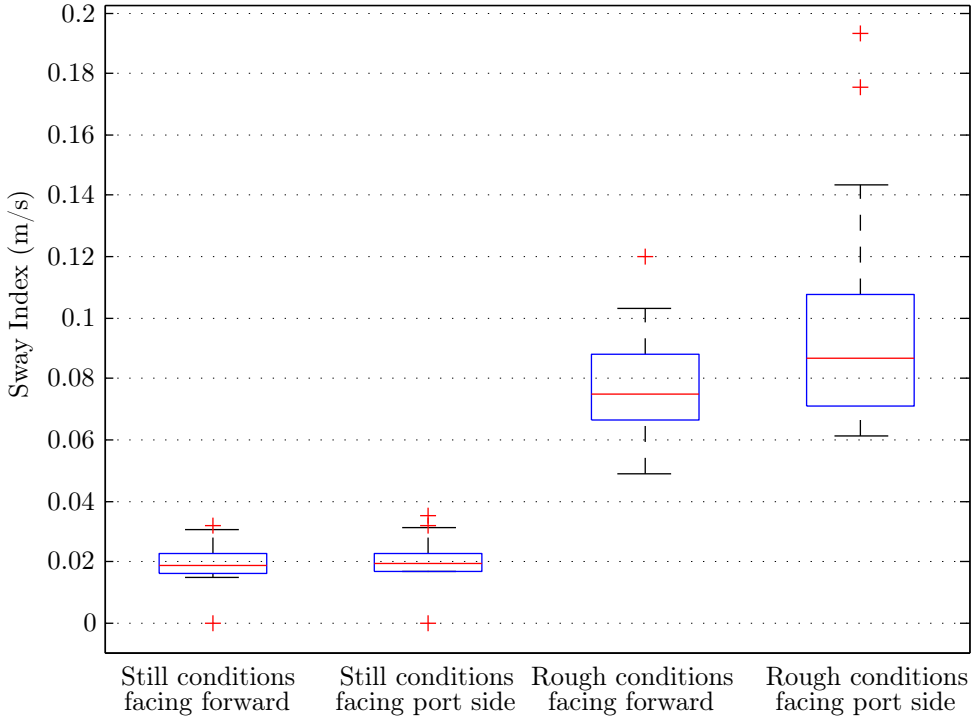

Figure 6.14 Deviation of the SI during four different testing conditions.

The SI for either facing the front or port side of the vessel is far greater during rough conditions when compared to still conditions, with a mean still-front to rough-front factor of 4 and a still-port to rough-port factor of $4,4$. This shows that more frequent, faster reactions and greater body sway activity is required to keep the body upright during rough conditions, compared with still conditions.

6.4.3 Conclusions

This experiment showed that the body experiences a fluctuation in ground reaction forces during rough sea conditions. Resultant forces with a maximum of up to $1,46$ and minimum of $0,67$ times the body's normal weight was measured and is characterized by the WF. A subject's SI during rough conditions is more than double the SI during still conditions. This indicates that seafarers therefore require more body activity and joint movement to keep themselves upright. Further research can be done to investigate the effects this might have on the body and whether this increase in body activity and extra forces aggregate the development of OA. Thresholds or guidelines can be established to show long term effects caused to the body. The damage caused to the knee and hip joints, due to the frequency and amplitudes of the measured ground reaction forces, needs to be determined.

Chapter 7

DISCUSSION, RECOMMENDATIONS AND CONCLUSION

This chapter gives a brief overview of the project. Suggestions are made for further studies and alterations which might improve the functionality of the Dorsiflexometer. A conclusion of the main findings is also presented.

7.1 Discussion

The Dorsiflexometer was designed and built with the intent of making physiological assessment methods accessible in the medical field. The machine aids in diagnosing patients with balance disorders and can further be used to identify certain activities which can help and speed up the rehabilitation process of injured athletes. It provides valuable information about a patient's postural control system and strategies used to maintain balance when perturbed. This information can be used by doctors to prescribe exercises or activities which can help patients improve their balance. Patient information is recorded with the use of a single force plate which records the body reaction forces while being exposed to forceful perturbations.

Two design methods were used to move the platform. The first design method made use of two gear sets driven by a Nema 34 stepper motor to oscillate the platform. This method was however not selected as it introduced vibration problems on the force plate, which is discussed in Chapter 3. The second method oscillates the platform with the use of a lead screw linear actuator also driven by a Nema 34 stepper motor. This method proved to be satisfactory and solved the vibration problem. An Arduino^{TM} micro-controller is used to control the rotational velocities and number of rotations of the stepper motor.

A computer program, written in Matlab, is used to operate the machine and micro-controller. The computer program simplifies the testing procedure in order for the machine to be operated by medical personnel with minimum training required, as discussed in Chapter 4. The program consists of a number of graphical user interfaces which instructs the operator of the requirements for each step during the testing procedure. Each subject's results and personal information is stored on a data base on the computer. The program outputs the measured results in digital format and calculates important balance metric factors regarding the test results. Qualified medical practitioners can assess the results and diagnose the patients accordingly. For a test, the patient is perturbed by firstly rotating the platform forwards, then backwards and then forward again to its starting position. The machine is therefore capable of conducting a static and dynamic test.

The movement of the body's centre of mass during such a perturbation gives insight in the balance behaviour and balance strategies used by subjects. The centre of mass movement cannot directly be recorded with a force plate. Therefore, two models which uses a subject's force plate recorded data to simulate the centre of mass movement in the sagittal plane, were derived. The first model simulates the body as a single inverted pendulum which only makes use of ankle flexion to maintain an upright posture. The entire body above the ankles is taken as a single segment. The second model simulates the body as a double inverted pendulum as discussed in Chapter 5. For the double inverted pendulum model, the body is split into two segments and uses both ankle and hip flexion to maintain an upright and stable posture. Human anthropometric data is used to combine body segments and calculate inertial forces for both single and double inverted pendulum models.

Various experiments were conducted to test the accuracy of the machine. The accuracy of the Dorsiflexometer was compared to the Biodex machine, which is a commercially available static balance testing machine. To show that the results obtained from the machine can be used to distinguish between balance capabilities, the balance metrics of subjects performing a single and then a double-legged stance test was compared. Furthermore, the results obtained from the inverted pendulums were compared to videographic results. A final experiment was conducted aboard the S.A Agulhas II to compare the balance metric factors of seafarers during still and rough sea conditions.

7.2 Recommendations

The platform was raised off the ground such that the mechanism which oscillates the platform could fit underneath it and in order for the platform to be

rotated about the patient's ankles. A step must thus be used for elderly people undergoing a balance assessment test. The mechanism rotating the platform can be designed to take up less space or that it doesn't need to be located underneath the platform. The platform can then be lowered making it easier for people to step onto the platform.

The linear actuator of the Dorsiflexometer is driven by a Nema 34 stepper motor. The motor is secured to a 'L' bracket which is directly bolted to the base plate. This fastening method of metal on metal causes the motor to be excessively noisy when turning. A casing enclosing the motor and other moving parts below the oscillating platform can be made to suppress the motor noise or a different fastening method can be used.

As an engineering requirement, the structure of the machine has to be strong and stable. The machine is therefore constructed from steel plates and pipes. The steel structure and force plate makes the Dorsiflexometer heavy and difficult to relocate. A wheel system can be designed such that the machine can be moved around with ease.

The Dorsiflexometer tests a subject's ability to balance by enforcing both dorsiflexion and plantar flexion of the ankle in the sagittal plane. Even though this gives an overall estimation of a subject's balance, a second degree of rotation can be added to the machine to further enforce eversion and inversion of the ankle in the frontal or coronal plane. The SIP and DIP model experiments can be retested by constraining the subjects undergoing the test to only use their ankles with which to balance as a verification of the model by means of physical struts of some form.

Statistical analysis should be used to determine and identify a correlation between the numerous balance metrics. This will help establish the weight bearing and parameter estimation of each balance metric. Underlying trends and patterns connecting the balance metrics with balance performance capabilities can further be discovered.

7.3 Conclusion

For this project, a new model of the Dorsiflexometer machine was designed, built and tested. The design of the new Dorsiflexometer is based on the principals and theory of the older model built by Botha (2005). The new Dorsiflexometer is operated from a complete new user interface program which gives the operator the ability to control the machine from a laptop computer. The results are outputted in digital format on the computer. A database containing the results of each tested patient, which can be used for comparison

reasons, are furthermore stored on the computer. A single force plate is used to measure the reaction forces of a patient while undergoing a balance assessment test. The machine has a new structural design. The platform and force plate which the patient stands on were lowered such that the platform now rotates about the ankles of the patient. A new rotational mechanism, working with a linear actuator and lever arm, is used to rotate the platform.

The capabilities of the new Dorsiflexometer was tested in several experiments to verify whether it is capable of accurately testing the balance abilities of a patient. Firstly the Dorsiflexometer was compared with the Biodex machine, which is commercially available and has similar static balance testing functions. The testing procedure of the Dorsiflexometer is much quicker and easier to conduct than its rival. The Dorsiflexometer results were similar to the results of the Biodex machine. Furthermore the Dorsiflexometer was used to distinguish between the balance capabilities of patients in either a single or double-legged stance.

A clear contrast was noted in the results of the single and double-legged stance experiment. This proved the potential of the machine to be used in the clinical setting to test the balance capabilities of injured or ill patients. Derived inverted pendulum models, which uses a subjects force plate recorded data to predict the movement of the COM, were tested. The model predicted data showed a close correlation with the videographic analysed results. At greater COM movement velocities, the SIP model struggled to react accordingly. The DIP model sustained the COM movement velocity and therefore models the movement of the body COM with greater accuracy. The DIP model simulation should be used to simulate the COM movement of a subject.

The development and improvements on the Dorsiflexometer proofed to be meaningful in the study of human balance. It is now recommended that the Dorsiflexometer be considered as being ready for field trials by medical practitioners. Future studies might refine this useful machine to be beneficial for different types of patients suffering from balance incompetencies.

List of References

Aagaard, P., Simonsen, E.B., Beyer, N., Larsson, B., Magnusson, P. and Kjaer, M. (1997). Isokinetic muscle strength and capacity for muscular knee joint stabilization in elite sailors. *International journal of sports medicine*, vol. 18, no. 7, pp. 521–525.

Arnold, B.L. and Schmitz, R.J. (1998). Examination of balance measures produced by the biodex stability system. *Journal of athletic training*, vol. 33, no. 4, p. 323.

BenAbdelkader, C. and Yacoob, Y. (2008). Statistical estimation of human anthropometry from a single uncalibrated image. *Computational Forensics*, pp. 200–20.

Benvenuti, F., Mecacci, R., Gineprari, I., Bandinelli, S., Benvenuti, E., Ferrucci, L., Baroni, A., Rabuffetti, M., Hallett, M., Dambrosia, J.M. *et al.* (1999). Kinematic characteristics of standing disequilibrium: reliability and validity of a posturographic protocol. *Archives of physical medicine and rehabilitation*, vol. 80, no. 3, pp. 278–287.

Biodex (2014). *Biodex Medical Systems*. Biodex Medical Systems, 20 Ramsey Road Shirley, New York 11967-4704.
Available at: `http://www.biodex.com/`

Bloem, B.R., Steijns, J.A. and Smits-Engelsman, B.C. (2003). An update on falls. *Current opinion in neurology*, vol. 16, no. 1, pp. 15–26.

Botha, J. (2003). Dorsiflexion of foot device.

Botha, J. (2005). *The Development of a Device for the Investigation of Dorsiflexion range of the Ankle with a Capacity to Measure Pathology, Recovery and Pharmacological Benefit*. Master's thesis, Univercity of Stellenbosch.

Botha, J., Dobson, R. and Driver-Jowitt, J. (2007). Development of a device to measure human response to dorsiflexural perturbation. *R & D Journal*, vol. 23, pp. 28–34.

Browne, J. and O'Hare, N. (2001). Review of the different methods for assessing standing balance. *Physiotherapy*, vol. 87, no. 9, pp. 489 – 495. ISSN 0031-9406.
Available at: `http://www.sciencedirect.com/science/article/pii/S0031940605606967`

Budynas, J.K.N.R.G. (2008). *Shigley's mechanical engineering design*. McGraw-Hill.

Chaudhry, H., Bukiet, B., Ji, Z. and Findley, T. (2011). Measurement of balance in computer posturography: Comparison of methods: A brief review. *Journal of Bodywork and Movement Therapies*, vol. 15, pp. 82 – 91. ISSN 1360-8592. Available at: `http://www.sciencedirect.com/science/article/pii/S1360859208000338`

Chaudhry, H., Findley, T., Quigley, K.S., Bukiet, B., Ji, Z., Sims, T. and Maney, M. (2004). Measures of postural stability. *Journal of rehabilitation research and development*, vol. 41, pp. 713–720.

Chaudhry, H., Findley, T., Quigley, K.S., Ji, Z., Maney, M., Sims, T., Bukiet, B. and Foulds, R. (2005). Postural stability index is a more valid measure of stability than equilibrium score. *Journal of rehabilitation research and development*, vol. 42, no. 4, p. 547.

Clark, S., Rose, D.J. and Fujimoto, K. (1997). Generalizability of the limits of stability test in the evaluation of dynamic balance among older adults. *Archives of physical medicine and rehabilitation*, vol. 78, no. 10, pp. 1078–1084.

Colobert, B., CrÃ©tual, A., Allard, P. and Delamarche, P. (2006). Force-plate based computation of ankle and hip strategies from double-inverted pendulum model. *Clinical Biomechanics*, vol. 21, no. 4, pp. 427 – 434. ISSN 0268-0033. Available at: `http://www.sciencedirect.com/science/article/pii/S0268003305002950`

Craig, J.J. (2005). *Introduction to robotics: mechanics and control*. Pearson/Prentice Hall Upper Saddle River, NJ, USA:.

Dean, E.M., Griffiths, C.J. and Murray, A. (1986). Stability of the human body investigated by sway magnetometry. *Journal of medical engineering & technology*, vol. 10, no. 3, pp. 126–130.

Dempster, W.T. (1955). Space requirements of the seated operator: geometrical, kinematic, and mechanical aspects of the body, with special reference to the limbs.

Diener, H.-C., Dichgans, J., Bacher, M. and Gompf, B. (1984). Quantification of postural sway in normals and patients with cerebellar diseases. *Electroencephalography and clinical neurophysiology*, vol. 57, no. 2, pp. 134–142.

Drillis, R., Contini, R. and Bluestein, M. (1964). Body segment parameters. *Artificial limbs*, vol. 8, no. 1, pp. 44–66.

Duncan, P.W., Weiner, D.K., Chandler, J. and Studenski, S. (1990). Functional reach: a new clinical measure of balance. *Journal of gerontology*, vol. 45, no. 6, pp. M192–M197.

Edmayr, W. (2011 October). Dorsiflexometer.

Elliott, C. and Murray, A. (1998). Repeatability of body sway measurements; day-to-day variation measured by sway magnetometry. *Physiological measurement*, vol. 19, no. 2, p. 159.

Felson, D.T. (2004). An update on the pathogenesis and epidemiology of osteoarthritis. *Radiologic clinics of North America*, vol. 42, no. 1, pp. 1–9.

Fernie, G.R. and Holliday, P. (1978). Postural sway in amputees and normal subjects. *The Journal of Bone & Joint Surgery*, vol. 60, no. 7, pp. 895–898.

Fischer, S.L. and Dickerson, C.R. (2012). Applying psychophysics to prevent overexposure: On the relationships between acceptable manual force, joint loading, and perception. *International Journal of Industrial Ergonomics*.

Fox, S.I. (2009). *Fundamentals of human physiology*. McGraw-Hill.

Furman, J. (1994). Posturography: uses and limitations. *Baillière's clinical neurology*, vol. 3, no. 3, p. 501.

Galley, P. and Forster, A. (1982). *Human movement: An introductory text for physiotherapy students*. C. Livingstone.

Gatev, P., Thomas, S., Kepple, T. and Hallett, M. (1999). Feedforward ankle strategy of balance during quiet stance in adults. *The Journal of physiology*, vol. 514, no. 3, pp. 915–928.

Greenwood, D.T. (2003). *Advanced dynamics*. Cambridge University Press Cambridge.

Guilak, F. and Hung, C.T. (2005). *Physical regulation of cartilage metabolism*. Lippincott Williams & Wilkins, Philadephia.

Guskiewicz, K.M., S.E, R. and S.W, M. (2001). Why the clinical test of sensory integration of balance (ctsib) for concussion baseline balance testing?

Haight, D.J. (2012). *The effects of walking speed on knee joint loading estimated via musculoskeletal modeling*. Ph.D. thesis, Colorado State University.

Incorporation, A.M.T. (2010 October). *AMTI Force and Motion*. Advanced Mechanical Technology, Inc., 176 Waltham Street, Watertown, MA 02472-4800 USA. Available at: `http://www.amti.biz/`

Ishida, A., Imai, S. and Fukuoka, Y. (1997). Analysis of the posture control system under fixed and sway-referenced support conditions. *Biomedical Engineering, IEEE Transactions on*, vol. 44, no. 5, pp. 331–336.

Ji, Z., Findley, T., Chaudhry, H. and Bukiet, B. (2004). Computational method to evaluate ankle postural stiffness with ground reaction forces. *Journal of Rehabilitation Research & Development*, vol. 41, no. 2.

Kapteyn, T., W. Bles, h.J.N., L. Kodde, C.M. and Mol, J. (1983). Standardization in platform stabilometry being a part of posturography. *Agressologie*, vol. 24, no. 7, pp. 321–326.

Karlsson, A. and Lanshammar, H. (1997). Analysis of postural sway strategies using an inverted pendulum model and force plate data. *Gait & Posture*, vol. 5, no. 3, pp. 198–203.

Levin, O. and Mizrahi, J. (1996). An iterative model for estimation of the trajectory of center of gravity from bilateral reactive force measurements in standing sway. *Gait & Posture*, vol. 4, no. 2, pp. 89 – 99. ISSN 0966-6362.
Available at: `http://www.sciencedirect.com/science/article/pii/0966636295010378`

Levine, D., Whittle, M.W., Beach, J.A. and Ollard, P.G. (1996). Test-retest reliability of the chattecx balance system in the patient with hemiplegia. *Journal of rehabilitation research and development*, vol. 33, no. 1, pp. 36–44.

Liston, R.A. and Brouwer, B.J. (1996). Reliability and validity of measures obtained from stroke patients using the balance master. *Archives of physical medicine and rehabilitation*, vol. 77, no. 5, pp. 425–430.

Lockhart, T.E., Woldstad, J.C. and Smith, J.L. (2003). Effects of age-related gait changes on the biomechanics of slips and falls. *Ergonomics*, vol. 46, no. 12, pp. 1136–1160.

Mackie, H., Sanders, R. and Legg, S. (1999). The physical demands of olympic yacht racing. *Journal of Science and Medicine in Sport*, vol. 2, no. 4, pp. 375–388.

Murray, M., Seireg, A., Sepic, S.B. *et al.* (1975). Normal postural stability and steadiness: quantitative assessment. *J Bone Joint Surg Am*, vol. 57, no. 4, pp. 510–516.

Nashner, L.M. and Peters, J.F. (1990). Dynamic posturography in the diagnosis and management of dizziness and balance disorders. *Neurologic clinics*.

Önell, A. (2000). The vertical ground reaction force for analysis of balance? *Gait & posture*, vol. 12, no. 1, pp. 7–13.

Pollock, A.S., Durward, B.R., Rowe, P.J. and Paul, J.P. (2000). What is balance? *Clinical rehabilitation*, vol. 14, no. 4, pp. 402–406.

Ratzlaff, C.R., Koehoorn, M., Cibere, J. and Kopec, J.A. (2012). Is lifelong knee joint force from work, home, and sport related to knee osteoarthritis? *International journal of rheumatology*, vol. 2012.

Redfern, M.S., Yardley, L. and Bronstein, A.M. (2001). Visual influences on balance. *Journal of anxiety disorders*, vol. 15, no. 1, pp. 81–94.

Schaafsma, J.D., Giladi, N., Balash, Y., Bartels, A.L., Gurevich, T. and Hausdorff, J.M. (2003). Gait dynamics in parkinson's disease: relationship to parkinsonian features, falls and response to levodopa. *Journal of the neurological sciences*, vol. 212, no. 1, pp. 47–53.

Seedhom, B. (2006). Conditioning of cartilage during normal activities is an important factor in the development of osteoarthritis. *Rheumatology*, vol. 45, no. 2, pp. 146–149.

Soal, K. and Bekker, A. (2013). Whole-body vibration comfort on the s.a. agulhas ii polar supply and research vessel during a voyage to antarctica. In: *48th United Kingdom Conference on Human Response to Vibration*.

Stokes T, Theunissen C, L.M.G.S.W.M.B. (2012). Full scale ice measurement mini-seminar on-board the s. a. agulhas ii. In: *Stias Wallenberg Conference*.

Winter, D.A. (1995). Human balance and posture control during standing and walking. *Gait & posture*, vol. 3, no. 4, pp. 193–214.

Winter, D.A. (2009). *Biomechanics and motor control of human movement*. John Wiley & Sons.

Wright, B. (1971). A simple mechanical ataxia-meter. *The Journal of physiology*, vol. 218, p. 27P.

Zinke-Allmang, M. (2008). *Physics for the Life Science*. Nelson Education Limited.

Appendices

Appendix A

MEASURING INSTRUMENTATION

The commercially available instrumentation that was used for the manufacturing of the Dorsiflexometer is presented in this appendix. Figure A.1, A.2 and A.3 presents the specifications of the AMTI force plate. The force plate is used to measure the reaction forces and moments of a patient while they are perturbed. Figure A.4 presents the AMTI mini amplifier which amplifies and converts the force plate signal. For more information regarding the AMTI instrumentation refer to Incorporation (2010).

Furthermore, the information sheet of the Nema 34 stepper motor, which drives the linear actuator to perturb the platform, is presented in Figure A.5. The micro-step driver and micro-controller, used to configure the movement and rotational speed of the stepper motor, is presented in Figure A.6 and A.7.

AMTI
FORCE AND MOTION

www.AMTI.biz | sales@amtimail.com

OR6-7-1000 SPECIFICATIONS

AMTI's OR6-7 is the "standard size" force plate for gait studies and is used in hundreds of labs around the world. High sensitivity, low crosstalk, excellent repeatability and long-term stability make this platform an ideal candidate for research and clinical studies.

Units: English ▼ Capacity: 1000 ▼

Dimensions (WxLxH)	18.25 x 20 x 3.25 in	**Mounting hardware**	Recommended
Weight	62 lb.	**Sensing elements**	Strain gage bridge
Channels	Fx, Fy, Fz, Mx, My, Mz	**Amplifier**	Required
Top plate material	Aluminum	**Analog outputs**	6 Channels
Temperature range	0 to 125°F	**Digital outputs**	None
Excitation	10V maximum	**Crosstalk**	< 2% on all channels
Fx, Fy, Fz hysteresis	± 0.2% full scale output	**Fx, Fy, Fz non-linearity**	± 0.2% full scale output

Channel	**Fx**	**Fy**	**Fz**	**Units**	**Mx**	**My**	**Mz**	**Units**
Capacity	500	500	1000	lb	10000	10000	5000	in-lb
Sensitivity	3	3	0.75	µv/v-lb	0.18	0.18	0.38	µv/v-in-lb
Natural frequency	280	280	460	Hz	-	-	-	Hz

Published specifications subject to change w ithout notice.

Last modified:2010-10-2

Figure A.1 AMTI force plate specifications.

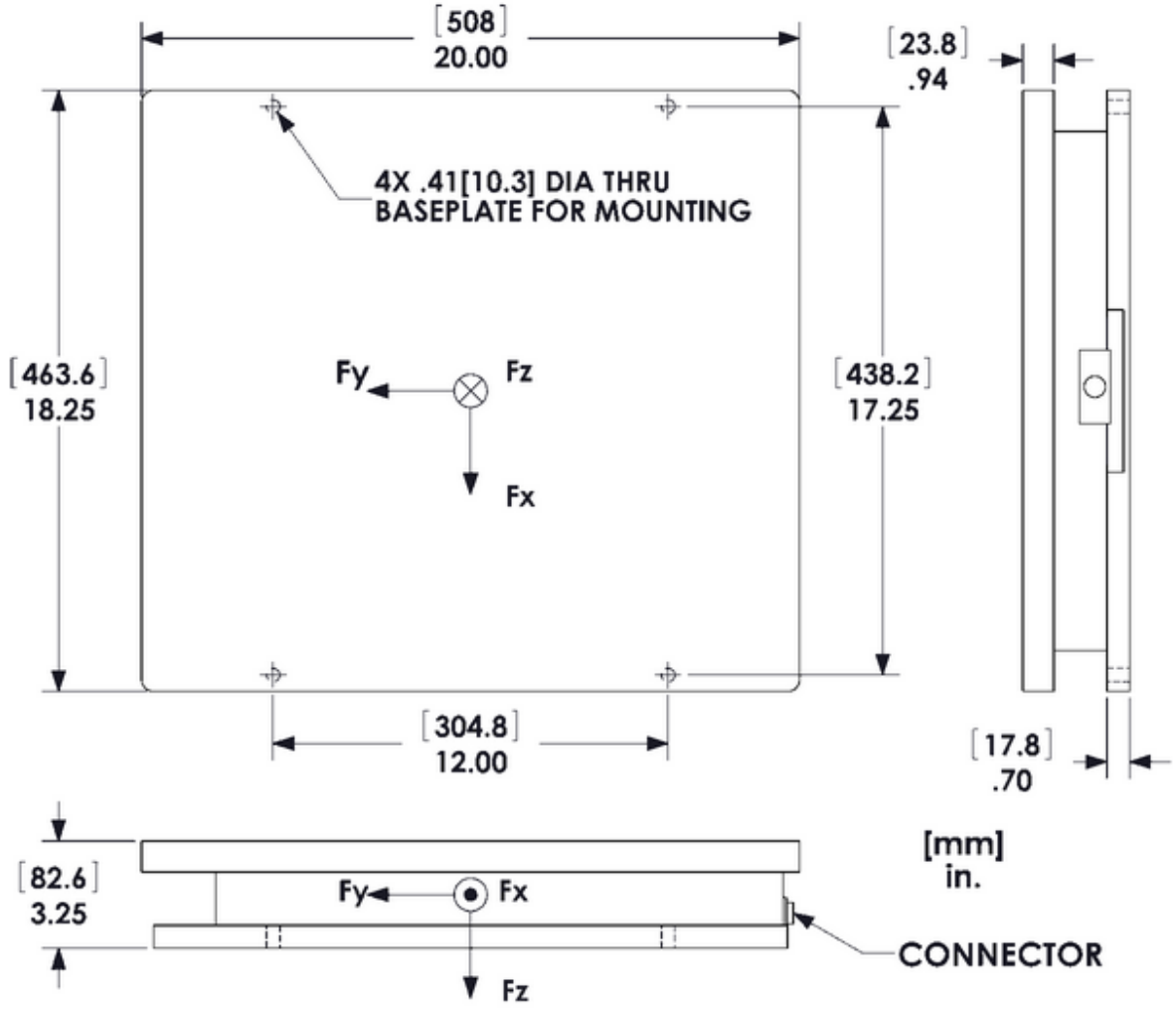

Figure A.2 AMTI force plate dimensions and specifications.

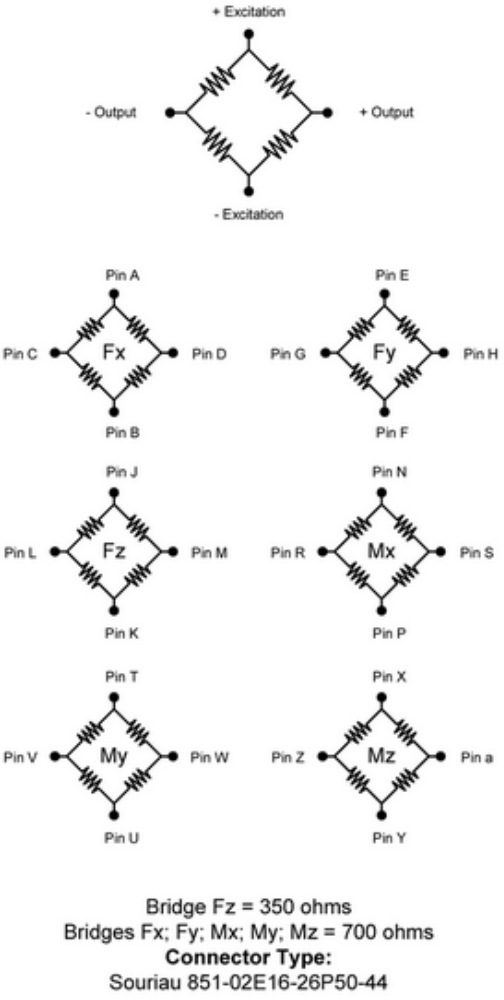

Figure A.3 AMTI force plate strain gage formation.

AMTI
FORCE AND MOTION

www.AMTI.biz | sales@amtimail.com

MINIAMP

Print-friendly version

The MiniAmp is a popular, economical solution for signal conditioning and amplification of AMTI?s multi-axis force plates and force sensors. Features include:

- Three user-selectable gains for each channel
- Three user-selectable excitation voltages for each channel
- Automatic balancing of strain gage bridges initiated by front-panel button or by software
- Two-pole, low-pass filter for each channel with a 1000 Hz cutoff
- Six channels of analog output with anti-aliasing filters
- Digital output via RS232 or USB (with converter)
- Manufactured under the ISO 13485:2003 and ISO 9001:2008 quality systems

MSA-6 specifications	
Analog inputs	Six four-arm strain gage bridge inputs (350 Ohm minimum)
Bridge excitation	Jumper selectable – 2.5, 5 or 10 VDC
Amplifier gains	Jumper selectable – 1000, 2000, 4000
Auto zero	Push button or software initiated
Anti-aliasing filter	1000 Hz low pass, 2-pole
Analog output range	+/- 10 volts
Synchronization	Genlock, external trigger
Digital output	12 bit
Data acquisition rates	Via RS232: 50, 60, 100, 120 or 200 datasets per second Via USB converter: 50, 60, 100, 120, 200, 240, 300, 400, 500, 600, 1000 or 1200 datasets per second
Power supply	External (included) 110-220 VAC, 50/60 Hz Output: 13.5-19V @ 0.30 amps
Connectors	Digital output: RS232 (USB via converter) Analog output: DB25S Sync/genlock: RCA phono Transducer Input: 26-pin circular type connector
Environmental operating conditions	0 to 125°F (-18 to 52°C)
Physical dimensions (WxLxH)	26 x 21 x 4 cm (10.25 x 8.25 x 1.72)
Weight	2 kg (4.5 lbs)

Figure A.4 AMTI Mini amplifier specifications.

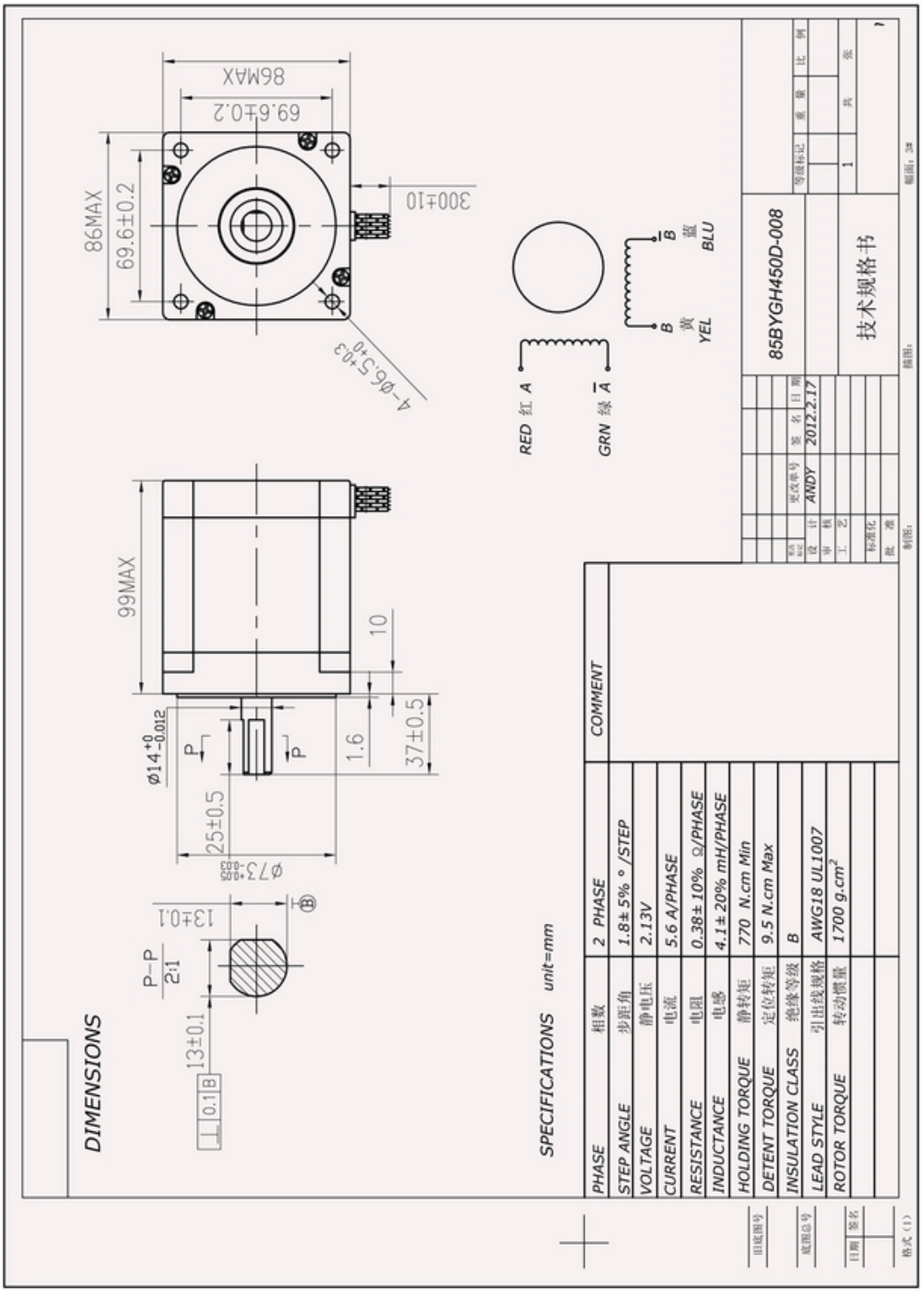

Figure A.5 Nema 34 stepper motor specifications.

Microstep Driver CW6060AC

Specification:

Mode	CW6060AC
Input Power	20~60V AC; 24~80V DC
Phrase Current	2.0A ~ 6.0A
Running Steps	1/2 、 1/4 、 1/8 、 1/16 、 1/32 、 1/64 、 1/128 、 1/256 steps; 1/5 、 1/10 、 1/25 、 1/50 、 1/125 、 1/250 steps.
Self-protection Way	overheating, overvoltage, overcurrent protection
Size	150mm × 98 mm × 45 mm
Weight	600g
Working Condition	Temperature: -15℃~40℃ Humidity: <90%
Input Method	Single Pulse

I/O Ports:

1、 AC 、 AC	Power Supply
2、 B+ 、 B-	One Phase Wires' Ports
3、 A+ 、 A-	The Other Phase Wires' Ports
4、 CP + 、 CP -	Step Pulse Input Ports (rising edge, duration> 10 μs)
5、 CW + 、 CW-	Motor running direction controlling ports.
6、 EN+、 EN-	The input signals is used to enable / disable, enable high Level performance, lov Level input driver does not work, then when not suspended.

Figure A.6 Stepper motor micro-step driver.

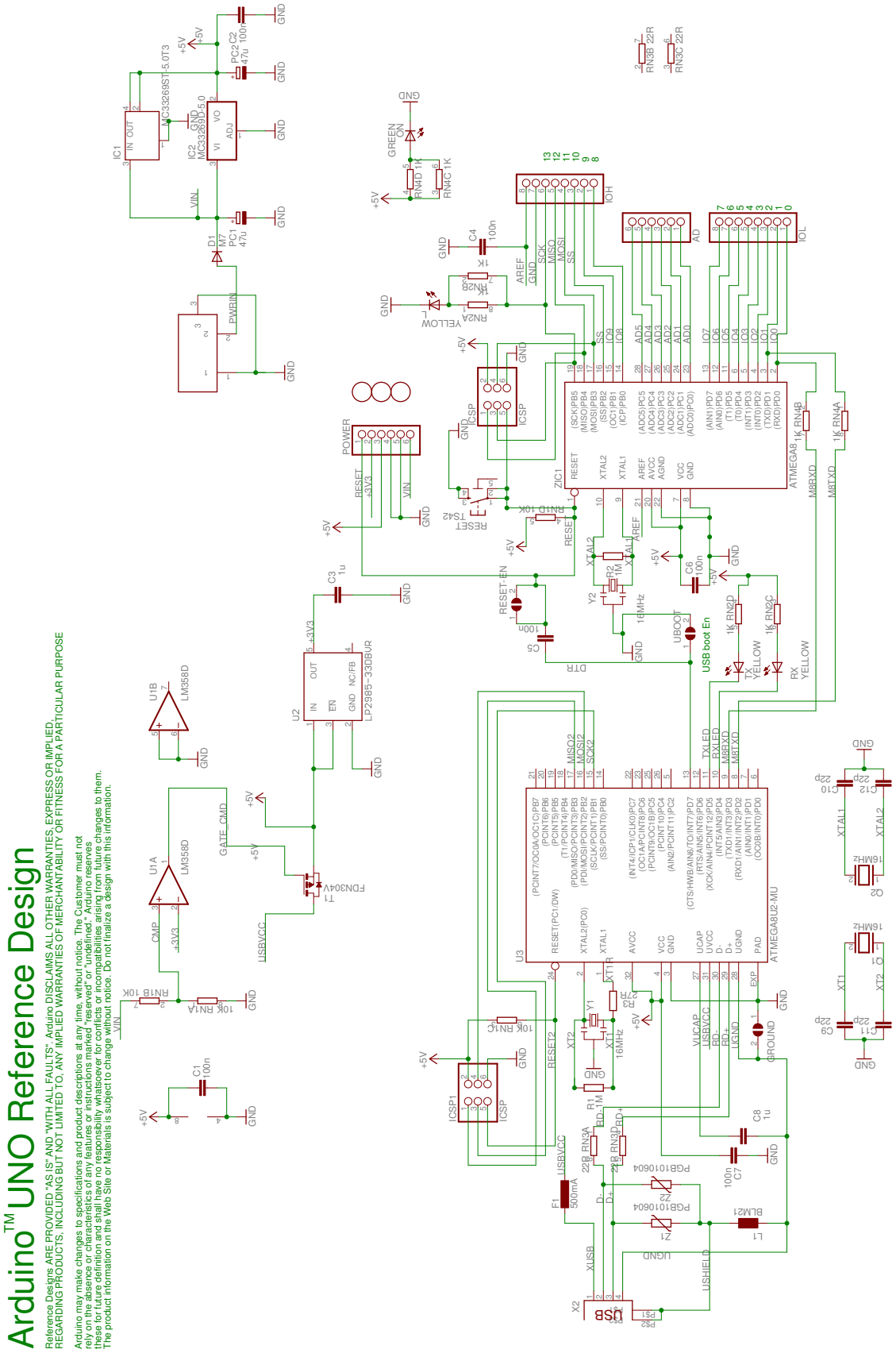

Figure A.7 Arduino micro-controller specifications.

Appendix B

MANUFACTURING AND ASSEMBLY DRAWINGS

The manufacturing and assembly drawings for the Dorsiflexometer are presented in the following appendix. The assembly tree in Figure B.1 shows the order of the drawings. The base plate, supporting struts, side brackets, platform, lever arm and motor mount were laser cut. The frame (frame pipe one and two) were bent from stainless steel piping. The rest of the parts were manufactured by the mechanical workshop of the Mechanical and Mechatronic Engineering of Stellenbosch University.

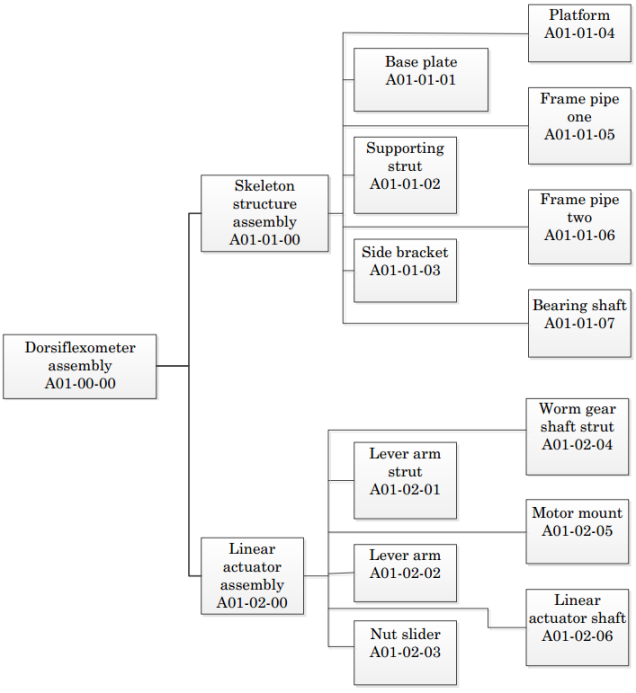

Figure B.1 Manufacturing drawings assembly tree.

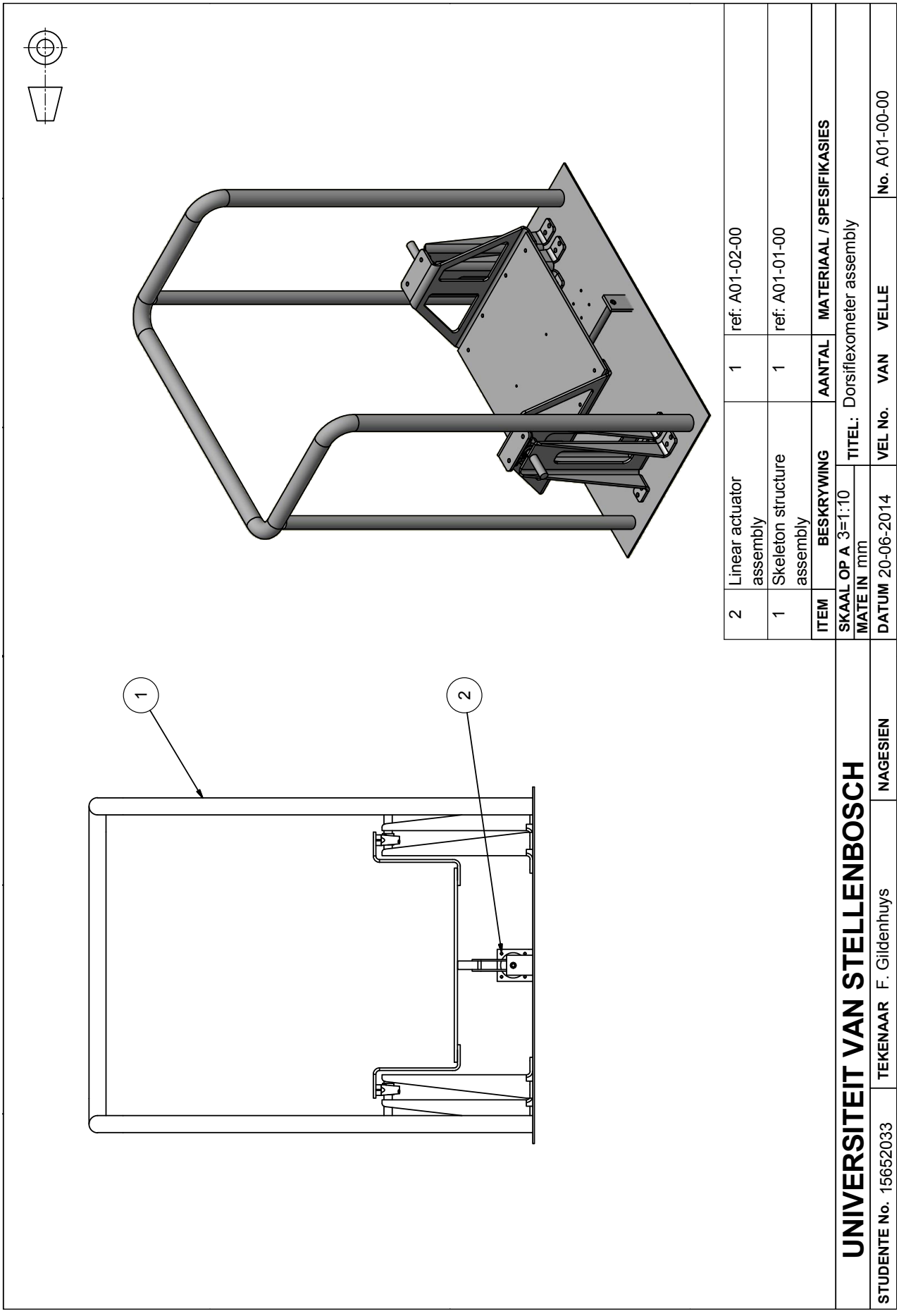

Figure B.2 Dorsiflexometer full assembly drawing.

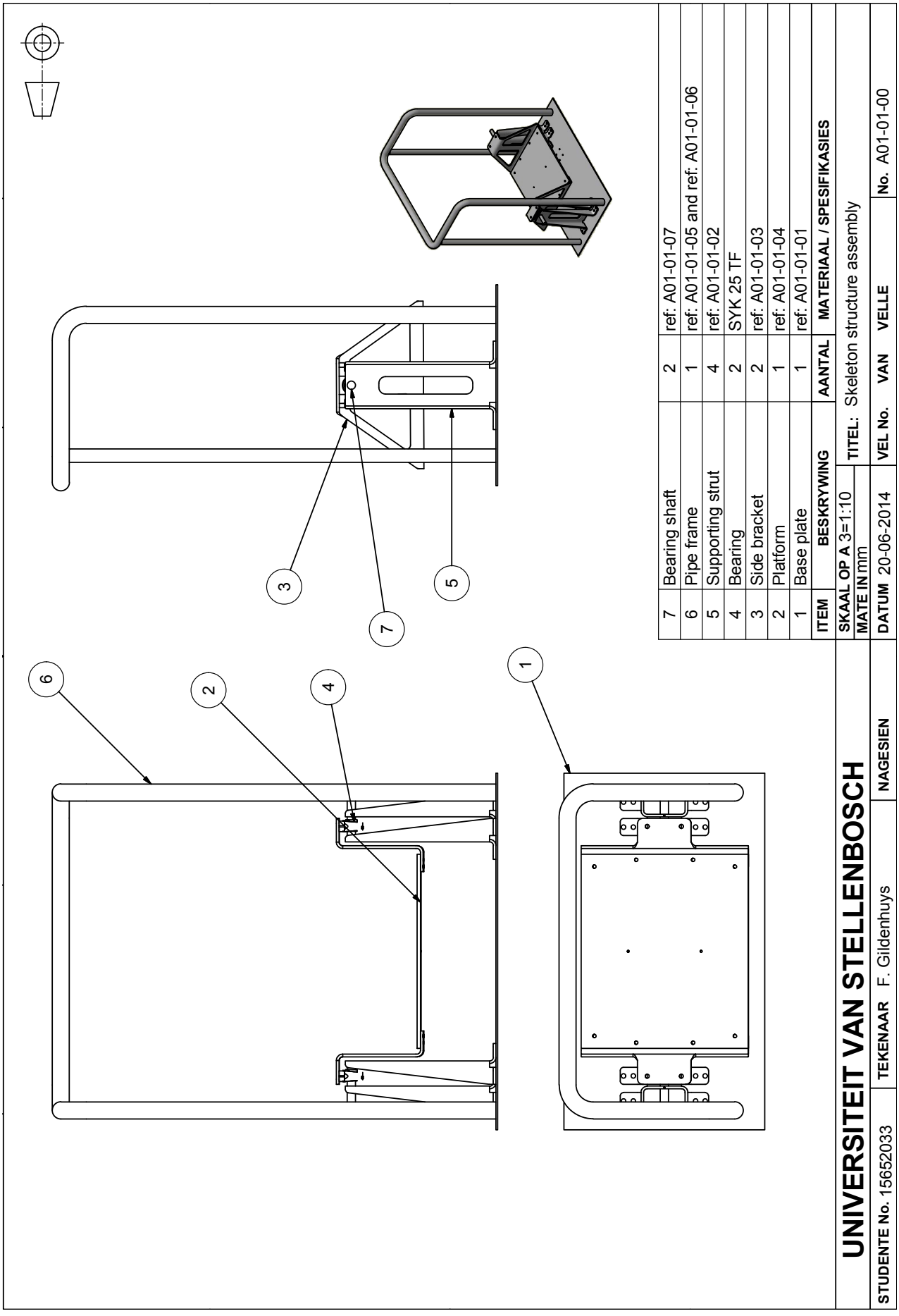

Figure B.3 Skeleton structure assembly drawing.

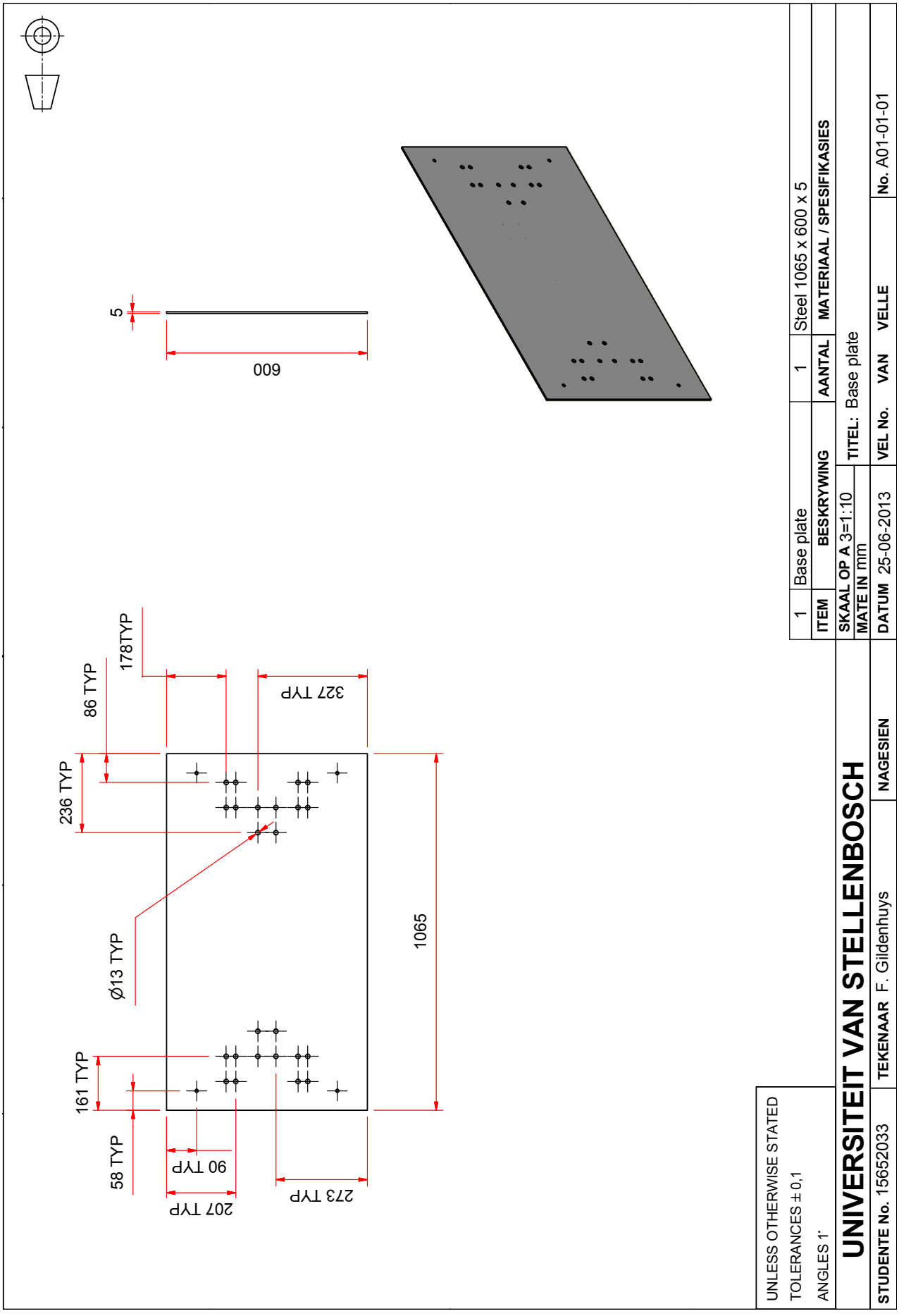

Figure B.4 Base plate manufacturing drawing.

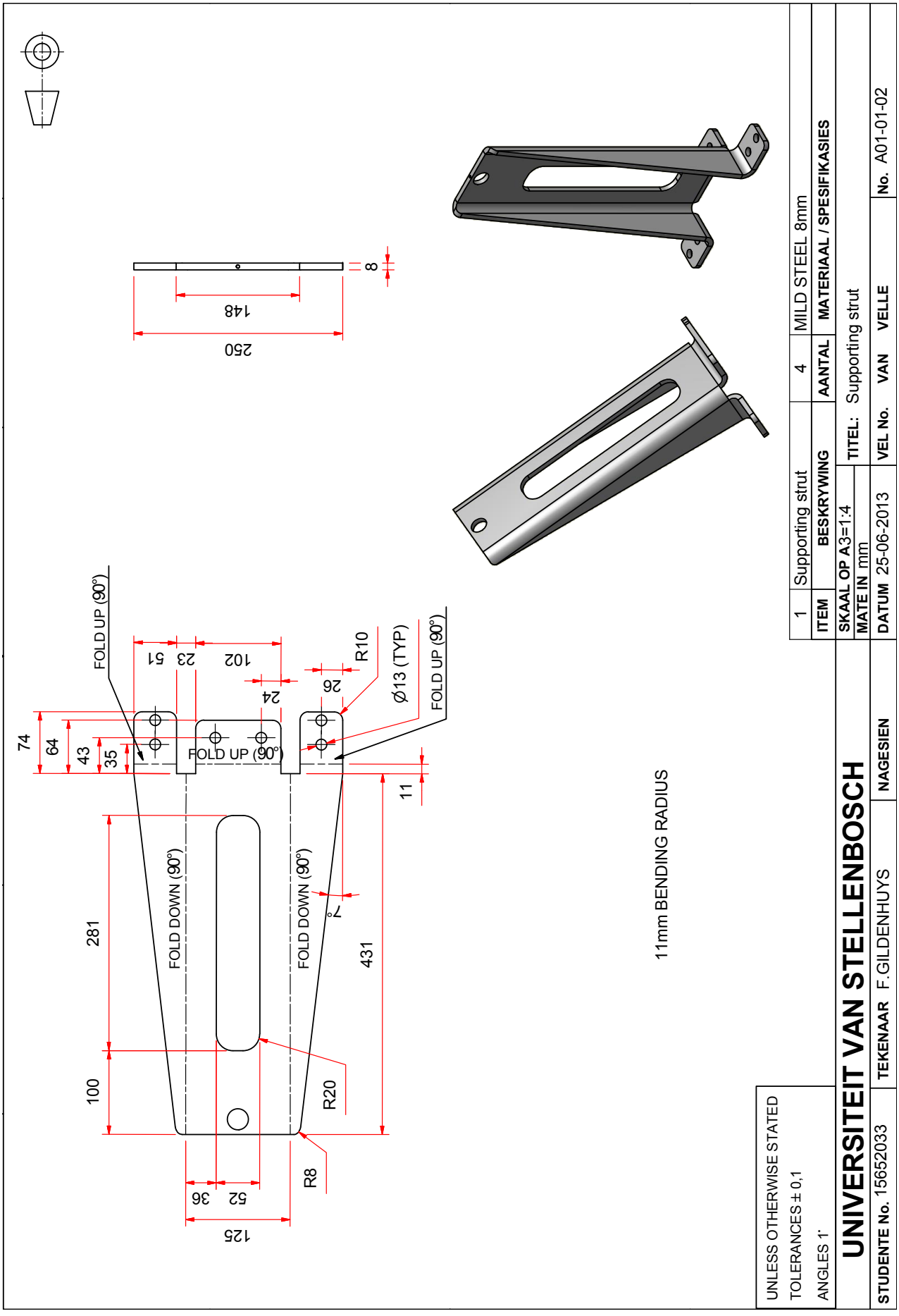

Figure B.5 Supporting strut manufacturing drawing.

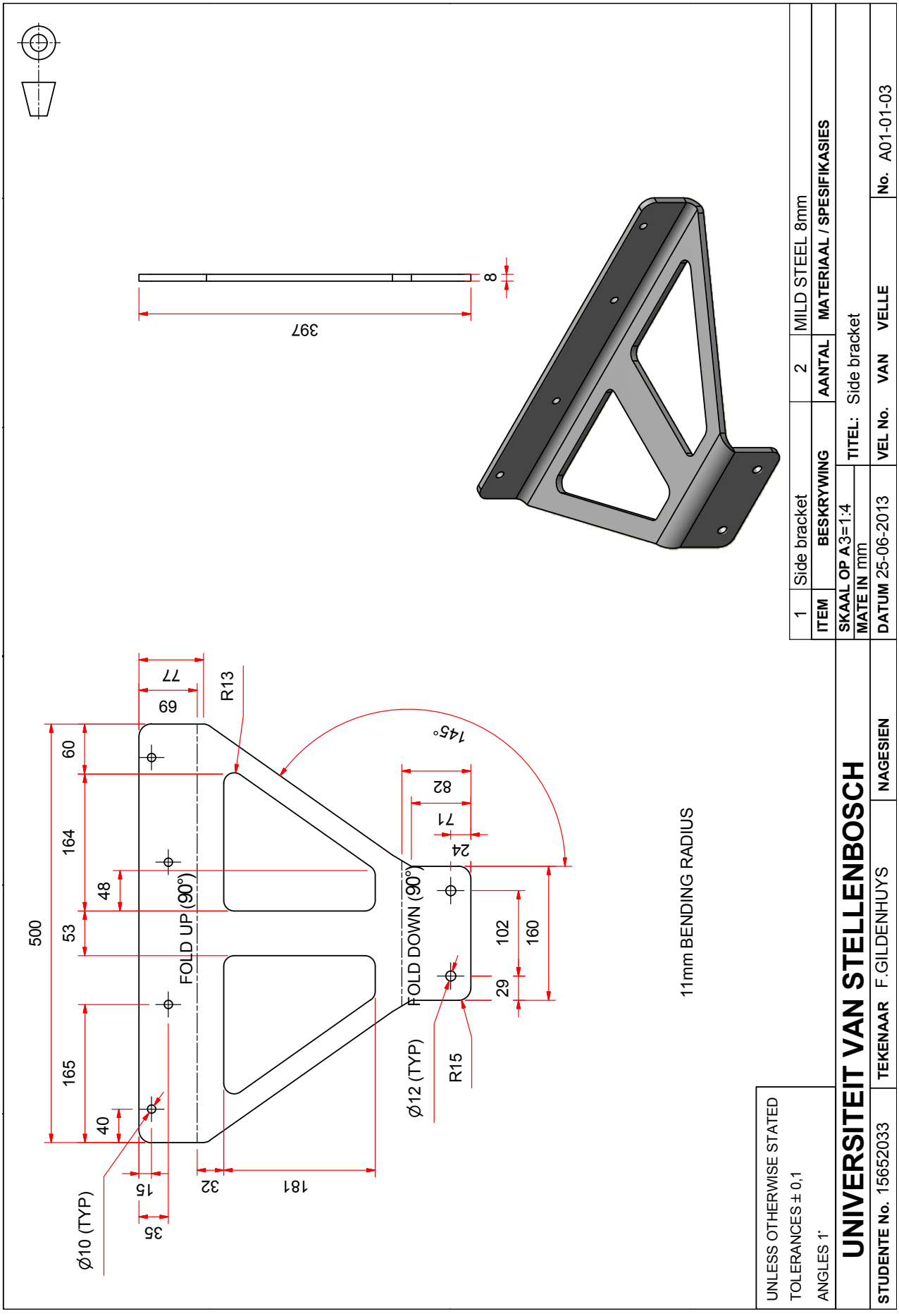

Figure B.6 Side bracket manufacturing drawing.

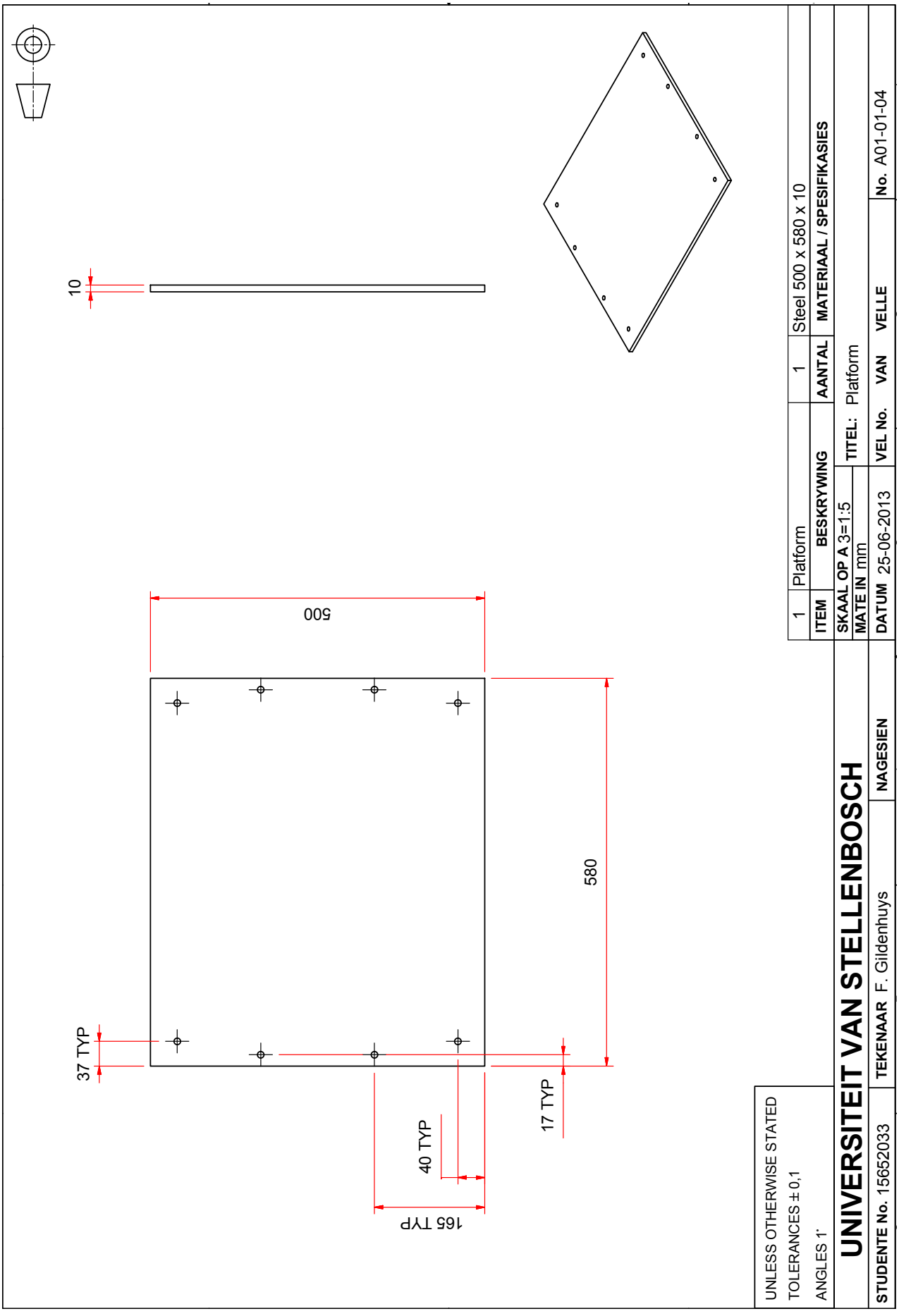

Figure B.7 Platform manufacturing drawing.

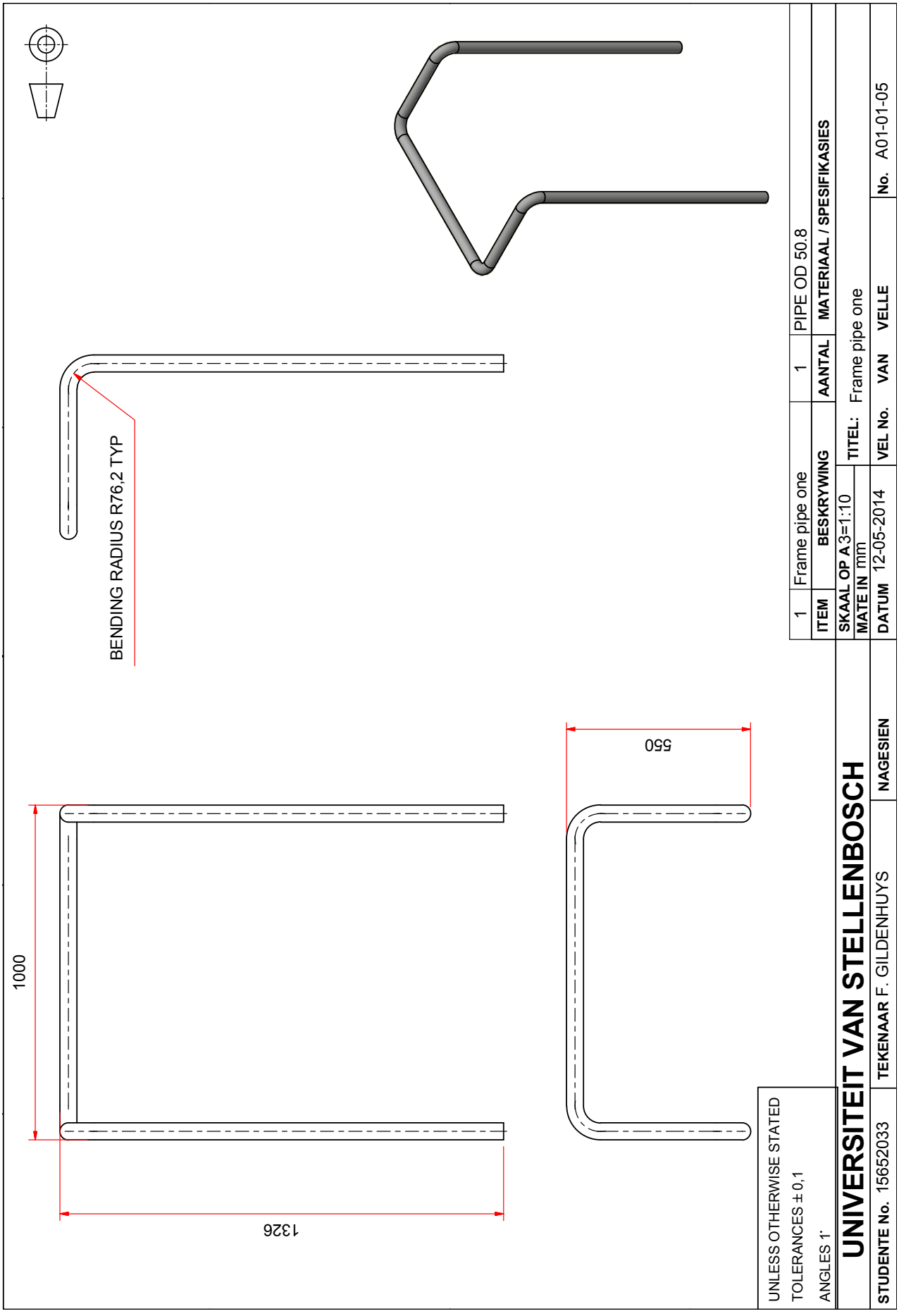

Figure B.8 Stainless steel pipe frame drawing one.

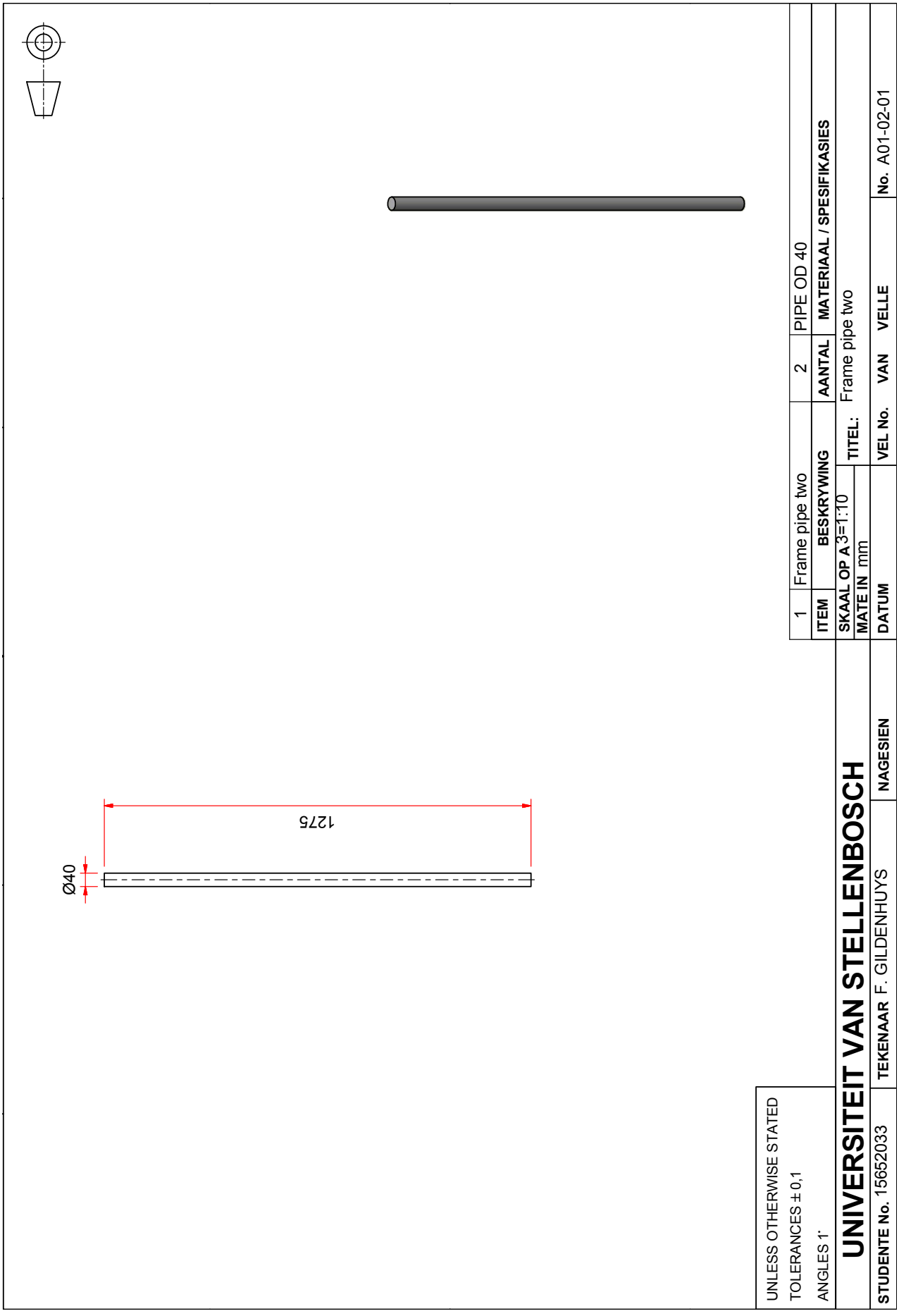

Figure B.9 Stainless steel pipe frame drawing two.

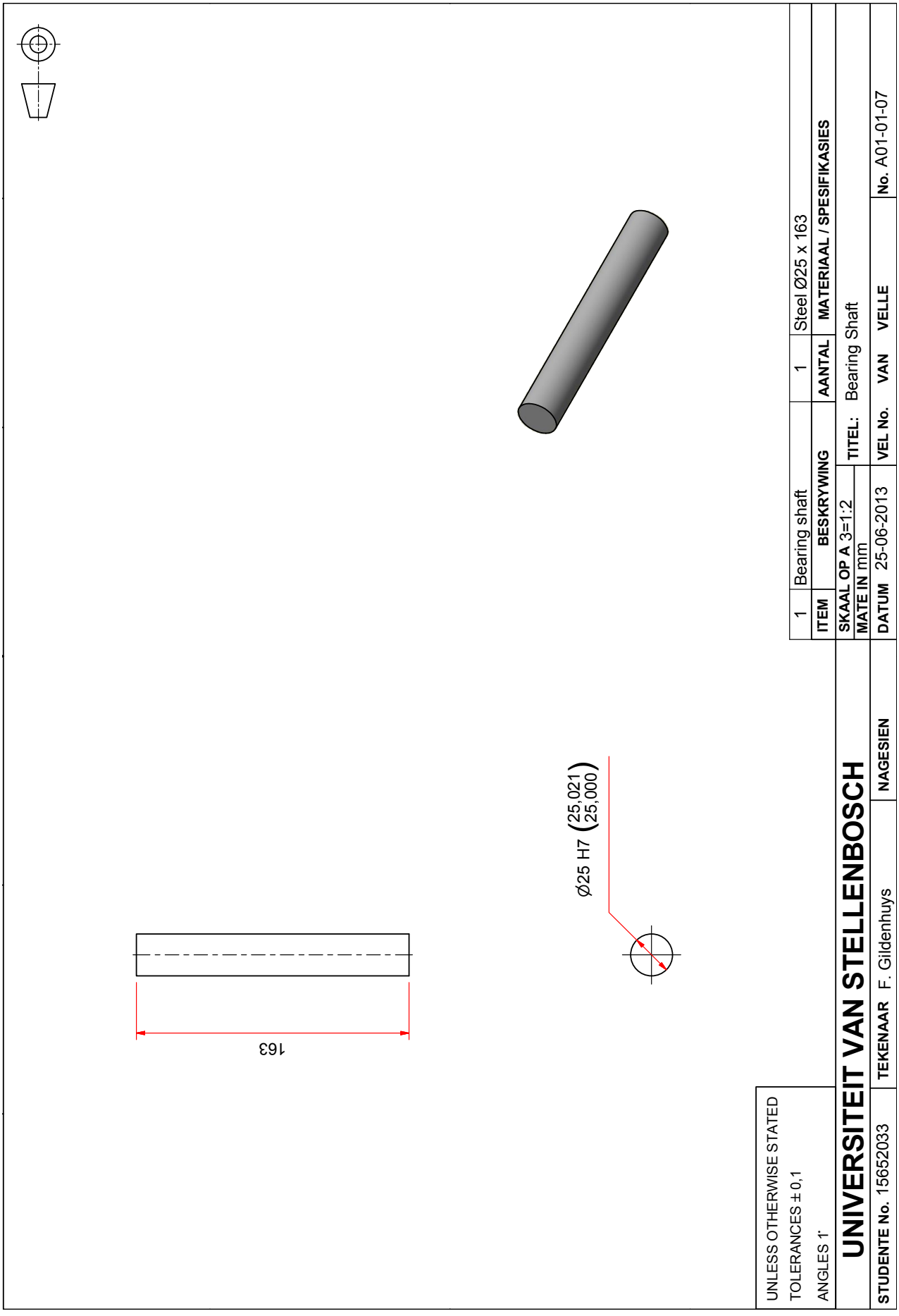

Figure B.10 Bearing shaft machine drawing.

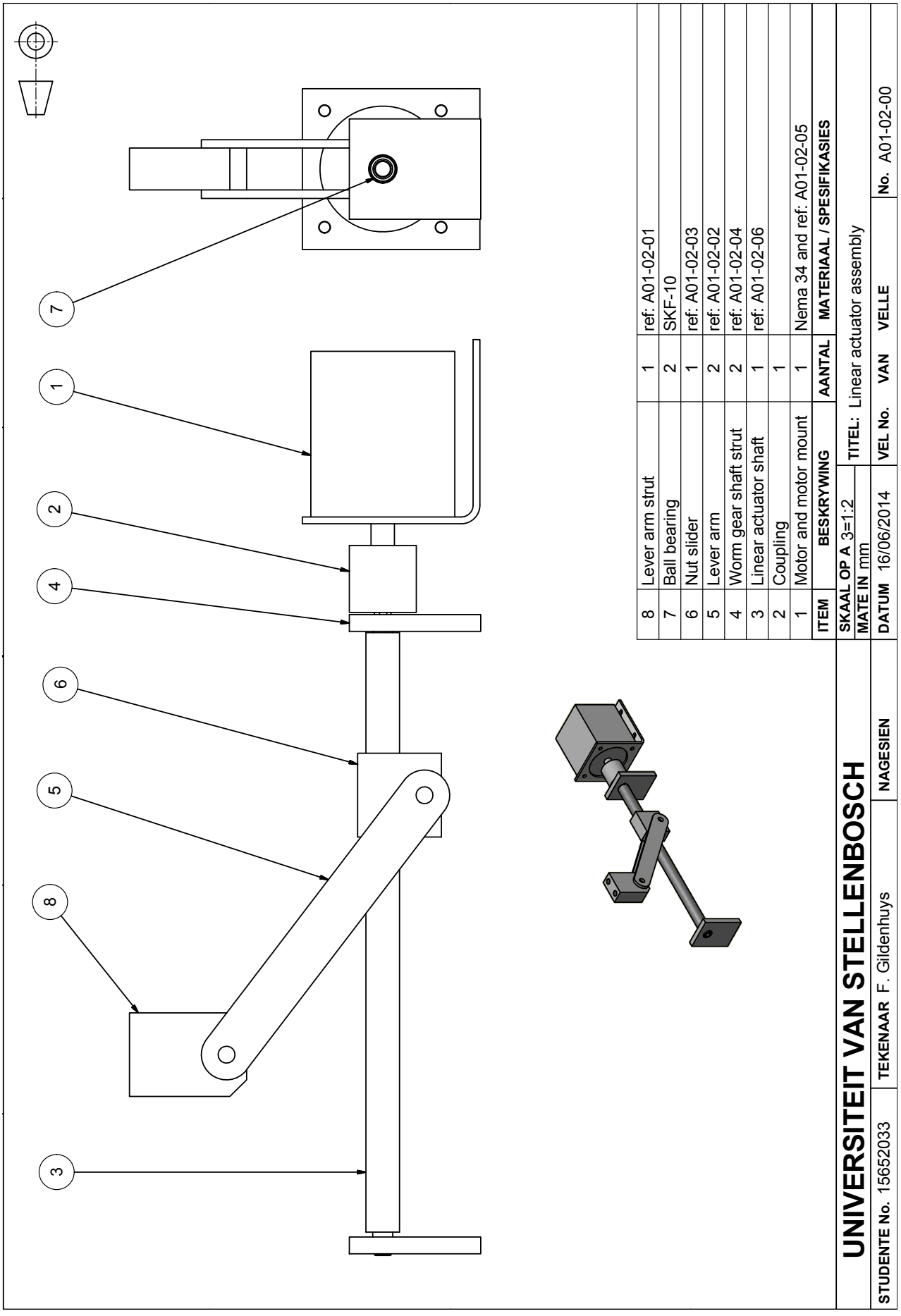

Figure B.11 Linear actuator assembly drawing.

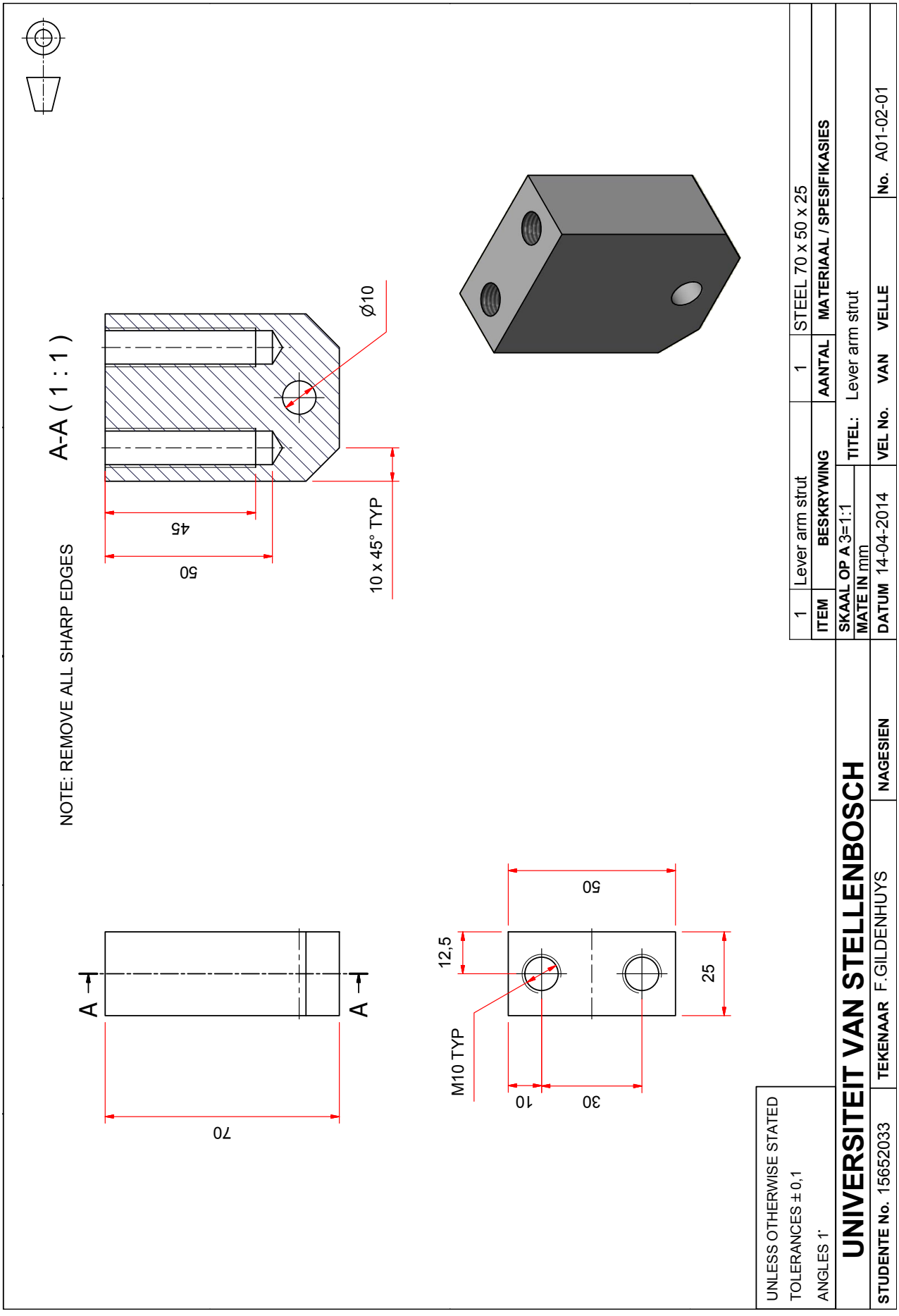

Figure B.12 Lever arm strut manufacturing drawing.

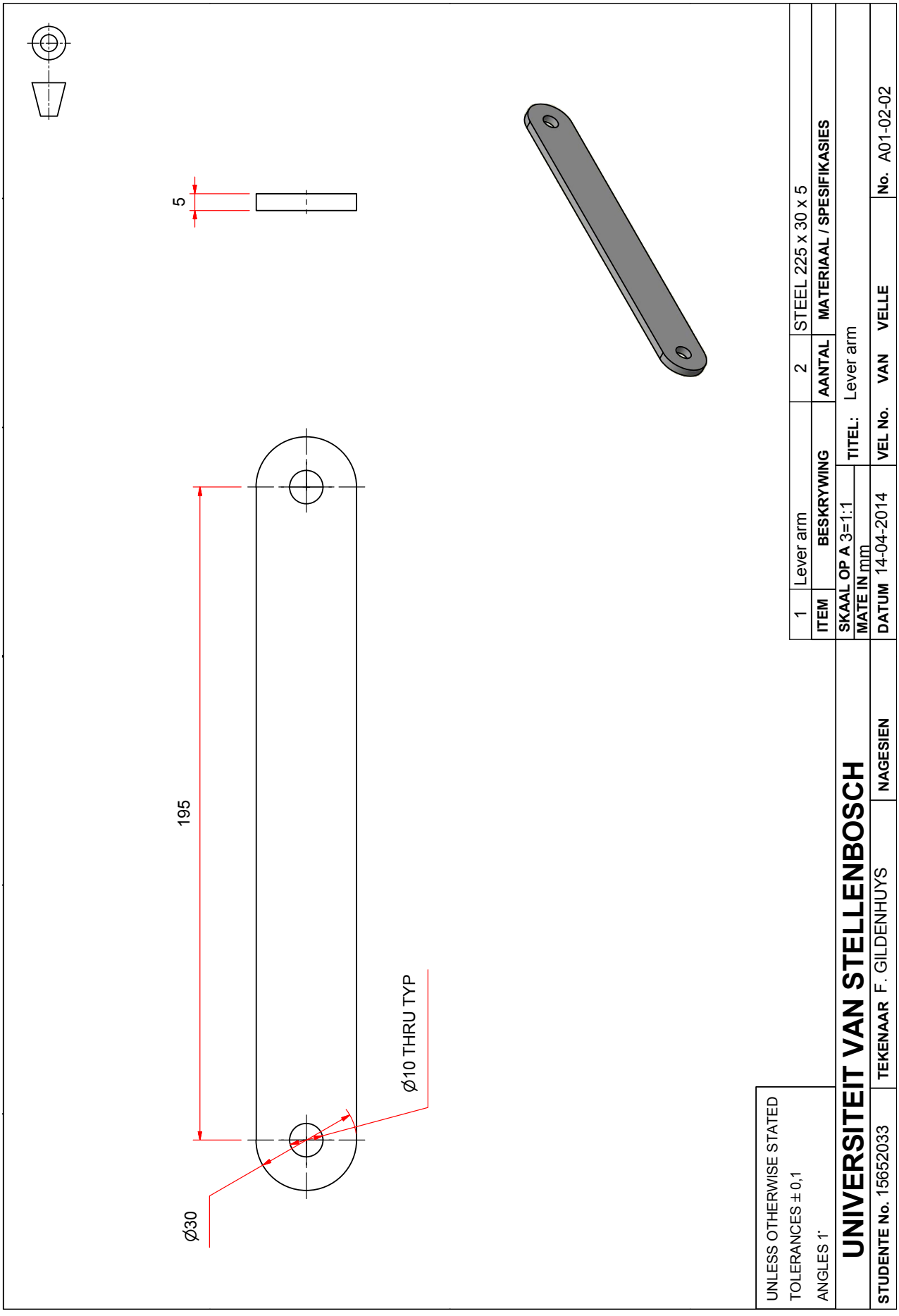

Figure B.13 Lever arm manufacturing drawing.

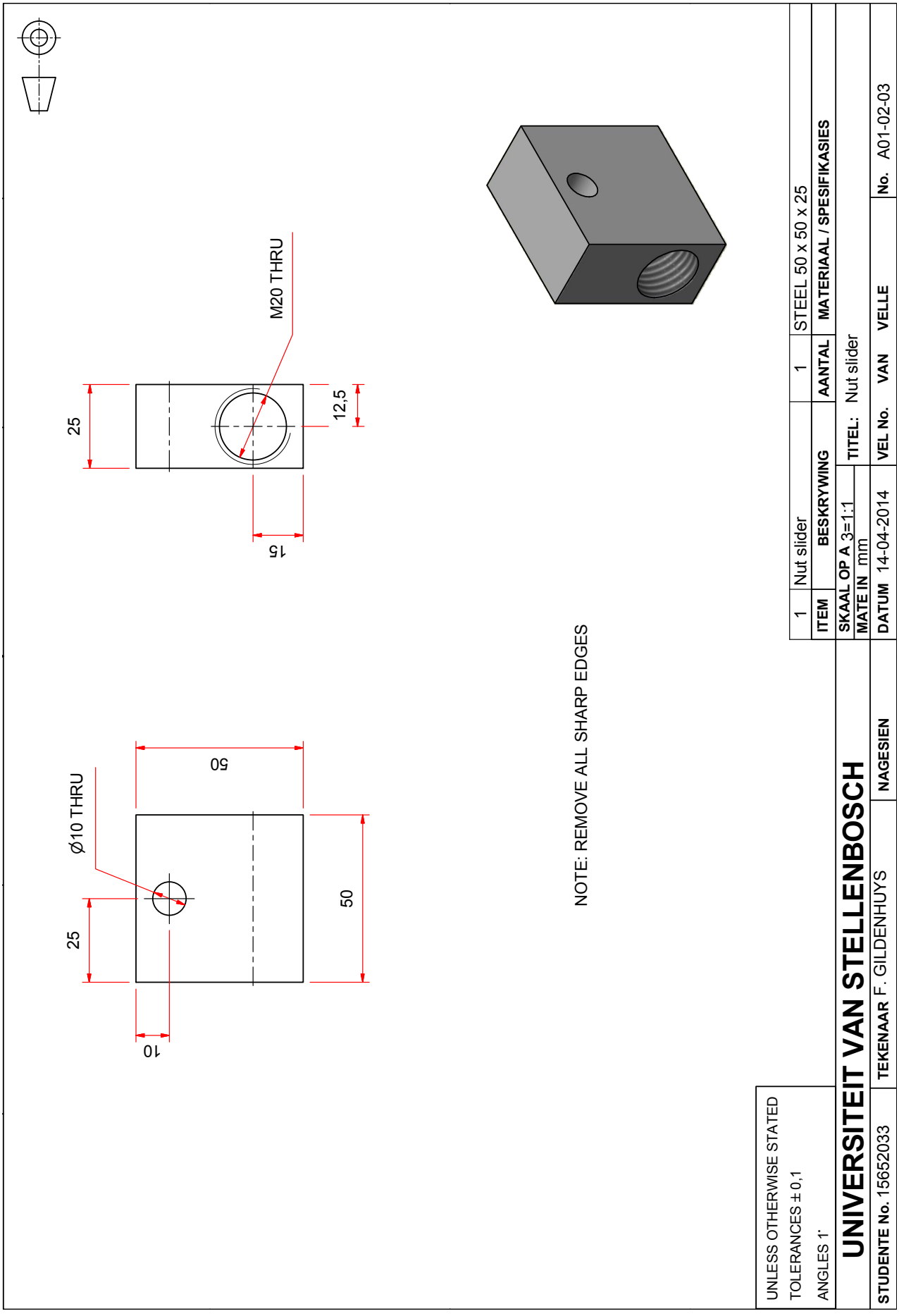

Figure B.14 Nut slider manufacturing drawing.

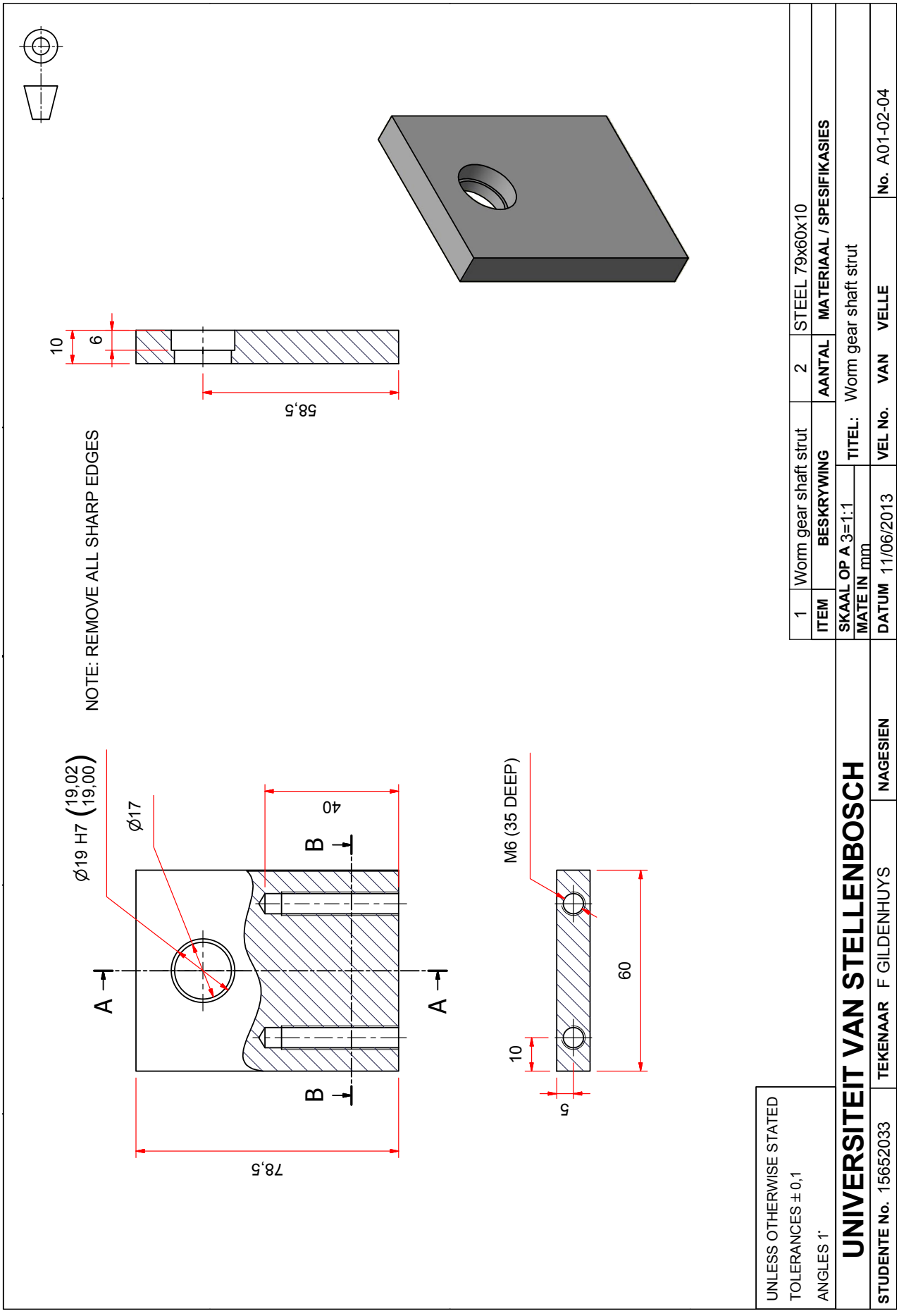

Figure B.15 Worm gear shaft strut manufacturing drawing.

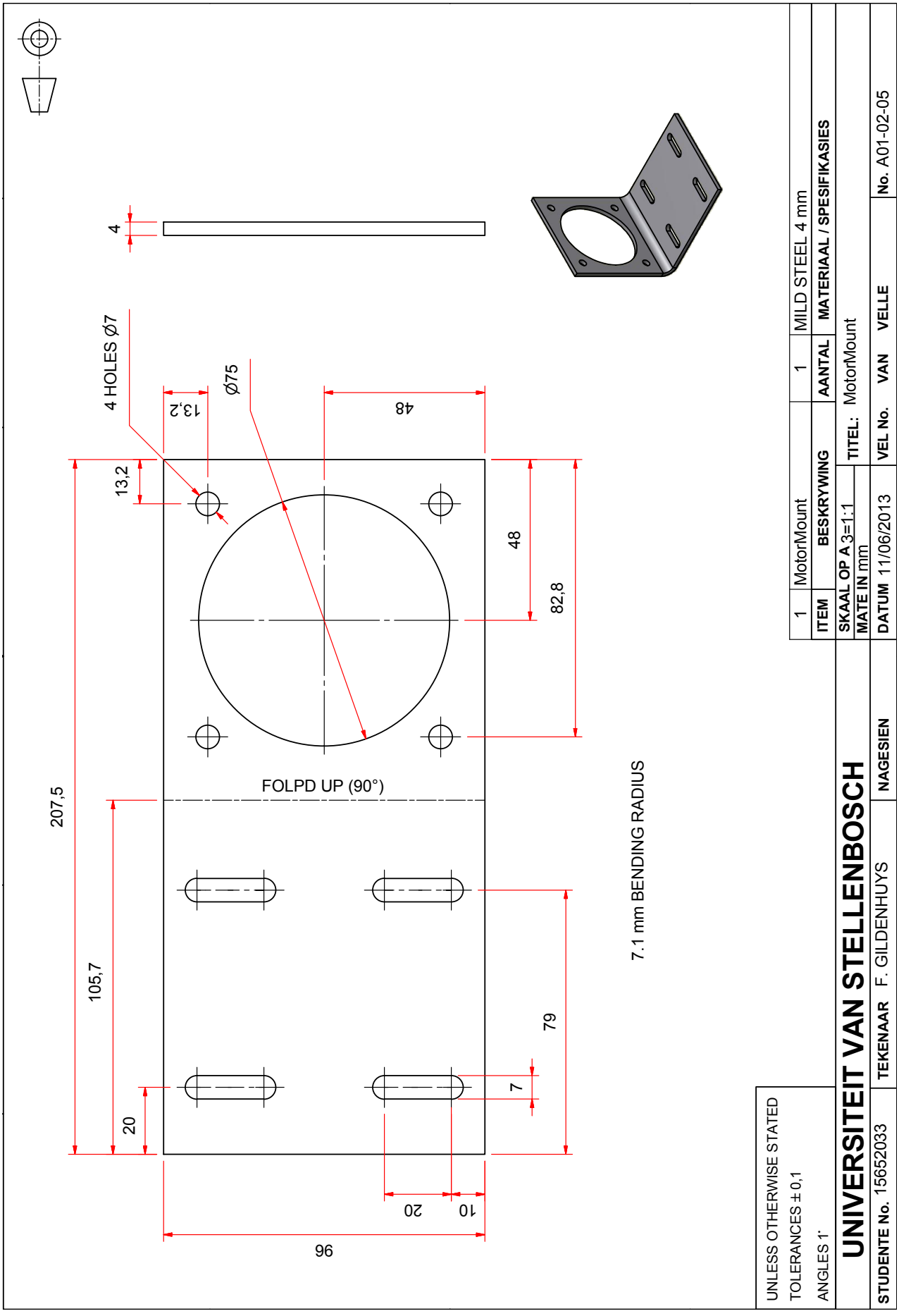

Figure B.16 Motor mount manufacturing drawing.

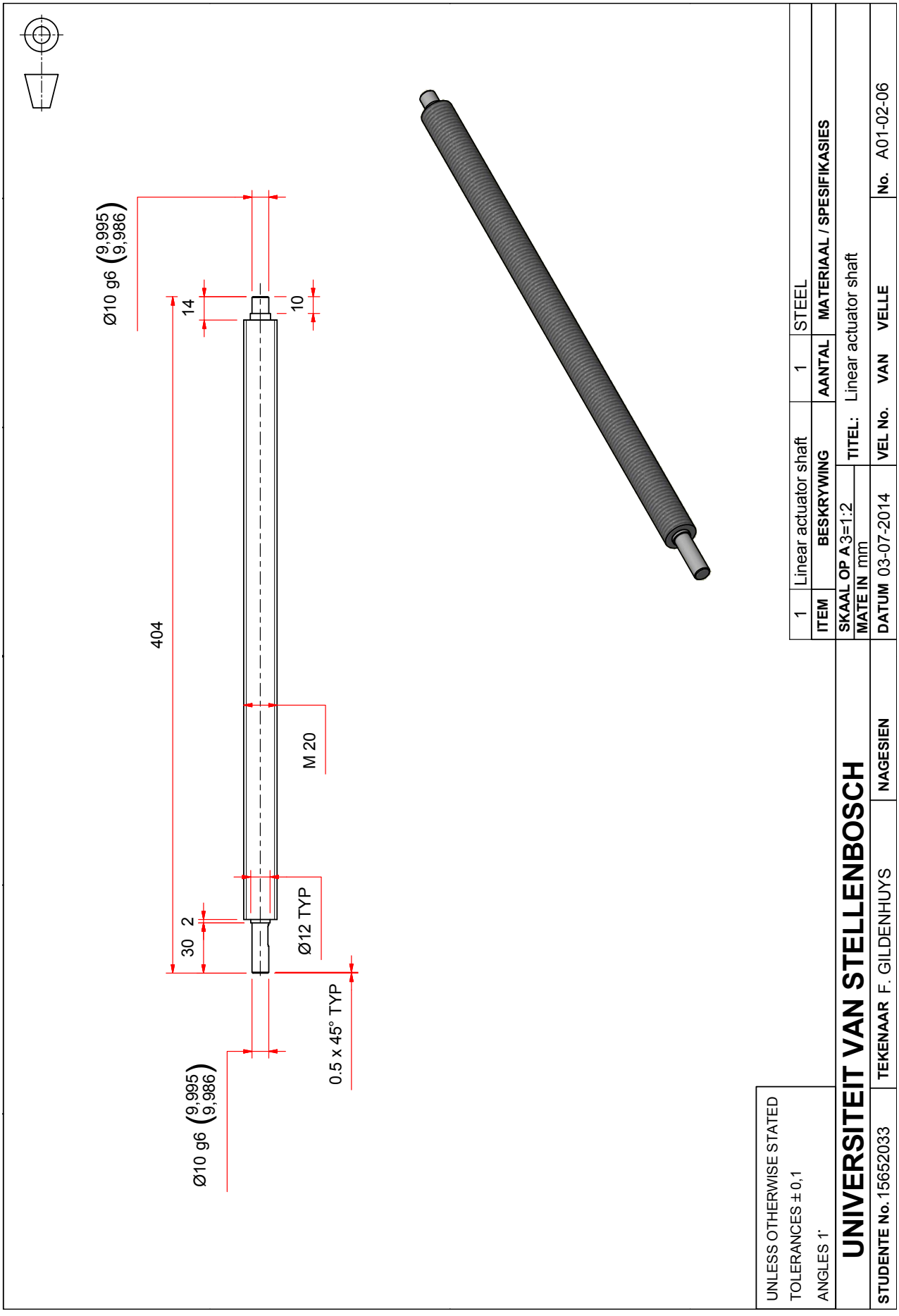

Figure B.17 Linear actuator shaft machine drawing.

Appendix C

LINEAR ACTUATOR TORQUE CALCULATIONS

The torque calculations for the power screw of the linear actuator is described in this appendix. The assumption was made that the torque, as a result of a subject stepping onto the platform, is directly transferred to the actuator block of the linear actuator as shown in Figure C.1. The force applied as a result of the subject stepping onto the platform is represented by F_1 and the countering force applied at the power screw is represented by F_2. If a subject weighing 120 kilograms steps onto the platform a counter force (F_2) of 775 Newton is applied to the power screw as shown in Equation C.0.1.

$$F_2 = \frac{120 \times 9.81 \times L_1}{L_2} \tag{C.0.1}$$

To overcome this force (F_2) a torque of 1,58 Newton meter is required by the stepper motor as shown in Equation C.0.2 (Budynas, 2008). The mean diameter (d_m) of the power screw is equal to 0.01875 m, the lead (l_{lead}) of a M20 course-pitch screw is equal to $0,0025$ m and the frictional coefficient (f) of oiled steel threads are equal to $0,15$.

$$T_R = \frac{F_2 d_m}{2}\left(\frac{l_{lead} + \pi f d_m \sec(30)}{\pi d_m - f l_{lead}\sec(30)}\right) \tag{C.0.2}$$

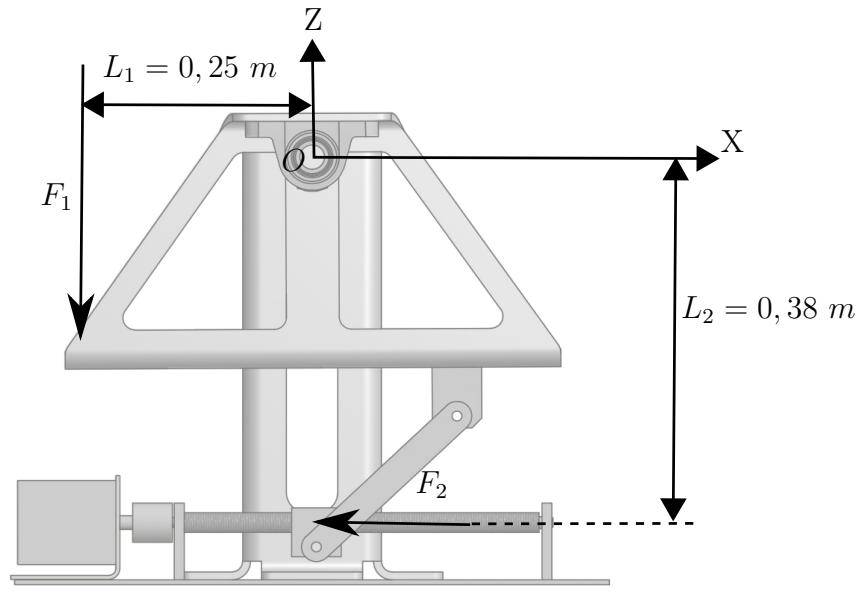

Figure C.1 Force on the power screw as a result of a subject stepping onto the Dorsiflexometer platform.